1974

The determination of nitrate and nitrite ions using forced-flow liquid chromatography with electrochemical detection

Ronald J. Davenport
Iowa State University

INFORMATION TO USERS

This material was produced from a microfilm copy of the original document. While the most advanced technological means to photograph and reproduce this document have been used, the quality is heavily dependent upon the quality of the original submitted.

The following explanation of techniques is provided to help you understand markings or patterns which may appear on this reproduction.

1. The sign or "target" for pages apparently lacking from the document photographed is "Missing Page(s)". If it was possible to obtain the missing page(s) or section, they are spliced into the film along with adjacent pages. This may have necessitated cutting thru an image and duplicating adjacent pages to insure you complete continuity.

2. When an image on the film is obliterated with a large round black mark, it is an indication that the photographer suspected that the copy may have moved during exposure and thus cause a blurred image. You will find a good image of the page in the adjacent frame.

3. When a map, drawing or chart, etc., was part of the material being photographed the photographer followed a definite method in "sectioning" the material. It is customary to begin photoing at the upper left hand corner of a large sheet and to continue photoing from left to right in equal sections with a small overlap. If necessary, sectioning is continued again — beginning below the first row and continuing on until complete.

4. The majority of users indicate that the textual content is of greatest value, however, a somewhat higher quality reproduction could be made from "photographs" if essential to the understanding of the dissertation. Silver prints of "photographs" may be ordered at additional charge by writing the Order Department, giving the catalog number, title, author and specific pages you wish reproduced.

5. PLEASE NOTE: Some pages may have indistinct print. Filmed as received.

Xerox University Microfilms
300 North Zeeb Road
Ann Arbor, Michigan 48106

The determination of nitrate and nitrite ions using forced-flow liquid chromatography with electrochemical detection

by

Ronald J. Davenport

A Dissertation Submitted to the
Graduate Faculty in Partial Fulfillment of
The Requirements for the Degree of
DOCTOR OF PHILOSOPHY

Department: Chemistry
Major: Analytical Chemistry

Approved:

Signature was redacted for privacy.

In Charge of Major Work

Signature was redacted for privacy.

For the Major Department

Signature was redacted for privacy.

For the Graduate College

Iowa State University
Ames, Iowa

1974

TABLE OF CONTENTS

I. INTRODUCTION

A chromatographic method for the separation and simultaneous determination of NO_2^- and NO_3^- is described in this thesis. The chromatographic detector is a Cd amperometric tubular electrode. The working range of the method is 0.05 - 1.0 mM for both NO_2^- and NO_3^-, and the detection limit is 0.01 mM.

This research was prompted by the increasing need to monitor the concentrations of NO_2^- and NO_3^- in the environment. Excessive amounts of NO_3^- and NO_2^- in food and H_2O can lead to methemoglobinemia in humans (especially infants) and livestock (142, 174). Methemoglobinemia results from the oxidation of the Fe(II) in hemoglobin by NO_2^- and, to a lesser extent, NO_3^- (54). The methemoglobin formed cannot reversibly combine with O_2 or CO_2. Death results from hypoxia in severe cases.

Nitrate is not as toxic as NO_2^-, but it can be converted to NO_2^- by the intestinal bacteria Escherichia coli (105). Nitrate is much more prevalent in the environment than NO_2^-. In one study of 197 meat products, the average concentrations found were 28 ppm NO_2^- and 181 ppm NO_3^- (181). Vegetables may contain as much as 3517 ppm NO_3^-, while the normal maximum concentration of NO_2^- is 5.5 ppm (143). The maximum limit set by the U.S. Public Health Service for NO_3^- in potable H_2O is 45 ppm (0.72 mM), and the generally accepted

maximum for NO_2^- is 0.2 ppm (4 μM) (190).

Ruminants are particularly susceptible to NO_3^- and NO_2^- poisoning. Grasses and cornstalks often used as feed may accumulate toxic levels of NO_3^- at certain times of the year (78a).

Carcinogenic nitrosamines may form in meat from nitrates and nitrites added during processing (70, 107, 196, 197). Nitrosamines may also form in the stomach after ingestion of NO_3^- and NO_2^- (106).

Because of the need for rapid, convenient, and accurate methods for the determination of NO_3^- and NO_2^-, a chromatographic method utilizing electrochemical detection was developed. Chromatographic methods are rapid, convenient, and easily automated. Electrochemical detectors are sensitive and sufficiently accurate for most analyses.

The Cd tubular detector was developed after preliminary studies were made to discover those experimental conditions that would optimize detector response. Cyclic voltammetry with a rotating Cd-disk electrode was used for those preliminary studies. Then the chromatograph and detector were developed and evaluated. Experimental procedures were developed for the analysis of hay, cornstalks, and H_2O. The reduction product of NO_3^- and NO_2^- was shown with a Cd coulometric detector to be NH_2OH. Cyclic voltammetry with a rotating ring-disk electrode showed NO_3^- is rapidly reduced to NO_2^-, and NO_2^- is reduced more slowly to NH_2OH.

II. LITERATURE REVIEW

No reliable and satisfactory gravimetric method has been developed for the determination of NO_2^-, but nitron can be used to quantitatively precipitate NO_3^- (37, 88, 230). Nitrite and many other ions interfere. When the gravimetric method has been applied to the determination of NO_3^- in H_2O, the procedure was long, and the technique was insensitive. The working range of concentrations was 0.12 - 0.60 g NO_3^-/l (198).

Nitrite is quite reactive and can be determined by titration with an oxidizing agent such as MnO_4^- (132, 215), Ce(IV) (216, 230), chloramine T (61, 230), and OCl^- (132). Nitrite can also be determined iodometrically (132).

Nitrate is less reactive and must be titrated with strong reducing agents such as Ti(III) (17) or Mn(II) (139). Nitrate can be titrated with indigocarmine (40, 41), or can be determined by reacting it with excess Fe(II), which is back-titrated with $K_2Cr_2O_7$ (103, 178) or MnO_4^- (132). Complexometric titrations of NO_3^- can be performed with titrants containing $Pb(OAc)_2$ or $Ba(OAc)_2$ (31, 136). An indirect method, involving the reaction of NO_3^- with urea, has been reported (43). Nitrate can be titrated with $HClO_4$ in a nonaqueous solvent after it is reduced to NO_2^- (217).

An advantage of titrimetric methods is that they require no elaborate equipment. However, they are best suited to the

analysis of more concentrated samples than those of interest here.

Manometric methods have been used to analyze mixtures of NO_3^- and NO_2^-. Both ions are reduced to NO at Hg in solutions of 19 N H_2SO_4 (227, 230). The concentration of NO_2^- can be calculated from the volume of N_2 produced by reduction with sulfamic acid (227). Alternatively, NO_3^- and NO_2^- are reduced to N_2O with HCOOH, which is decomposed to CO_2 (18). The N_2O is measured volumetrically, and the CO_2 formed is collected and weighed on soda asbestos. The concentrations of NO_2^- and NO_3^- are calculated from the stoichiometry of the reactions.

Ammonia is formed if NO_3^- and NO_2^- are reacted with Al (14), Raney-nickel catalysts (33), or Devarda's alloy (204). The NH_3 can be distilled and determined titrimetrically or spectrophotometrically (137). However, phosphate is present in many samples and interferes with the Devarda's method (73).

Microdiffusion methods have been developed, which use Zn or $FeSO_4$ to reduce NO_3^- to NH_3 (74, 145). For the analysis of soil with these methods, the working range is only 1 - 6 ppm NO_3^--N, and the amount of Zn used for the reduction is critical to the precision of the analysis.

Both NO_2^- and NO_3^- absorb light in the ultraviolet region of the spectrum, and they can be determined spectro-

photometrically (21, 79, 163, 172, 214). Absorbance measurements at 302 nm and 355 nm can be used to calculate NO_2^- and NO_3^- concentrations in a mixture (93, 234). The working range is narrow, and Ba(II), Pb(II), Zn(II), and Cu(II) interfere.

Most spectrophotometric methods for NO_2^- and NO_3^- employ color-forming reagents for greater sensitivity. Nitrate can be determined by reaction with brucine in concentrated solutions of H_2SO_4 (110, 135, 177), and NO_2^- can be determined with brucine in less acidic solutions (67, 193). The reaction of brucine with NO_3^- is not stoichiometric and is difficult to control (232). Calibration curves do not follow Beer's Law exactly (102), and the curves exhibit a minimum at high concentrations (102). Solutions containing 0.8, 23, and 38 mg NO_3^--N/l all produce absorbance readings of 0.6.

Other color-forming reagents that react with NO_3^- are phenoldisulfonic acid (14), diphenylamine (57, 108, 238), NH_4ReO_4 (98), 2-nitroso-1-naphthol-4-sulfonic acid (2), chromotropic acid (186, 233), methylene blue (125), and m-xylenol (14, 180).

Nitrite can be determined by diazotization of sulfanilic acid and reaction with α-naphthylamine (14, 173). Alternatively, NO_2^- can be determined by reaction with sulfanilamide and N-(1-naphthyl)ethylenediamine (14, 84, 175,

195, 231). Nitrate can be determined with either of these procedures if it is first reduced to NO_2^- with Zn powder (167), N_2H_4 (55, 118), or a Cd or Cd(Hg) reduction column (14, 77, 83, 99, 194). Certain enzymes (189, 229), bacteria (243), and algae (100) have been used to reduce NO_3^- to NO_2^-.

Other color-forming reagents that react with NO_2^- are phenylenediamine (16), antipyrine (151), α-thiolacetic acid (26), dithiazanine iodide (68), 2-mercaptoethanol (210), amino-G acid (138), malachite green (111), congo red (111), di-sodium 1-(4-amino-2-sulfophenylazo)-2-amino-8-hydroxy-naphthylene-6-sulfonate (120), and o-tolidine (80).

Some spectrophotometric procedures have been automated to decrease the manipulation required to perform them routinely (12, 15, 42, 150, 161, 236, 239). The Technicon Autoanalyzer uses a N-(1-naphthyl)ethylenediamine method (12) and can analyze 30 - 40 samples of H_2O per day for several constituents besides NO_3^- and NO_2^- (236). However, the results obtained from the automated method do not always agree with those from the manual procedure (89).

Various spectrophotometric methods recently were compared and evaluated (8, 156). The methods were used to analyze identical samples containing 1 ppm NO_3^- and 10 - 400 ppm Cl^-. Chloride interfered with all of the methods used. The best method was a modified brucine procedure, but it produced relative errors of 5.5 - 9.2%, depending on the Cl^- concen-

tration. Chloride is a common anion, yet it causes large errors in the standard spectrophotometric methods.

Many samples (especially extracts of silage and green feeds) are highly colored and turbid. These samples must be clarified with $ZnSO_4$ and $K_4Fe(CN)_6$ (3), $Al_2(SO_4)_3$ (126), ion-exchange resins (32, 112, 170), or acetone extractions (162) if they are to be analyzed spectrophotometrically.

Electrochemical methods may be better suited than spectrophotometric methods for the analysis of turbid and colored samples and samples that contain Cl^- and other salts that interfere with the standard methods. The majority of electrochemical methods for the determination of NO_3^- and NO_2^- are polarographic. Nitrite can be determined by oxidation at the dropping Hg electrode (DME) (9, 10). Nitrate and NO_2^- are predicted to be reduced to NH_2OH at +0.41 and +0.91 V vs. SCE, respectively, from the thermodynamics of the reductions (122). However, the kinetics are very slow. Nitrate is reduced only at very negative potentials in concentrated solutions of H_2SO_4 (152, 185). The reduction occurs at more positive potentials in solutions of various polyvalent cations (25, 47, 76, 158, 211, 222, 223). Solutions containing La(III) (13, 59, 76, 85, 146, 205, 211, 222, 223), Ce(IV) (59, 85, 211, 223), Th(IV) (69), Nd (III) (101, 211), and Zr(IV) (59, 157, 187, 235) are particularly effective. In the case of La(III), the

increased reversibility of the reduction of NO_3^- is known to be due to the formation of an electroactive NO_3^- complex (128). The calibration curves obtained with these polarographic methods are not strictly linear, and they are somewhat inconvenient to use.

The polarographic waves from the reduction of several species are enhanced in the presence of NO_3^-, although NO_3^- itself is not reduced at the DME in the medium used. The catalytic enhancement of the reduction waves for complexes of Cr(III) (92, 94, 220, 237), Mo(VI) (46, 90, 91, 115, 130), U(VI) (72, 95, 129, 131, 133, 134, 164), and V(V) (219) with NO_3^- has been reported. Nitrite also enhances these waves and can be determined (22, 46, 91, 92, 164).

Some of these catalytic reactions do not result in linear calibration curves (115). The commonly used U(VI) method allows the determination of NO_3^- in the concentration range of 2×10^{-7} to 2×10^{-5} M (95), but several cations and anions interfere (164). Phosphate and F^- interfere because they complex some of the uranium species in the solution.

Nitrate and NO_2^- can be determined polarographically after reaction with some organic compounds to form electroactive derivatives. Such reagents as semicarbazide (11), 2,6-xylenol (30, 52, 59, 96, 97, 226), and sodium naphthionate (20) have been used. The 2,6-xylenol method is useful in

the range of 2×10^{-5} to 1×10^{-3} M NO_3^-. The reaction of NO_3^- with 2,6-xylenol requires ten minutes, and Cl^- is a serious interference (97).

The nitrate-selective electrode has been widely used (23, 24, 49, 50, 63, 66, 78b, 127, 148, 149, 153, 155, 184, 188). Both the membrane type and the liquid-anion exchanger type of electrode give linear response over the concentration range of 1×10^{-4} to 1×10^{-1} M (56). Relative errors are as small as 2% (38). When soil is analyzed, the relative error is generally 5%, and the relative standard deviation is 12.5% (66). Therefore, the nitrate-selective electrode compares well with spectrophotometric methods (147, 154, 159, 169, 176, 179), and it gives better results than the Devarda's method in the analysis of plant extracts (160). Nitrite can be determined if it is oxidized to NO_3^- with MnO_4^- (166).

Disadvantages of the nitrate-selective electrodes are their long response times and short lifetimes of only 1 - 3 weeks (56). Many ions (especially Cl^-) interfere with their use. For best results, temperature control and buffer solutions must be used (1, 71). The electrodes are not accurate if the NO_3^- concentration is less than 5 μg N/ml (36). Therefore, $Al_2(SO_4)_3$ solutions containing 10 μg NO_3^--N/ml are often used to extract NO_3^- from plant material (19, 39).

Coulometry has been used to determine NO_3^- and NO_2^- with greater precision and accuracy than that obtained with other methods. Electrogenerated Ti(III) (44, 45), Fe(II) (82), and U(III) (60, 65) have been used. Nitrite has been determined by potentiostatic oxidation in a rotating Pt cell (48). These procedures are precise, but some are time consuming.

Other techniques have been reported for the determination of NO_3^- and NO_2^-. These include fluorometry (64, 183), atomic absorption (104), fourier transform infrared spectrophotometry (242), X-ray diffraction (192), and thermometric methods (191).

The analysis of a mixture of NO_3^- and NO_2^- could be expedited if the mixture was separated chromatographically. A detector that is responsive to both NO_2^- and NO_3^- would allow the determination of the NO_2^- and NO_3^- concentrations with a single injection of the sample. This chromatographic method would be faster, more convenient, and more easily automated than the methods discussed above.

The use of gel-permeation chromatography to separate NO_3^- from NO_2^- has been reported, but the chromatographic behavior of ions is strongly dependent upon the sample matrix in gel-permeation chromatography (200). A few ion-exchange separations of NO_3^- and NO_2^- have been reported. The strongly basic Wofatit SBW anion-exchange resin was used with an

eluent of 1 N NaCl and 0.1 N NaOH, or 1 N Na_2SO_4 and 0.1 N NaOH (88). Another reported separation scheme used Dowex-2 resin and 1.25 M NaCl eluent (81). This separation required 25 minutes for elution. A high-resolution separation was achieved with a column of Zipax, coated with a strongly basic anion-exchange resin (203). The eluent was H_2O at a pressure of 1200 psi. The elution required 3 minutes. These separations were monitored either spectrophotometrically (88, 200, 203) or with an ion-exchange membrane that swelled or contracted as ions were eluted onto it (81). This membrane detector had working ranges of 0.010 - 0.075 M $NaNO_3$ and 0.010 - 0.040 M $NaNO_2$. The working ranges of the spectrophotometric detectors were not reported.

The sensitivity of electrochemical methods make their application as chromatographic detectors attractive. However, the polarographic procedures discussed above cannot be directly applied to the chromatographic detector. The normal DME is not suitable for the analysis of flowing streams because the drop-time is irregular due to turbulence near the drop. Therefore, the currents measured are erratic (113b). Vibrating and spinning DME's have been adapted to the analysis of flowing streams, but they are cumbersome and complicated (168).

Tubular electrodes are simple and easily adapted to chromatographic analysis (27-29, 144, 207-209). Tubular

graphite electrodes have been used to monitor $Fe(CN)_6^{-3}$, $Fe(CN)_6^{-4}$, Ag^+, Fe^{+3}, Fe^{+2}, MnO_4^-, Mn^{+2}, Tl^{+3}, and Tl^{+1} (207-209). In a tubular Pt electrode, $Fe(CN)_6^{-3}$ has been detected at concentrations as low as 0.01 μM (27).

In addition to the tubular electrodes, other amperometric detectors, having very large surface area to interstitial volume ratios, have been reported. These electrodes are called coulometric detectors if they electrolyze every equivalent of electroactive species entering them. They are very sensitive, and their response is not a function of the flow rate of the eluent (113b, 123, 212, 218, 240). Coulometric detectors have been used to monitor I^-, Fe^{+3}, Cu^{+2} (113b, 241), various species of U and Pu (124), alkaline earths, various transition metals, halides, carboxylic acids, amino acids, phenols, and monosaccharides (218).

Although the catalytic enhancement of the U(VI) wave at amalgamated Ag and amalgamated Au cathodes has been reported (213) and could be adapted to a chromatographic detector, it would be subject to the same chemical interferences as the polarographic method. Direct reduction of NO_3^- and NO_2^- at an electrode would be simpler and more impervious to interferences. The reduction of NO_3^- at a rotating Cd-disk electrode (RCDE) was observed by several workers, but it was not evaluated for analytical applications by them (86, 122, 224, 225). Recently, Davenport and

Johnson evaluated the reduction of both NO_3^- and NO_2^- at a RCDE and suggested the possibility of developing a Cd tubular chromatographic detector (53). This thesis reports that development.

III. INSTRUMENTATION

A. Electronic Circuitry

1. Four-electrode potentiostat

The electronic instrument used was that for the simultaneous and independent potentiostatic control of two electrodes, described earlier (171). The portion of the circuit for potentiostatic control of electrode I-1 in Figure 1 of Reference 171 was modified according to the design described in Reference 35. The modification permitted the control of the potential or current in electrode I-1 with simultaneous potentiostatic control of electrode I-2. The circuit was constructed in our laboratory, but an equivalent instrument is available commercially from Pine Instrument Co. of Grove City, Pennsylvania. Instead of a recorder with a potentiometric input for recording the current in electrode I-2 (171), a difference amplifier was used to monitor the difference in the voltages at the outputs of amplifiers A-2 and F-2.

Voltages were measured with a digital voltmeter, Model 345, from Data Technology, Inc. of Palo Alto, California. Current-potential curves were recorded on a X-Y recorder, Model 815, from Bolt, Beranek, and Newman, Inc. of Santa Ana, California. Instruments used for determining values of current, voltage, and resistance were calibrated with standards from the Physics Instrument Services of Iowa State

University.

All potentials are reported as volts (V) vs. the saturated calomel electrode (SCE).

2. Three-electrode potentiostat

The three-electrode potentiostat used for all chromatographic experiments was an Electroscan 30 from Beckman Instruments, Inc. of Fullerton, California. An internal potentiometer was used to apply a potential to the working electrode. The Initial Voltage Control on the Electroscan was calibrated with the digital voltmeter described above.

Chromatograms were recorded on the strip chart recorder in the Electroscan. Both the chart speed and the current span were calibrated. A 1.30-KΩ precision resistor mounted in a dummy cell was used to calibrate the current span.

B. Rotating Cadmium-Disk Electrode

The rotating Cd-disk electrode (RCDE) was constructed by Pine Instrument Co. from reagent grade Cd (99.9%) from Mallinckrodt Chemical Works. The reagent grade Cd sticks were melted in a crucible over a bunsen burner. The resulting metal slug was machined into the disk electrode and sheathed in a Teflon sleeve. The geometric area of the Cd disk was 0.456 cm^2.

The electrode surface was polished to a mirror finish with a 600 grit Buehler Handimet strip followed by 30 μm, 6 μm, and 1 μm Buehler AB Metadi Diamond on a nylon lapping

cloth. Before each experiment, the disk surface was polished with 0.3 μm Buehler AB Polishing Alumina on a Buehler Microcloth.

The electrode was rotated in a Model PIR synchronous rotator from Pine Instrument Co.

C. Rotating Glassy-Carbon Disk/Platinum-Ring Electrode

A rotating ring-disk electrode (RRDE) that had a glassy-carbon disk and a Pt ring was obtained from Pine Instrument Co. The face of the electrode was polished to a mirror finish using the procedure described for the RCDE.

The disk radius was 0.3787 cm, the inner radius of the ring was 0.3989 cm, and the outer radius of the ring was 0.4214 cm. The other geometric parameters of the electrode were $\alpha = 0.168$, $\beta = 0.211$, and $N = 0.170$. The significance of these parameters has been discussed by Albery and Hitchman (7b).

D. Voltammetric Cell

The cell used for all voltammetric studies was constructed in the Department of Chemistry Glass Shop at Iowa State University from a 400-ml Pyrex beaker. The Pt wire counter electrode was placed in a side arm of the cell and was separated from the test solution by a fritted-glass disk. The side arm was filled with the supporting electrolyte. The reference electrode was a Beckman SCE, placed in a side arm connected to a Luggin capillary by a ground glass stopcock.

The Luggin capillary was filled with the supporting electrolyte, and the SCE side arm was filled with a saturated solution of Na_2SO_4.

E. Tubular Chromatographic Detector

The Cd tubular electrode, shown in Figure III. 1, was constructed by melting reagent grade (99.9%) Cd rods from J. T. Baker Chemical Co. in a test tube. The resulting rod was turned to 1/2" o.d. and was cut 7/8" long. The interior dimensions of the tube were 1/16" i.d. x 1/2". The base of the electrode was tapped for a 1/4" - 28 thread, and the electrode was connected to the chromatograph with a flanged tube and tube-end fitting from Chromatronix, Inc. of Berkeley, California. A Cu wire, soldered to the base of the electrode, was used for electrical contact to the potentiostat.

The Cd electrode was pressed into a concentric, tubular Teflon holder, shown in Figure III. 1. The upper, circular faces of the electrode and holder were covered with paraffin so only the interior of the tube was in electrical contact with the solution.

The Teflon holder was machined to fit a 24/25 female, standard taper glass joint. The glass joint formed the walls of the detector cell and contained the Pt wire counter electrode, the Beckman SCE, and several milliliters of effluent. Excess effluent was removed from the cell by

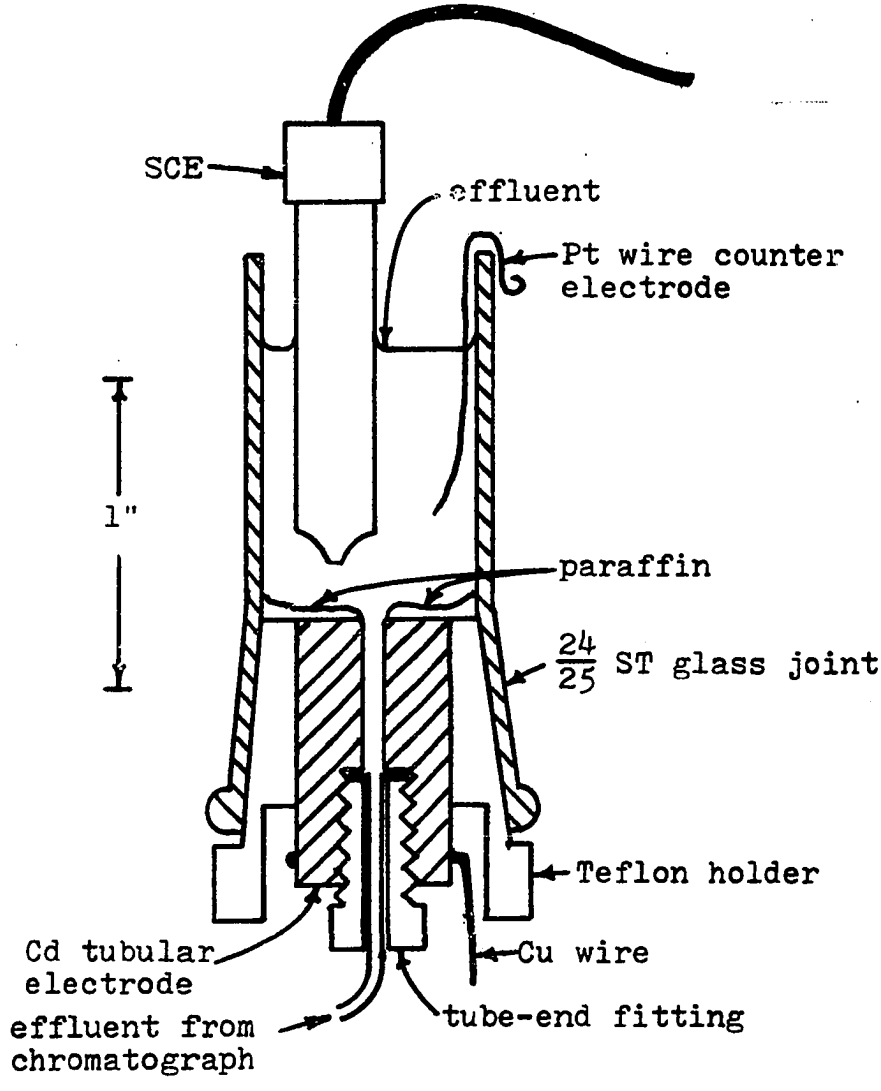

Figure III. 1. Cd tubular electrode and detector cell

suction.

F. Coulometric Chromatographic Detector

The coulometric electrode, shown in Figure III. 2, was also constructed from melted Cd rods from J. T. Baker Chemical Co. The outer diameter of the electrode was 1/2", and the interior of the electrode was a hole 3/16" i.d. and 1" long. From the 3/16" i.d. hole, a 60^{o} taper led to a 1/16" i.d. lip which was 1/16" thick. The base of the electrode was tapped for a 3/8" - 24 thread. The male half of a Glass-to-Cheminert Union from Chromatronix, Inc. was screwed into the base, and a flanged tube and tube-end fitting was inserted in the male union to connect the electrode to the chromatograph.

The interior of the electrode was filled to capacity with two hundred thirty 0.010" diam. x 1" Cd (99.999%) wires from Research Organic/Inorganic Chemical Corp. of Sun Valley, California. The tapered section of the tube was filled with a wad of a 5" length of the Cd wire (see Figure III. 2).

This electrode fit in the aforementioned Teflon holder, and the same detector cell was used as described previously. A Cu wire was soldered to the end of the electrode, and paraffin covered the upper surface of the Cd tube.

G. Liquid Chromatograph

The forced-flow liquid chromatograph used is shown schematically in Figure III. 3. The design and construction

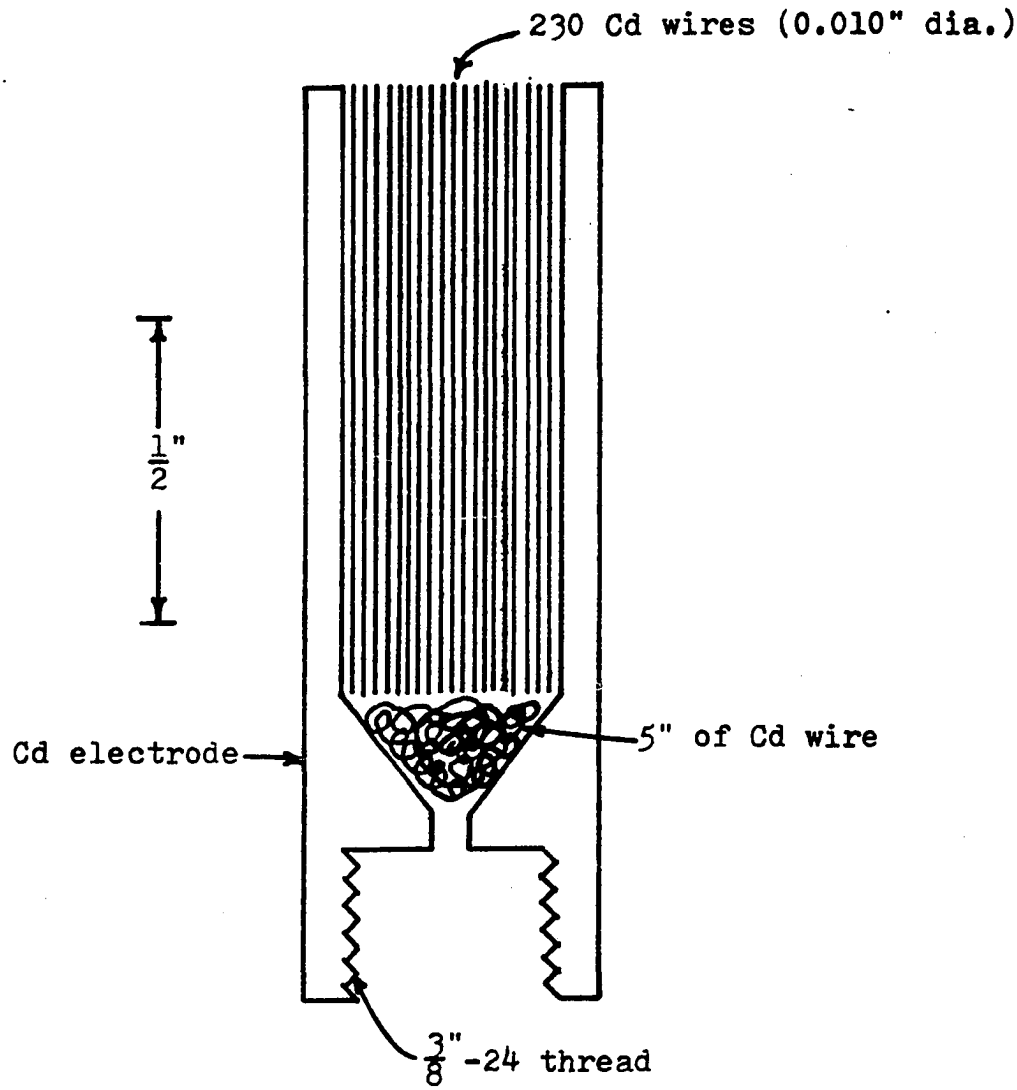

Figure III. 2. Cd coulometric electrode

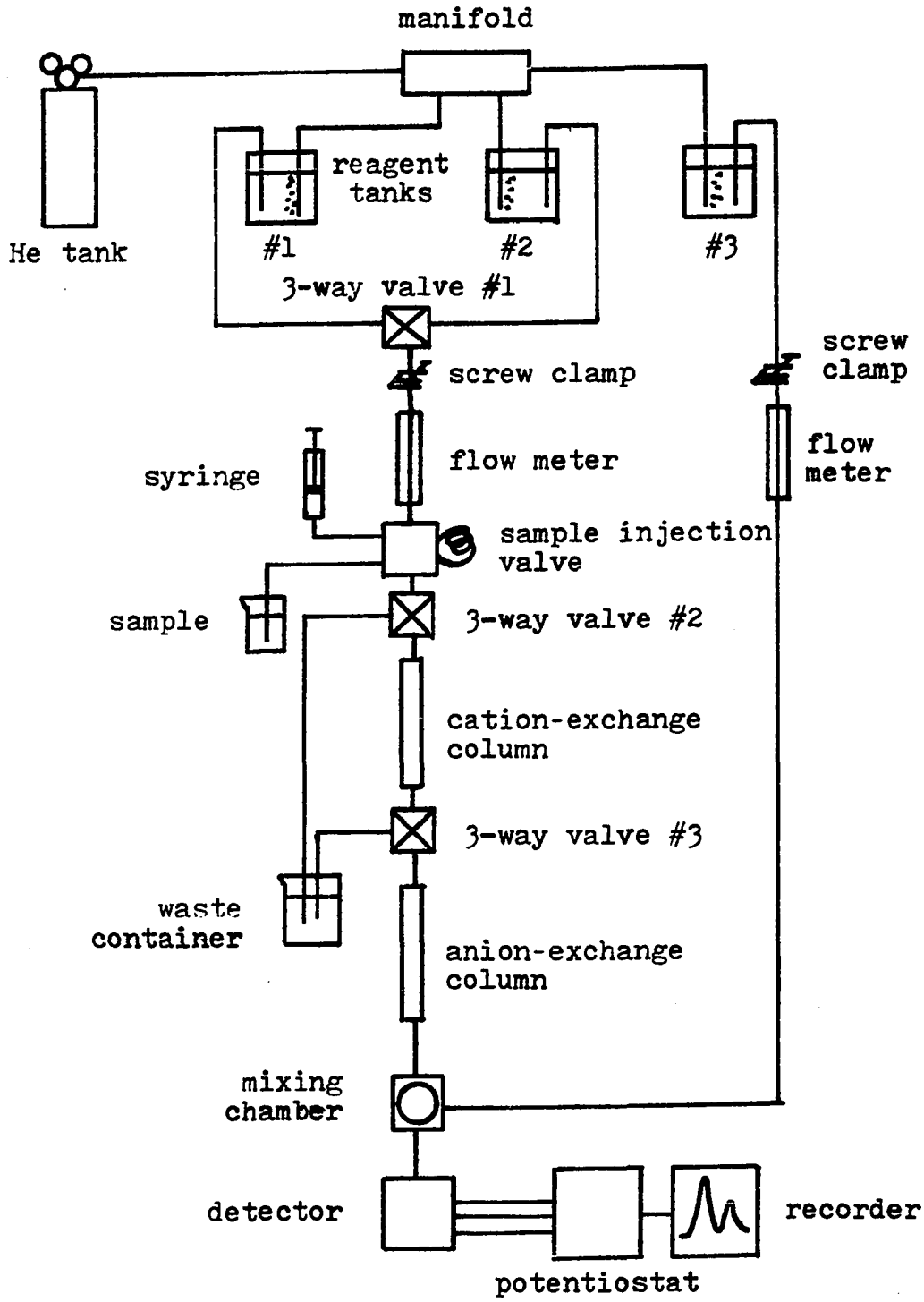

Figure III. 3. Forced-flow liquid chromatograph

of the chromatograph was based on that reported by Seymour, Sickafoose, and Fritz (206). The components shown in Figure III. 3 were connected using Teflon tubing (0.063" o.d. x 0.031" i.d.) and tube-end fittings from Chromatronix, Inc.

A He tank and two-stage regulator were used to apply pressure (at about 25 psi) through a manifold to each of three reagent tanks. The manifold was made locally from Kel-F, but equivalent pieces are commercially available from Chromatronix, Inc. The reagent tanks were glass reagent grade acid bottles and held 2 l of solution. The bottle caps on the tanks were constructed locally from nylon. The caps were tapped for tube-end fittings so that tubing could be attached from the manifold to the tanks, and from the tanks to the chromatograph. The plastic liners from the commercial acid bottle caps were inserted in the nylon caps to inhibit deterioration from acidic solutions splashed onto the caps during deaeration.

Reagent tanks #1, #2, and #3 held the 0.010 M $HClO_4$ eluent, 2 M HCl, and 0.20 M H_2SO_4 electrolyte, respectively.

Three 3-way valves from Chromatronix, Inc. were used to control the flow of eluent through the chromatograph. Valve #1 allowed solution from either tank #1 or #2 to flow into the chromatograph. Bubbles of He trapped in the eluent stream were shunted to a waste container through valve #2.

The sample injection valve was also from Chromatronix.

Two sample loops were used. One was calibrated by acid-base titritmetry and contained 0.665 ml. The other contained 0.33 ml and was calibrated by a length measurement.

Both the cation-exchange column and the anion-exchange column were borosillicate glass tubes (6 mm o.d. x 1 mm i.d. x 11 cm), and they were attached to the chromatograph through Chromatronix Glass-to-Cheminert Unions.

The cation-exchange column contained 80 - 100 mesh Dowex 50x8, a strongly acidic resin in the H^+ form. The purpose of this column was to remove from the eluent cations that would be deposited on the Cd electrode surface, thereby poisoning it. To regenerate the resin, 2 M HCl from reagent tank #2 was pumped through the cation-exchange column and into a waste container through valve #3.

The anion-exchange column contained 180 - 250 mesh Amberlite IRA-900, a strongly basic, macroreticular resin in the ClO_4^- form. This column was used for the analytical separation.

The effluent was mixed with the 0.20 M H_2SO_4 from reagent tank #3 in a 1:1 volumetric ratio in a Teflon mixing chamber from Pine Instrument Co. Gilmont flow meters, from Cole-Parmer Instrument Co. of Chicago, Illinois, were adapted to the chromatograph to measure the flow rate of the eluent and the 0.20 M H_2SO_4. The flow meters were calibrated by collecting volumes of H_2O for known periods of time. The

flow rates were adjusted with screw clamps on the Teflon tubing.

IV. THE REDUCTION OF NITRATE AND NITRITE AT A ROTATING CADMIUM-DISK ELECTRODE

A. Introduction

Some fundamental investigations of the reduction of NO_3^- and NO_2^- at Cd cathodes must be made before samples can be analyzed chromatographically with a Cd detector. The electrochemistry of Cd must be studied, at least as it pertains to the analytical applications of the electrode. The potentials at which NO_3^- and NO_2^- are reduced at Cd cathodes, and the experimental conditions that maximize the rate of the reductions must be found before the chromatographic detector can be operated with optimum sensitivity and linearity of response.

These investigations are more conveniently accomplished with a rotating disk electrode (RDE) than with a tubular electrode. Various media can be studied quickly by immersing the RDE in a cell filled with each solution. A tubular electrode requires a pumping apparatus and an electrolyte resevoir, which is often inconvenient to refill. The extent to which a reaction is limited by the rate of mass transport is easily determined with a RDE by increasing the rotational velocity of the electrode. The rates of mass transport obtainable with a RDE are many times greater than those conveniently achieved with a tubular electrode.

The advantage of a tubular electrode is that it is easily adapted to the analysis of chromatographic effluents.

The experimental conditions that maximize the rate of the reductions at the rotating Cd-disk electrode (RCDE) will maximize the sensitivity and linearity of response of the Cd tubular detector.

The equations concerning hydrodynamics and mass transport to a RDE were solved by Levich (144). The maximum current for a reversible electrochemical reaction is limited by the rate of convective-diffusional transport of the electroactive species to the electrode. The limiting current can be calculated from Equation IV. 1.

$$I_\ell = 0.62\ nFAD^{2/3}\nu^{-1/6}w^{1/2}C^b \qquad \text{(IV. 1.)}$$

In Equation IV. 1,

I_ℓ = limiting current (ma)

n = equivalents per mole of electroactive species

F = Faraday's constant (C/equivalent)

A = geometric area of disk electrode (cm^2)

D = diffusion coefficient of electroactive species (cm^2/sec)

ν = kinematic viscosity of the solution (cm^2/sec)

w = rotational velocity of electrode (rad/sec)

C^b = bulk concentration of electroactive species (moles/l)

The limiting current is a linear function of $w^{\frac{1}{2}}$ and C^b for reversible reactions; however, I_ℓ is independent of $w^{\frac{1}{2}}$ and C^b if the reaction rate is entirely limited by the kinetics of the electrochemical reaction. Many moderately

reversible reactions are partially limited by kinetics at high rates of mass transport, and plots of I_ℓ *vs.* $w^{\frac{1}{2}}$ or I_ℓ *vs.* C^b are not linear at large values of $w^{\frac{1}{2}}$ or C^b. The experimental conditions that produce the largest values of I_ℓ and the most linear plots of I_ℓ *vs.* $w^{\frac{1}{2}}$ or I_ℓ *vs.* C^b, are the optimum conditions for application of that reaction for quantitative analysis.

B. Experimental

1. Chemicals and reagents

All chemicals used were reagent grade quality from J. T. Baker, Inc. All H_2O used was triply distilled with a deionization between the first and second distillation. The second distillation was from an alkaline solution of $KMnO_4$. Prepurified N_2 (99.999%) from Air Products was used for deaeration.

Stock solutions of $NaNO_3$ and $NaNO_2$ were prepared by dissolving sufficient quantities of the salts (dried 4 hours at 90°C) in H_2O to make 100 ml of 0.1 M solutions.

The supporting electrolyte was prepared by diluting quantities of Baker reagent grade acids with H_2O.

2. Experimental procedures

The voltammetric cell was filled with 400 ml of supporting electrolyte. To prevent air from being drawn into the cell by the rotation of the electrode, the cell was covered with a flat Teflon lid. The lid had a hole in the

center that was slightly larger in diameter than the electrode.

Nitrogen used for deaeration of the electrolyte was saturated with H_2O vapor by bubbling it through H_2O in a gas washing bottle. Deaeration was accomplished by dispersing the N_2 through the electrolyte while the electrode was rotated at 41.9 rad/sec. After deaeration, N_2 was blown over the surface of the solution to exclude O_2 from the cell.

The RCDE was potentiostated between -0.85 and -1.20 V whenever it was in the electrolyte to prevent oxidation of the electrode surface.

Aliquots of stock solutions added to the electrolyte were mixed by momentarily rotating the RCDE at 167 or 261 rad/sec.

Current-potential (I-E) curves were obtained and are shown only for the cathodic scan unless otherwise noted.

C. Results and Discussion

1. Usable potential range of the RCDE

The potential region that can be investigated with a RCDE is narrow compared to that of most electrodes used in electroanalysis. In a deaerated solution of 0.10 M H_2SO_4 - 5.0 mM $HClO_4$ (the electrolyte used in the chromatographic detector), Cd is oxidized at potentials more positive than -0.8 V (Figure IV. 1). The product of the oxidation is Cd^{+2} (114), and the dissolution of the electrode produces a large

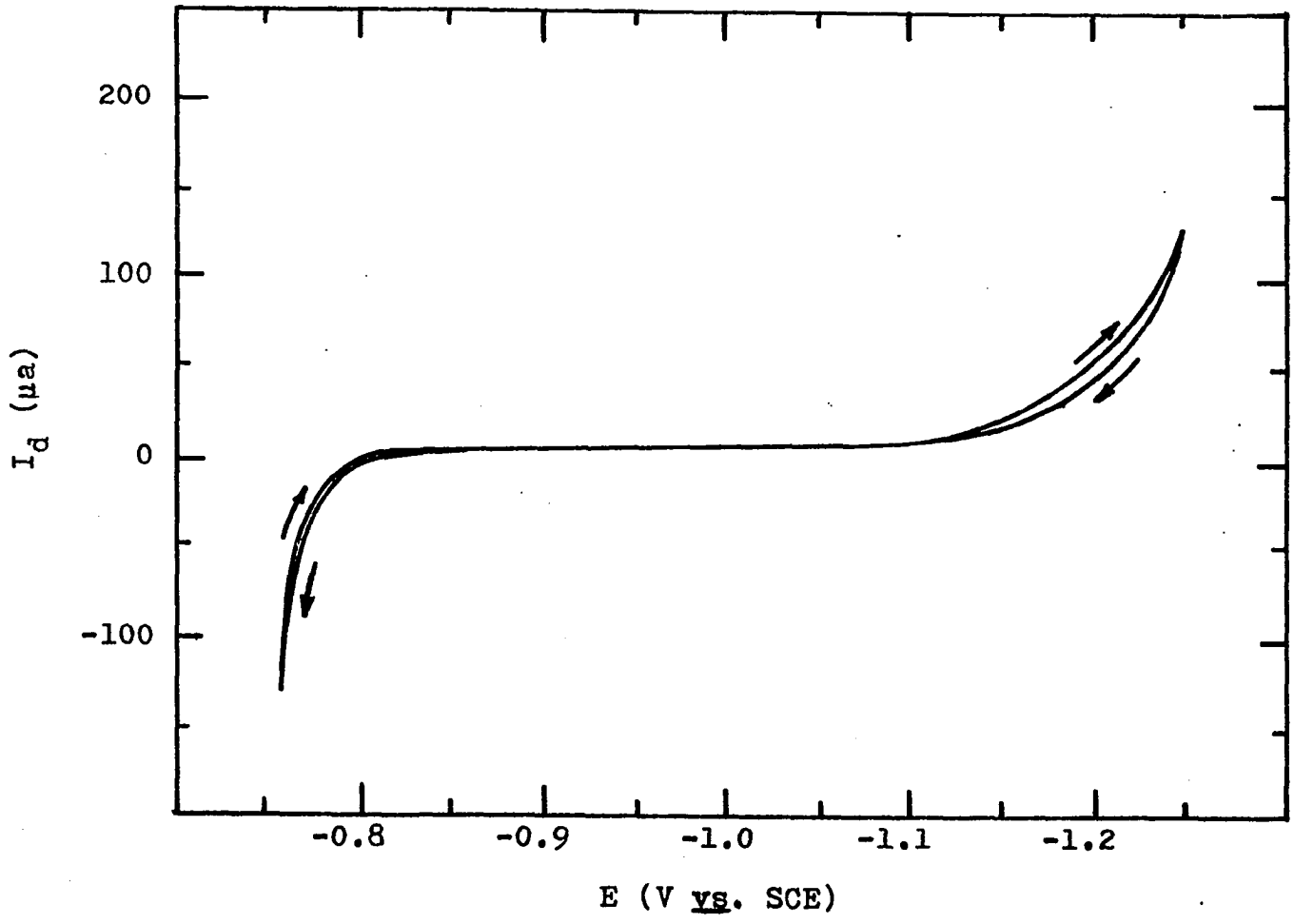

Figure IV. 1. Current-potential curve of RCDE 0.10 M H_2SO_4 - 5.0 mM $HClO_4$ electrolyte. Scan rate 1.0 V/min. Rotational velocity 41.9 rad/sec.

anodic current. The reduction of H^+ from the electrolyte at the RCDE produces a large cathodic current, which limits the negative end of the voltage scan to about -1.2 V. The measurement of current for an electroactive species can only be done at potentials where the Cd is not being oxidized and the reduction current from H_2 evolution is not excessive. Therefore, the analytically useful range of potentials at the RCDE in this medium spans only 0.4 V.

2. Voltammetry of nitrate and nitrite at the RCDE

Both NO_3^- and NO_2^- are reduced at the RCDE within the aforementioned potential limits. The I-E curves of 0.987 mM $NaNO_3$ and of 0.993 mM $NaNO_2$ in 0.10 M H_2SO_4 - 5.0 mM $HClO_4$ are reproduced in Figure IV. 2. Neither voltammetric wave is affected significantly by changes in the scan rate of the electrode potential. The waves typically exhibit some noise, especially at high rotational velocities or large concentrations of NO_3^- and NO_2^-.

The NO_3^- wave is considerably larger than the NO_2^- wave, but the waves have similar shapes. Neither wave exhibits a limiting-current plateau. Therefore, the current measured at the disk, I_d, is dependent upon the potential at which it is measured. This dependence of I_d on electrode potential is indicative of slow heterogeneous kinetics in the reduction process, and it will be discussed in greater detail below.

Although a true limiting current cannot be measured, I_d

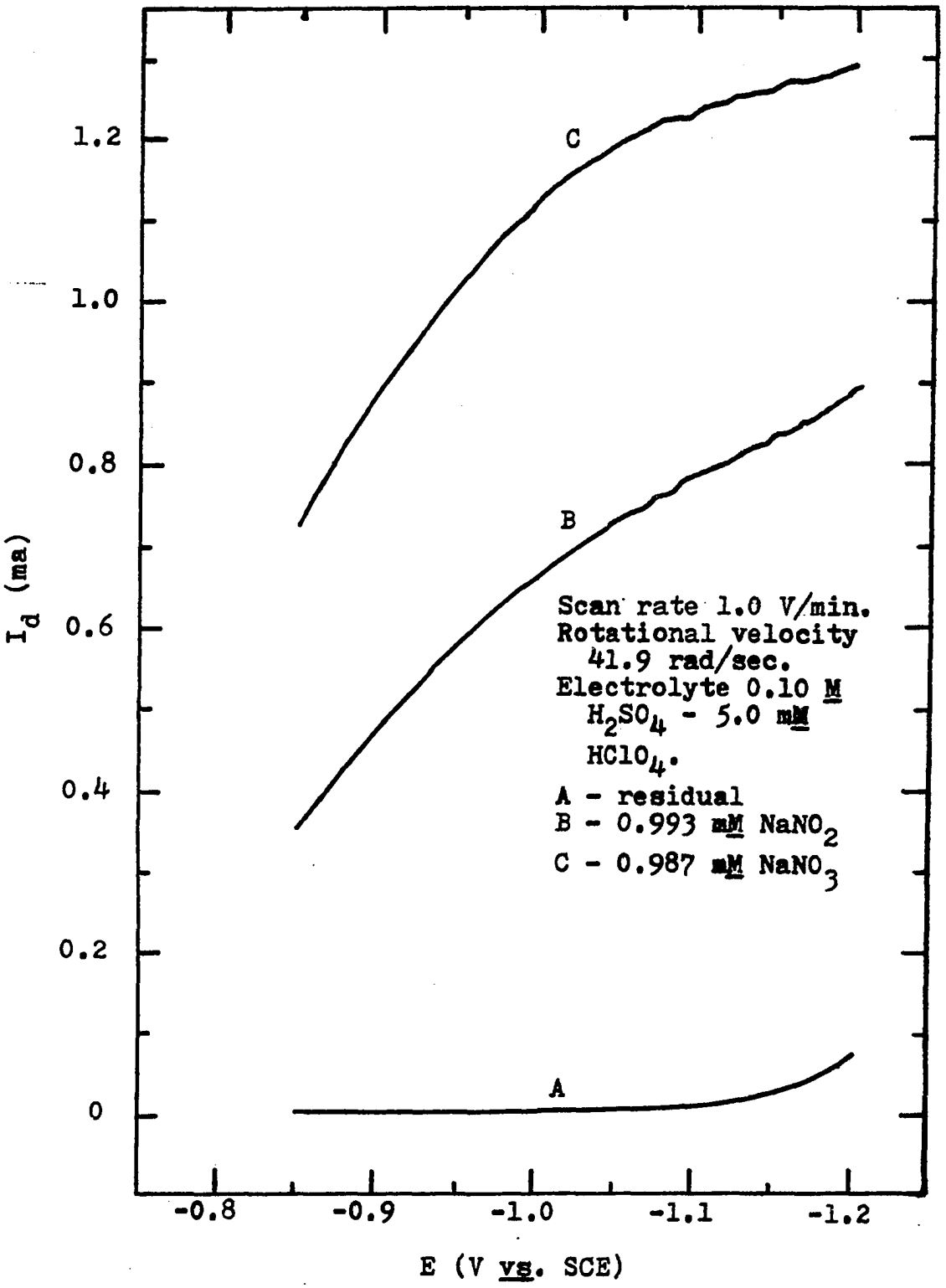

Figure IV. 2. Current-potential curves of NO_2^- and NO_3^- at RCDE

at a given electrode potential can be measured and related to $w^{\frac{1}{2}}$ and C^b. The disk current, measured at -1.0 V, is a linear function of NO_3^- and NO_2^- concentrations (Figure IV. 3). The plot of I_d vs. NO_3^- concentration is linear to 1.1 mM; whereas the NO_2^- curve deviates from linearity above 0.9 mM. Both plots are curved at higher concentrations. The positive intercepts exhibited by both curves in Figure IV. 3 are due to a small, non-faradaic charging current resulting from the potential scan of the RCDE.

3. Electrolyte study

The disk current from the reduction of both NO_3^- and NO_2^- is not a linear function of $w^{\frac{1}{2}}$. The current is partially limited by mass transport and partially by the kinetics of the reduction process. The degree to which I_d is limited by kinetics is affected by the choice of acid used as the supporting electrolyte. It can be seen from the curvatures and slopes of the plots of I_d vs. $w^{\frac{1}{2}}$ in Figures IV. 4 and IV. 5, that the reductions of NO_3^- and NO_2^- occur with slightly faster kinetics in 0.10 M $HClO_4$ than in 0.10 M H_2SO_4. The reductions are considerably less reversible in 0.10 M HCl than in 0.10 M $HClO_4$, and are entirely limited by kinetics at large values of $w^{\frac{1}{2}}$ in 0.10 M H_3PO_4. Excessive evolution of H_2 in 0.10 M H_3PO_4 necessitated measurement of I_d at -0.85 V. The measurement of I_d at a more positive potential than -1.0 V increased the

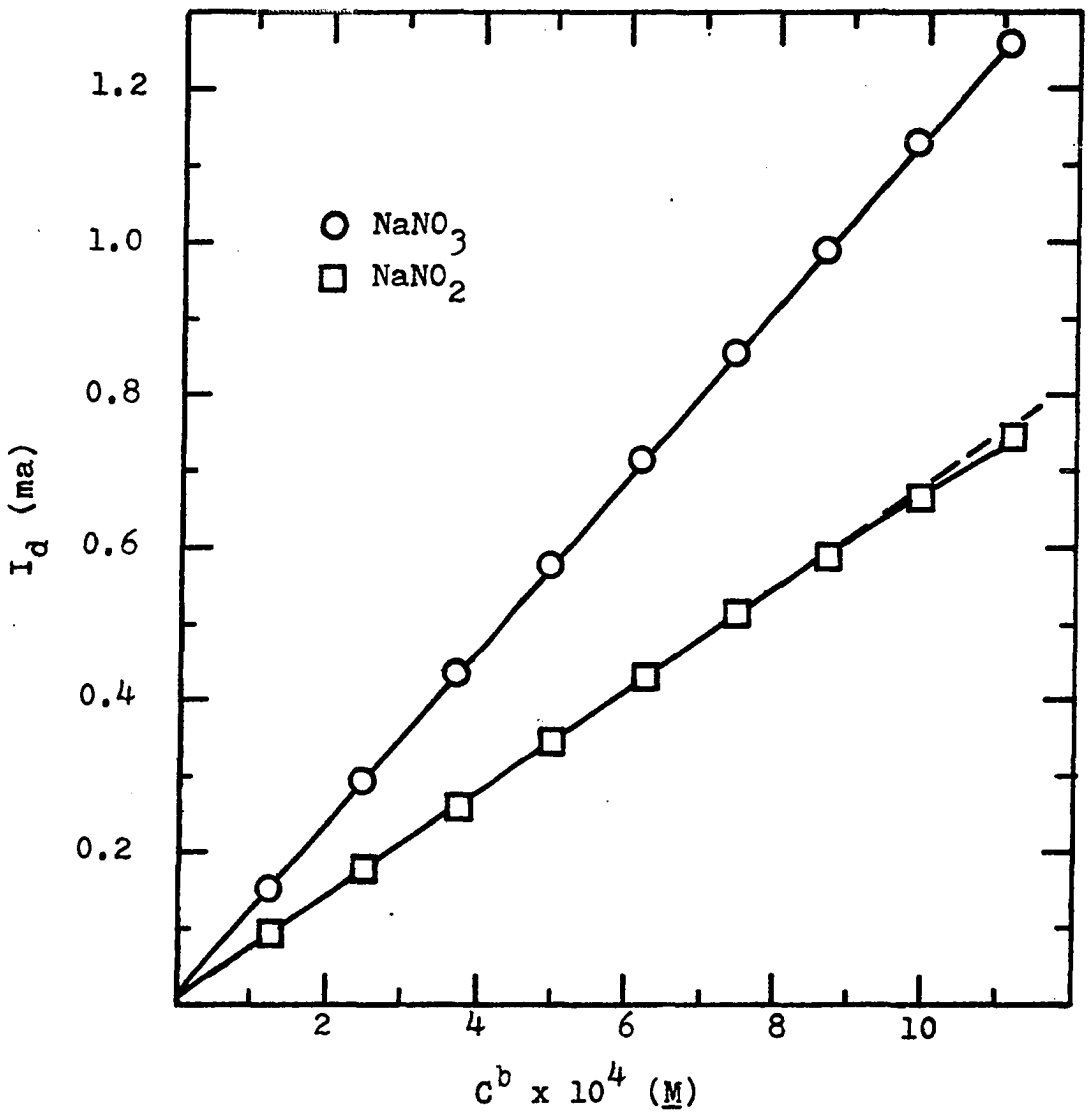

Figure IV. 3. Concentration study of NO_2^- and NO_3^- at RCDE Rotational velocity 41.9 rad/sec. Scan rate 1.0 V/min. Electrolyte 0.10 M H_2SO_4 - 5.0 mM $HClO_4$. I_d measured at -1.0 V.

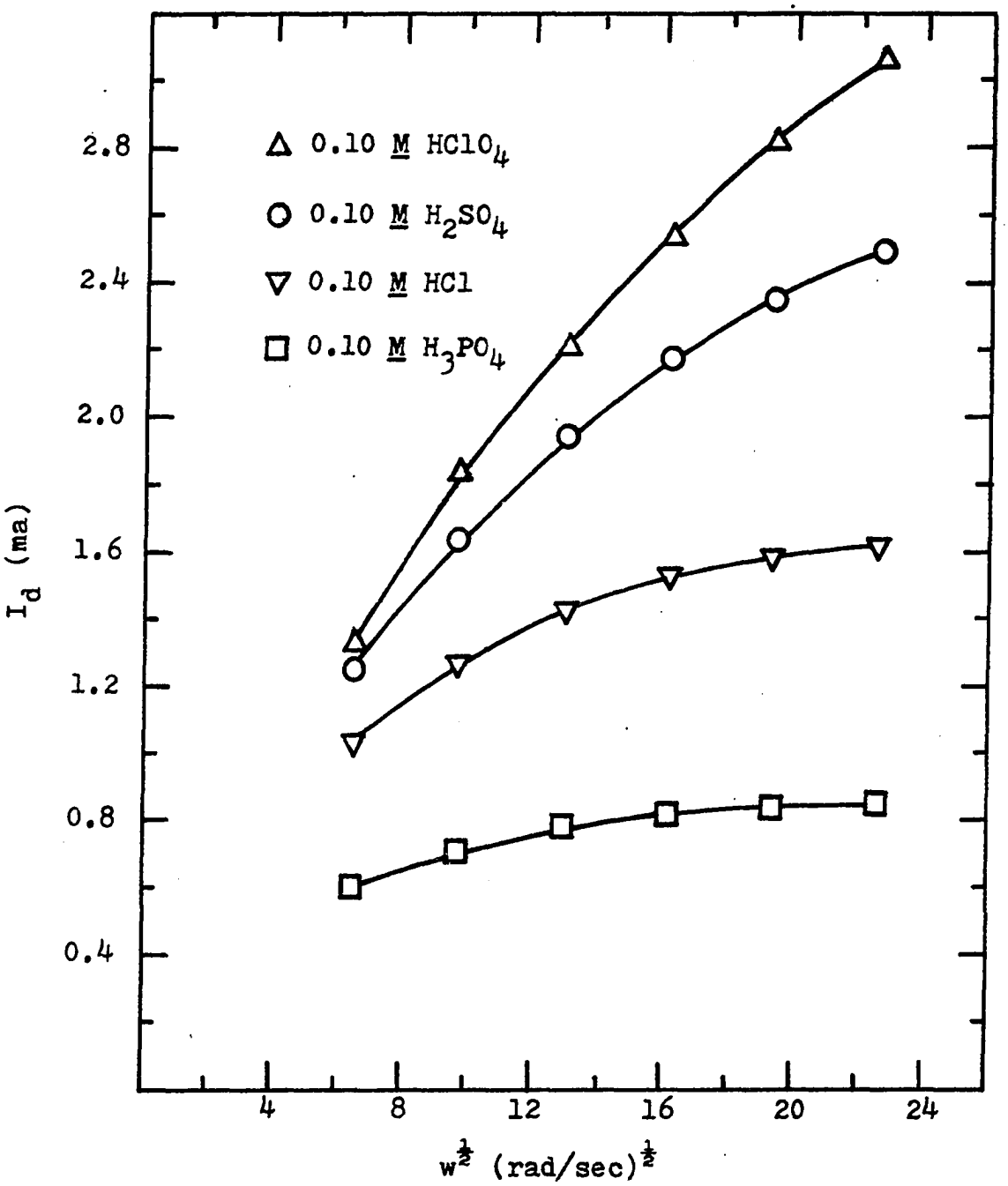

Figure IV. 4. Electrolyte study
RCDE. 0.987 m$\underline{M}$ $NaNO_3$. Scan rate 1.0 V/min. I_d measured at -1.0 V (I_d measured at -0.85 V for 0.10 $\underline{M}$ H_3PO_4 data).

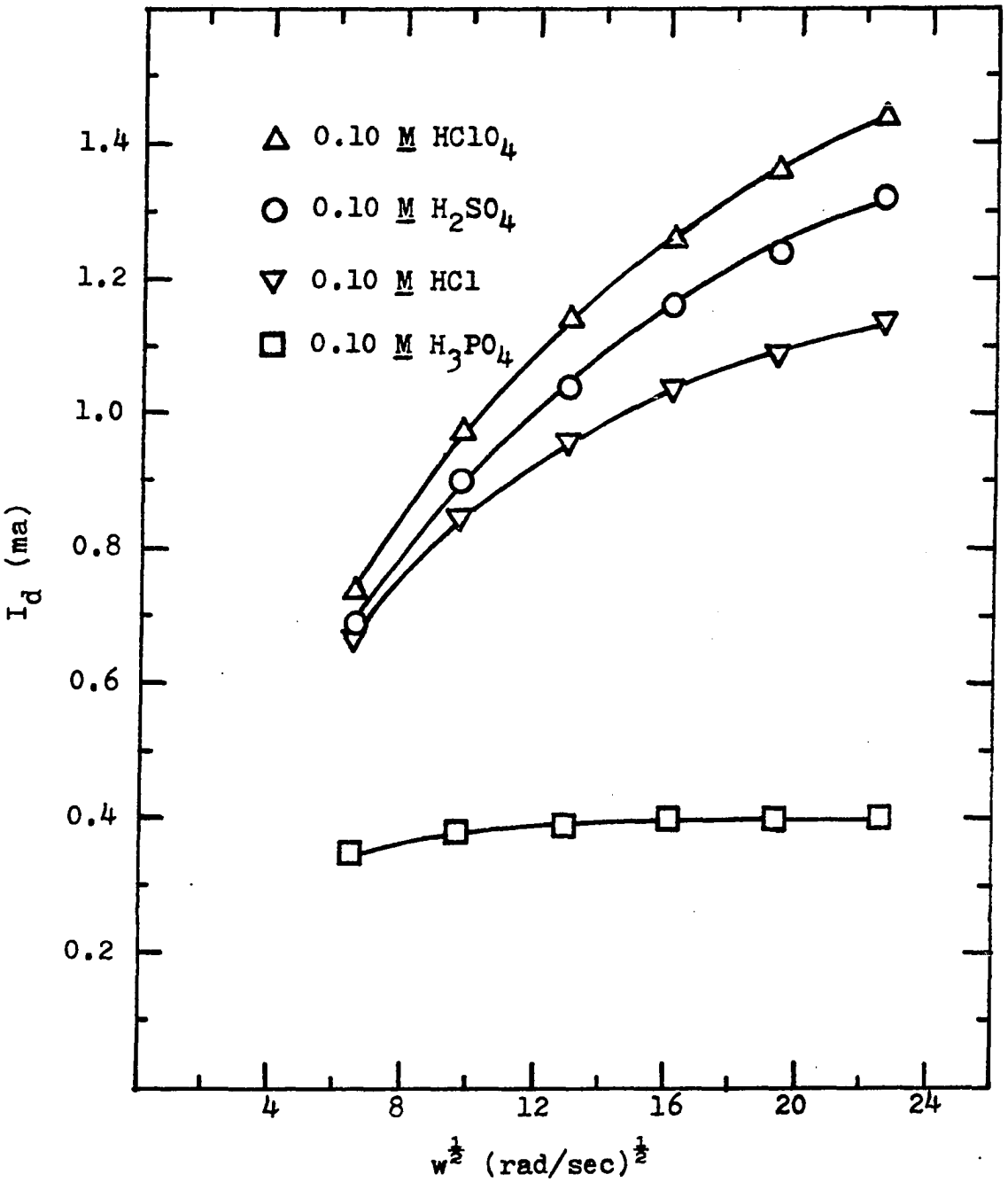

Figure IV. 5. Electrolyte study
RCDE. 0.993 m$\underline{M}$ $NaNO_2$. Scan rate 1.0 V/min. I_d measured at -1.0 V (I_d measured at -0.85 V for 0.10 $\underline{M}$ H_3PO_4 data).

curvature of the plots of I_d *vs.* $w^{\frac{1}{2}}$, as will be shown later in this chapter.

The acidity of the electrolyte also affects the kinetics of the reductions. As shown by the greater slope and linearity of the plot of I_d *vs.* $w^{\frac{1}{2}}$ in Figure IV. 6, the reduction of NO_3^- is kinetically faster in 0.10 *M* H_2SO_4 than in 0.010 *M* H_2SO_4. The use of a more acidic electrolyte might increase the rate of the reductions still more, but in solutions of H_2SO_4 more concentrated than 0.10 *M*, the reduction current for the evolution of H_2 interferes with the measurement of the reduction current from NO_2^- and NO_3^-. Therefore, 0.10 *M* acid was concluded to be an optimum concentration.

The reagent grade $HClO_4$ available locally was analyzed with anodic stripping voltammetry and was found to contain approximately 10^{-8} *M* Cu(II) (8a). Reagent grade H_2SO_4 contained much less Cu(II). Therefore, 0.10 *M* H_2SO_4 was used as the supporting electrolyte for all succeeding experiments to avoid the deposition of Cu on the RCDE.

4. *Effects of various anions and cations*

Most of the reported ion-exchange separations of NO_3^- and NO_2^- use an eluent containing Cl^- (81, 88). From the data in Figures IV. 4 and IV. 5, it is concluded that Cl^- inhibits the reduction of NO_3^- and NO_2^-. An investigation was made to see if this inhibition was characteristic of

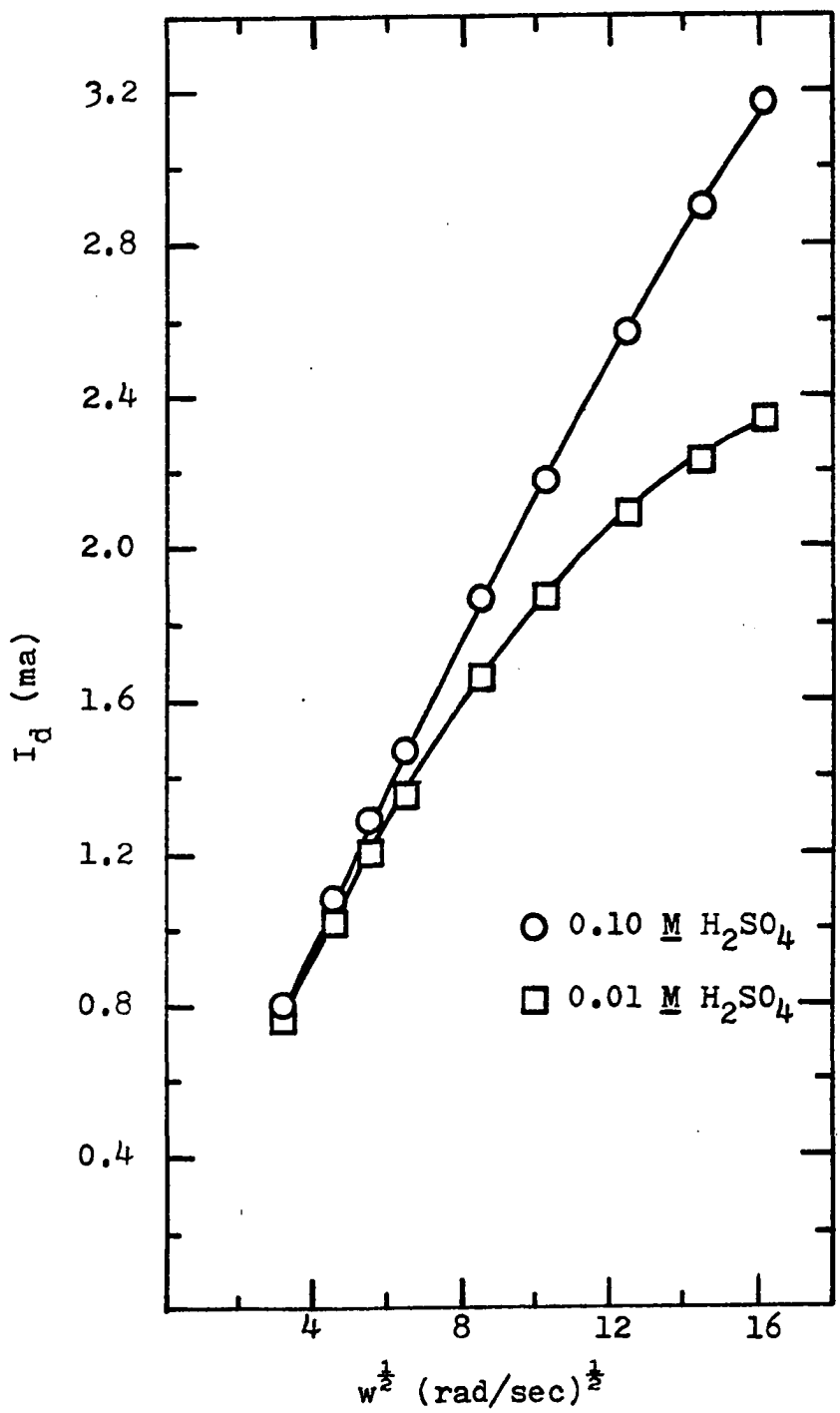

Figure IV. 6. Study of electrolyte acidity RCDE. 0.988 mM $NaNO_3$. Scan rate 1.0 V/min. I_d measured at -1.15 V.

other halides that might be substituted for Cl^- in a chromatographic eluent. Voltammetric waves of 0.989 m$\underline{M}$ $NaNO_3$ were obtained with supporting electrolytes consisting of 0.10 $\underline{M}$ H_2SO_4 and 0.02 $\underline{M}$ NaI, 0.02 $\underline{M}$ NaBr, or 0.02 $\underline{M}$ NaCl. Voltammetric waves were also obtained in 0.10 $\underline{M}$ H_2SO_4 - 0.02 $\underline{M}$ $NaHSO_4$ for comparison. The $NaHSO_4$ maintained the ionic strength equal to that of the other solutions. A plot of I_d $\underline{vs.}$ $w^{\frac{1}{2}}$ for each solution is shown in Figure IV. 7. Chloride and Br^- have an equal effect and inhibit the reduction slightly. In their presence, I_d is smaller and the curvature of the I_d $\underline{vs.}$ $w^{\frac{1}{2}}$ plot is greater than that obtained in the solution of 0.10 $\underline{M}$ H_2SO_4 - 0.02 $\underline{M}$ $NaHSO_4$.

Iodide has a much more pronounced effect. The disk current is entirely kinetically limited, except at the lowest rotational velocities. This may be because I^- is strongly adsorbed on Cd cathodes (182), and the adsorbed layer of I^- electrostatically repels the NO_3^-. On the other hand, the NO_3^- ions may have to compete with the I^- for the active sites on the electrode surface at which reduction occurs. Iodide may also react with reduction intermediates of NO_3^- and disrupt the reduction mechanism. Whatever the cause, the inhibition is severe, and the presence of I^- in the electrolyte must be avoided.

Another series of $w^{\frac{1}{2}}$ studies were made to investigate the effect that various cations in the electrolyte might

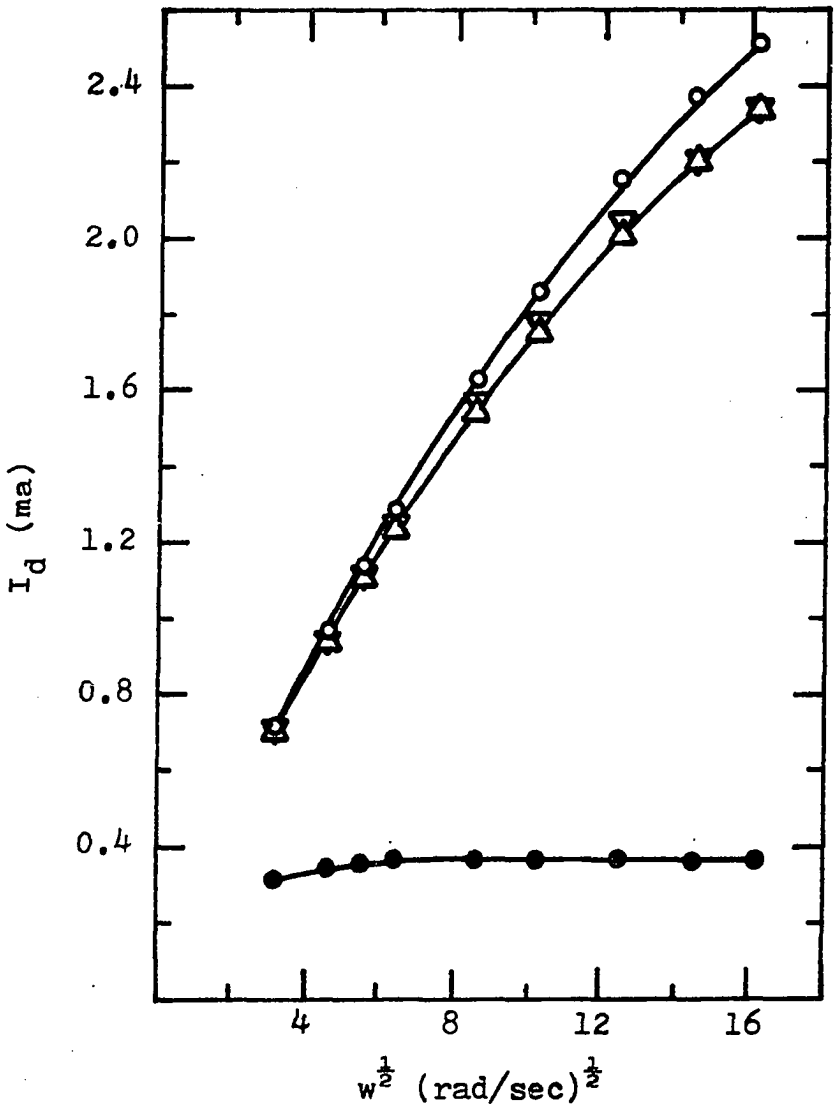

Figure IV. 7. Halide study
RCDE. 0.989 m$\underline{M}$ $NaNO_3$. Scan rate 1.0 V/min.
I_d measured at -1.15 V.
o 0.10 $\underline{M}$ H_2SO_4 - 0.02 $\underline{M}$ $NaHSO_4$
Δ 0.10 $\underline{M}$ H_2SO_4 - 0.02 $\underline{M}$ NaCl
▽ 0.10 $\underline{M}$ H_2SO_4 - 0.02 $\underline{M}$ NaBr
● 0.10 $\underline{M}$ H_2SO_4 - 0.02 $\underline{M}$ NaI

have on the reduction of NO_3^-. Voltammograms of 0.984 m<u>M</u> $NaNO_3$ in solutions of 0.10 <u>M</u> H_2SO_4 that contained 0.005 <u>M</u> K_2SO_4, 0.01 <u>M</u> $MgSO_4$, or 0.01 <u>M</u> $La(HSO_4)_3$ were obtained, and plots of I_d <u>vs</u>. $w^{\frac{1}{2}}$ were made (Figure IV. 8).

The values of I_d were smallest in the solution containing 0.01 <u>M</u> La^{+3}. Nitrate is known to be complexed by La^{+3} (128), so the smaller currents may be due to a decrease in the bulk concentration of free NO_3^- because of complexation with La^{+3}. The decrease in I_d is not as large in the case of La^{+3} as in the presence of I^-. Therefore, the presence of various cations in the electrolyte is expected to change the rate of the reductions relatively little.

5. <u>Treatment of the RCDE surface</u>

The RCDE used in these studies was constructed from polycrystalline Cd. The crystal planes on the electrode surface are not visually apparent when the RCDE is polished as described in Chapter III. If the RCDE is potentiostated at 0.0 V for 90 seconds, the Cd on the polished surface is oxidized to Cd^{+2}. The polycrystalline inner structure of the electrode is exposed and is apparent to visual inspection.

The reductions of NO_3^- and NO_2^- occur more reversibly at the oxidized surface than at the polished surface. Voltammetric waves of 0.993 m<u>M</u> $NaNO_2$ and 0.987 m<u>M</u> $NaNO_3$, obtained at both polished and oxidized electrode surfaces,

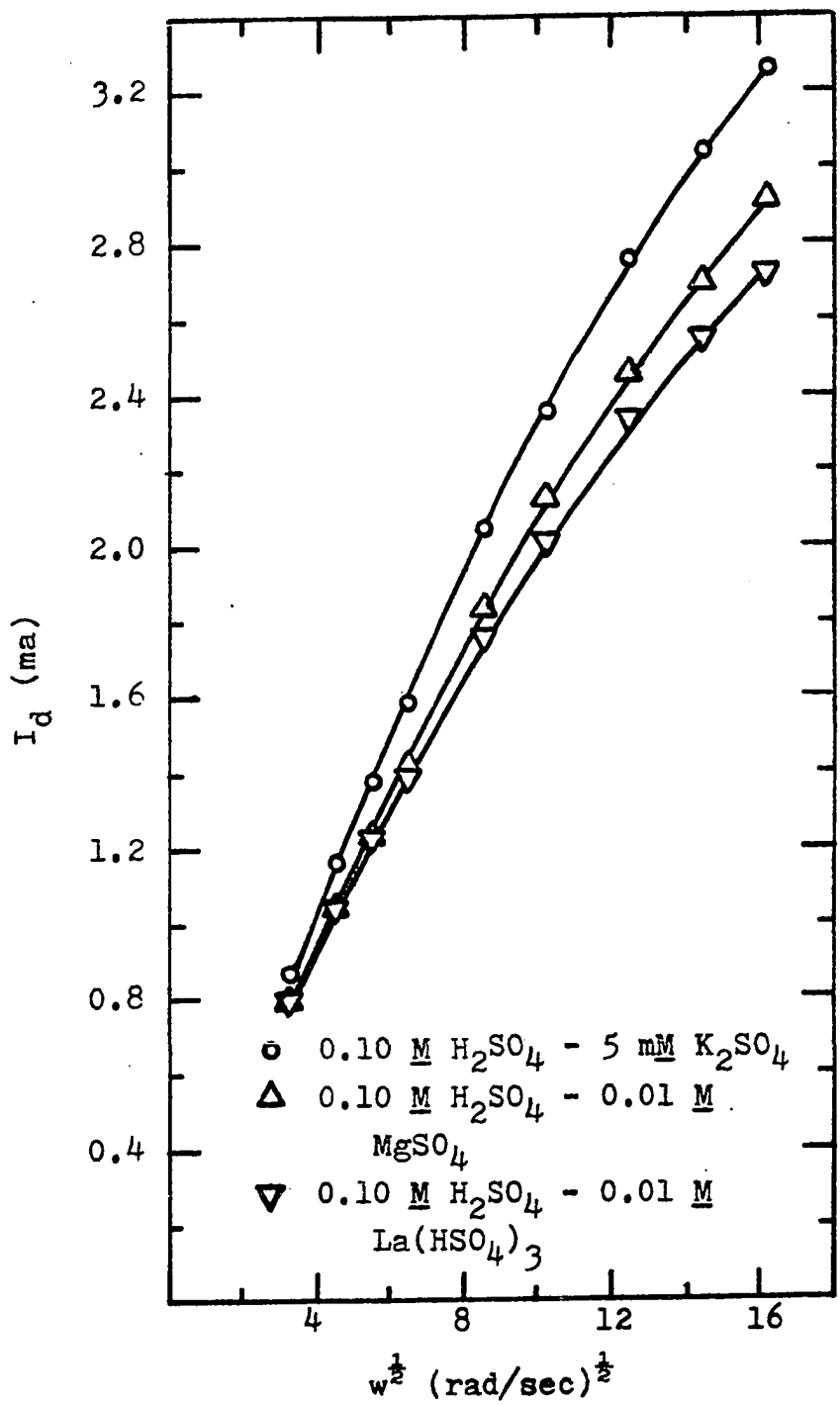

Figure IV. 8. Cation study
RCDE. 0.984 mM $NaNO_3$. Scan rate 1.0 V/min.
I_d measured at -1.15 V.

are reproduced in Figure IV. 9. The waves are larger and exhibit more of a limiting-current plateau when the oxidized RCDE surface is used, and the slope of a plot of I_d *vs.* $w^{\frac{1}{2}}$ is much greater (Figure IV. 10).

The increased current is apparently not due to increased electrode surface area from oxidation of the Cd. The values of I_d are smaller when the RCDE is sanded with 600 grit sandpaper than when the electrode is polished. It is concluded that oxidation of the surface exposes more active sites to the solution than are present on the polished surface. The active sites may be on particularly reactive crystal planes, which are exposed when the RCDE is oxidized. The RCDE was normally polished before it was used to achieve good day-to-day reproducibility, even though the rates of the reductions were decreased.

The chromatographic detectors were made of polycrystalline Cd and were never polished. Therefore, the reductions of NO_2^- and NO_3^- in the detectors are probably somewhat more reversible than expected if only the data obtained with the polished RCDE is considered.

6. Fundamental considerations

The increase in I_d following oxidation of the RCDE is not predicted by Equation IV. 1. The limiting current in Equation IV. 1 is related to the geometric area of the electrode, not the true surface area or an "activated"

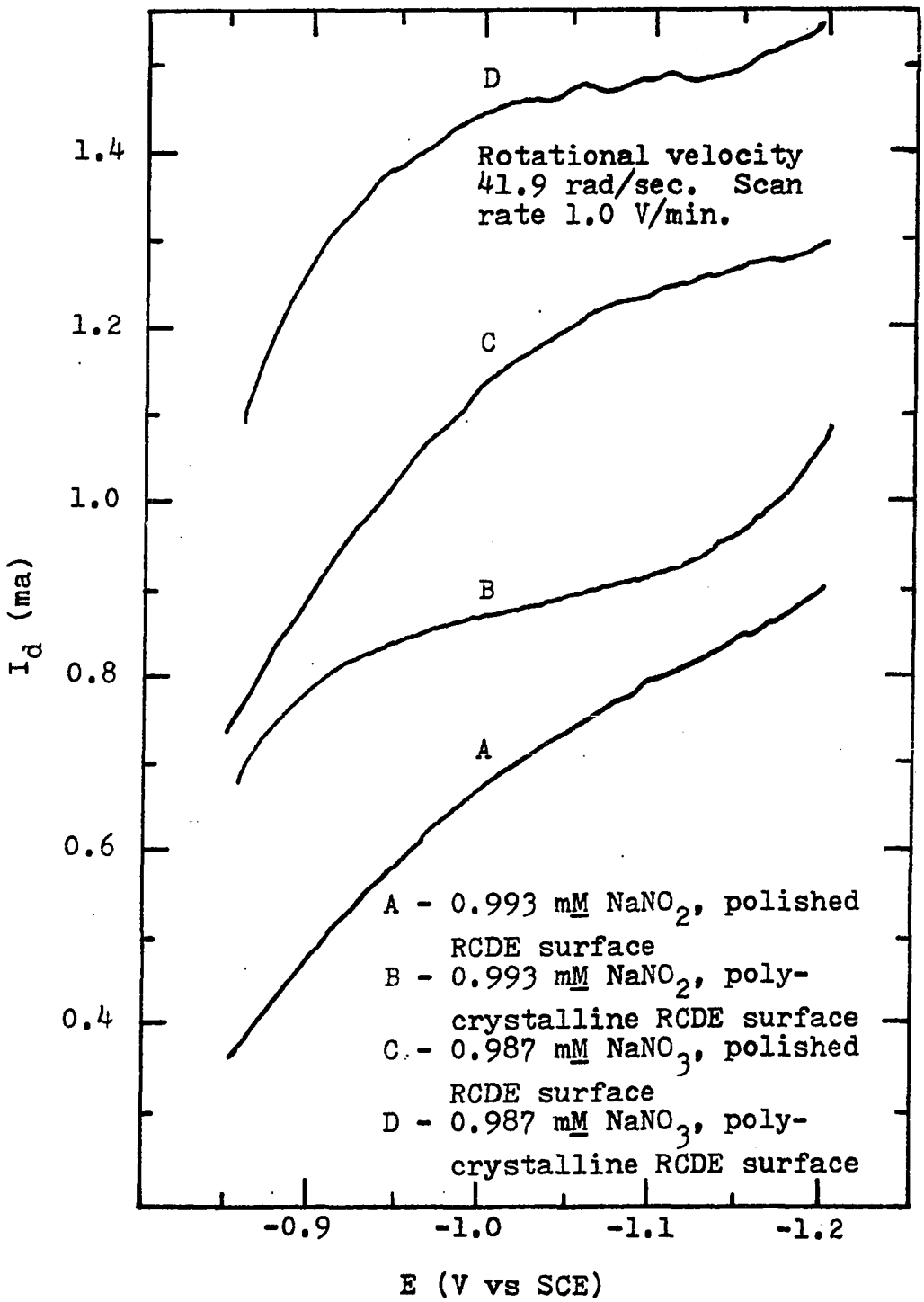

Figure IV. 9. Effect of oxidation of the RCDE on reductions of $NaNO_2$ and $NaNO_3$ in 0.10 M H_2SO_4 - 5.0 mM $HClO_4$

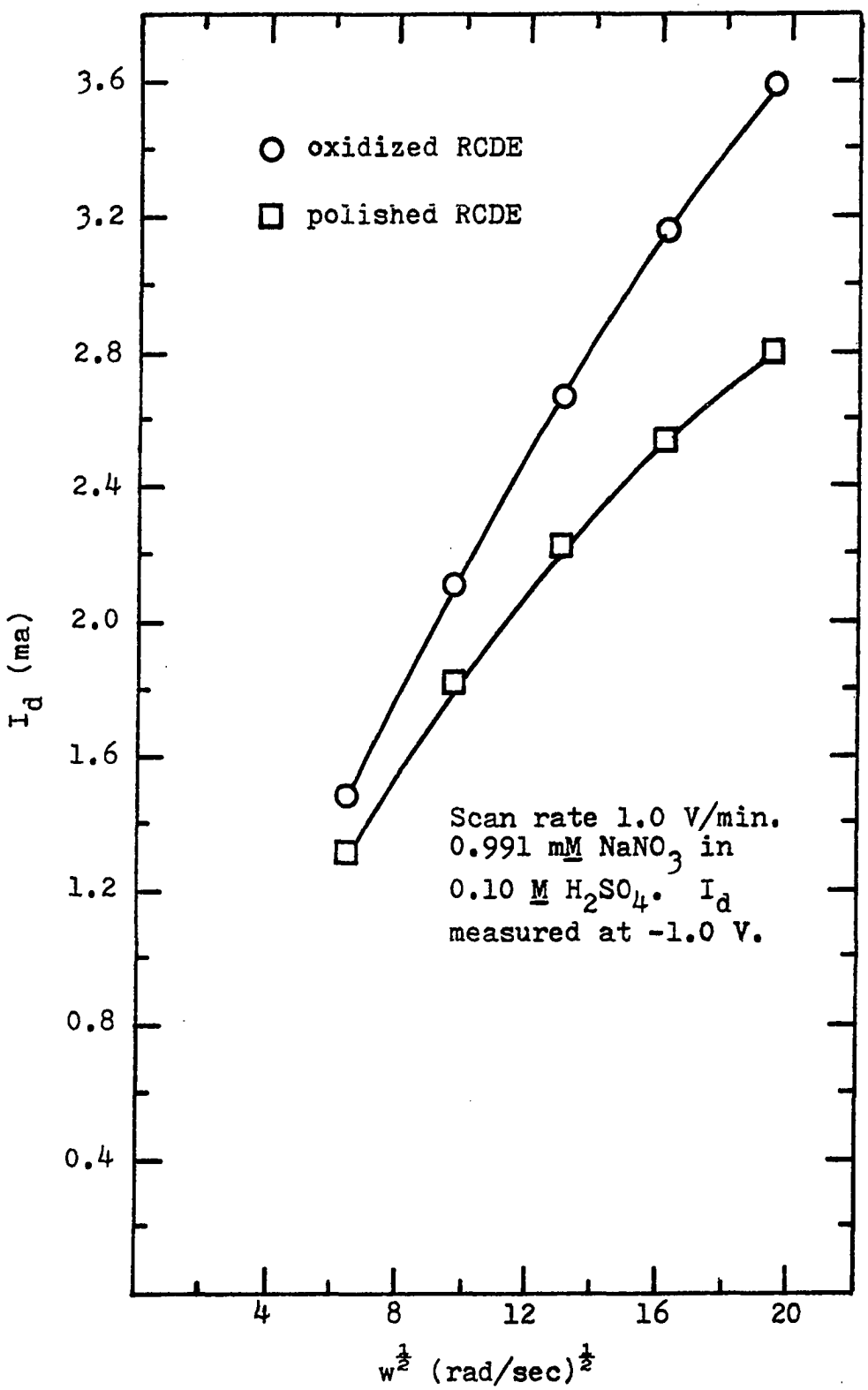

Figure IV. 10. Effect of oxidation of RCDE on $w^{\frac{1}{2}}$ study

surface area. The rate of the reduction of NO_3^- and NO_2^- at Cd does seem to be related to the number of active sites on the Cd surface. A quantity, A', will designate the area of the electrode containing active sites. The area, A', can be increased by oxidation of the surface, but the geometric area, A, is constant.

A consideration of the fundamental equations leading to Equation IV. 1 may elucidate the relationship between A' and A. The reduction of a species, O, which consumes h hydrogen ions and leads to the soluble product, P, can be represented by the equation below:

$$O + hH^+ + ne^- \rightarrow P \qquad \text{(IV. 2.)}$$

The heterogeneous rate constant, k, for such a reduction is given by Equation IV. 3 (4).

$$k = k_c \exp\{-\beta nFE/RT\} \qquad \text{(IV. 3.)}$$

In Equation IV. 3,

k_c = specific rate constant (cm/sec)

β = symmetry parameter

E = electrode potential (V)

R = gas constant (joule/^oK)

T = temperature (^oK)

The other parameters have their usual electrochemical significance.

The reverse of Equation IV. 2 is negligible in the case of NO_3^- and NO_2^- because of the large overpotentials of the

reductions. Equation IV. 4 relates the surface concentrations of the reactants to I_d.

$$I_d = nFA'kC_o^s(C_{H^+}^s)^h \qquad \text{(IV. 4.)}$$

In Equation IV. 4,

C_o^s = concentration of species, O, at the electrode surface

$C_{H^+}^s$ = concentration of H^+ at the electrode surface

The activated surface area is used in Equation IV. 4 because the rate of the reduction is dependent on the number of active sites on the electrode. All activity coefficients are assumed here to be unity.

The surface concentrations can be related to I_d by the Nernst diffusion-layer model (4):

$$I_d = (C_o^b - C_o^s)nFAD/\delta \qquad \text{(IV. 5.)}$$

where,

δ = diffusion-layer thickness

The disk current is proportional to the geometric area of the electrode, regardless of the rate of the reduction.

The surface concentration of H^+ can be related to C_o^s from the stoichiometry of Equation IV. 2.

$$C_{H^+}^b - C_{H^+}^s = h(C_o^b - C_o^s) \qquad \text{(IV. 6.)}$$

Substitution of the expressions for C_o^s and $C_{H^+}^s$ from Equations IV. 5 and IV. 6 into Equation IV. 4 gives:

$$I_d = nFA'k\left(C_o^b - \frac{I_d\delta}{nFAD}\right)\left(C_{H^+}^b - \frac{hI_d\delta}{nFAD}\right)^h \qquad \text{(IV. 7.)}$$

The quantity, $\frac{hI_d\delta}{nFAD}$, can be evaluated and compared to $C_{H^+}{}^b$ if h and δ are known. The true value of h for the reduction of NO_3^- is unknown, but the stoichiometry of the reduction of NO_3^-, given in Equation VI. 2, shows that a maximum of $7H^+$ may be consumed prior to the rate-determing step. The diffusion-layer thickness can be calculated from Equation IV. 8 (4).

$$\delta = 1.61\ D^{1/3}\nu^{1/6}\omega^{-1/2} \qquad \text{(IV. 8.)}$$

The rotational velocity normally used was 41.9 rad/sec. The value of ν was 0.01 cm^2/sec, and the literature value of the diffusion coefficient of NO_3^- is 1.9×10^{-5} cm^2/sec (228). If I_d is 1 ma, and h is 7, then the following equality exists:

$$\frac{hI_d\delta}{nFAD} = 4 \times 10^{-3} \text{ moles/l} \qquad \text{(IV. 9.)}$$

Since $C_{H^+}{}^b$ equals 0.1 M, the last factor in Equation IV. 7 can be approximated by $(C_{H^+}{}^b)^h$. Solving Equation IV. 7 for I_d gives:

$$I_d = \frac{nFA'kC_o{}^b(C_{H^+}{}^b)^h}{1 + k(A'/A)\ (\delta/D)\ (C_{H^+}{}^b)^h} \qquad \text{(IV. 10.)}$$

Substitution of Equation IV. 3 into Equation IV. 10 gives:

$$I_d = \frac{nFA'C_o{}^b\ (C_{H^+}{}^b)^h\ k_c\exp\{-\beta nFE/RT\}}{1 + (A'/A)\ (\delta/D)\ (C_{H^+}{}^b)^h\ (k_c\exp\{-\beta nFE/RT\})} \qquad \text{(IV. 11.)}$$

Two opposite cases are clearly predicted by brief examination of Equation IV. 11. The second term in the denominator of Equation IV. 11 is much less than unity if the rate of the reduction is slow, the bulk concentration of H^+ is low, and the ratio of A'/A is small. The reduction is entirely limited by kinetics, and Equation IV. 11 can be rewritten.

$$I_d = nFA'C_o{}^b(C_{H^+}{}^b)^h\, k_c \exp\{-\beta nFE/RT\} \qquad \text{(IV. 12.)}$$

The disk current is independent of the rate of mass transport, but is proportional to $C_o{}^b$.

The second term in the denominator of Equation IV. 11 is larger than unity when k is large (i.e. E is a large negative potential), $C_{H^+}{}^b$ is large, and the ratio A'/A is a maximum. The reduction is reversible, and Equation IV. 11 can be rewritten.

$$I_d = nFAC_o{}^b\, D/\delta \qquad \text{(IV. 13.)}$$

Substitution of Equation IV. 8 into Equation IV. 13 gives Equation IV. 1. The disk current is limited solely by the rate of mass transport, and is proportional to $C_o{}^b$ and $w^{\frac{1}{2}}$.

The reduction of NO_3^- and NO_2^- at Cd lies between these extremes, and the kinetic rate is comparable to the rate of mass transport.

Equation IV. 11 predicts many of the observations that have been made. Increasing $C_{H^+}{}^b$ increases the reversibility

of the reductions (Figure IV. 6). Oxidation of the RCDE increases the ratio A'/A, and increases the linearity of I_d *vs.* $w^{\frac{1}{2}}$ plots (Figure IV. 10).

The rate of the reductions increases at more negative potentials, as predicted by Equation IV. 11. Plots of I_d *vs.* $w^{\frac{1}{2}}$ exhibit greater slopes when I_d is measured at -1.0 V than at -0.90 V (Figure IV. 11).

The disk current is proportional to C^b in both the reversible case and the kinetically limited case. The two proportionality constants are different, however, and at large concentrations of NO_3^- and NO_2^-, there is curvature in plots of I_d *vs.* C^b because of the transition from mass-transport limitation to kinetic limitation. At very large concentrations, the reduction of NO_3^- or NO_2^- consumes so large a quantity of H^+ at the electrode surface that $C_{H^+}{}^s$ cannot be approximated by $C_{H^+}{}^b$. This adds to the curvature of the I_d *vs.* C^b plots.

7. Reduction of dissolved oxygen

Oxygen is reversibly reduced at Cd cathodes (121). The voltammetric wave from O_2 in air-equilibrated electrolyte is shown in Figure IV. 12. This wave has a definite limiting-current plateau from -0.85 to -1.0 V. The reduction of H^+ becomes significant at more negative potentials. Unlike the reductions of NO_2^- and NO_3^-, a plot of I *vs.* $w^{\frac{1}{2}}$ for air-equilibrated electrolyte is linear to a rotational velocity

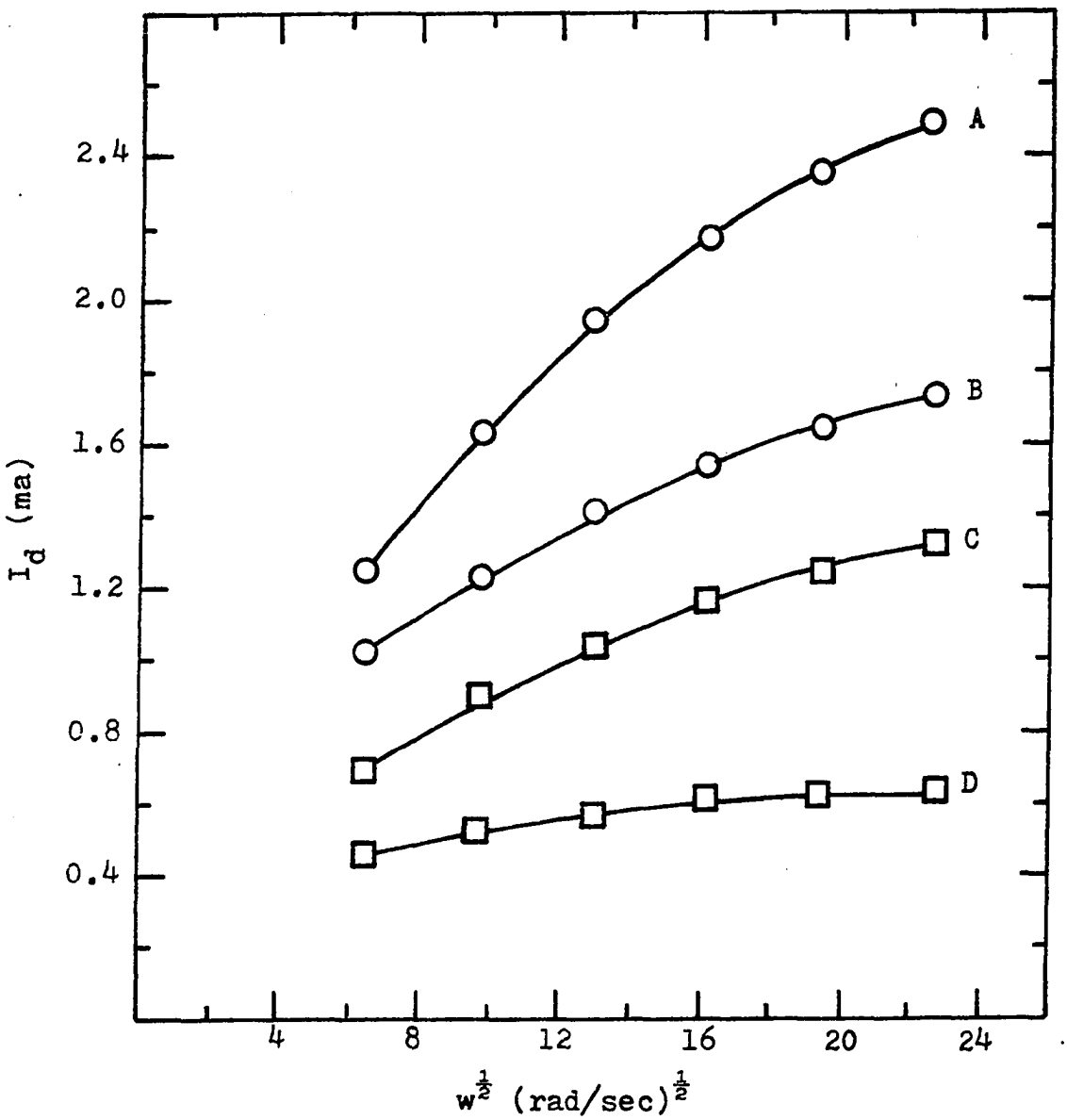

Figure IV. 11. Study of the potential dependence of the reductions of $NaNO_2$ and $NaNO_3$

RCDE. Scan rate 1.0 V/min. Electrolyte 0.10 M H_2SO_4.

A - 0.987 mM $NaNO_3$, I_d measured at -1.0 V

B - 0.987 mM $NaNO_3$, I_d measured at -0.9 V

C - 0.993 mM $NaNO_2$, I_d measured at -1.0 V

D - 0.993 mM $NaNO_2$, I_d measured at -0.9 V

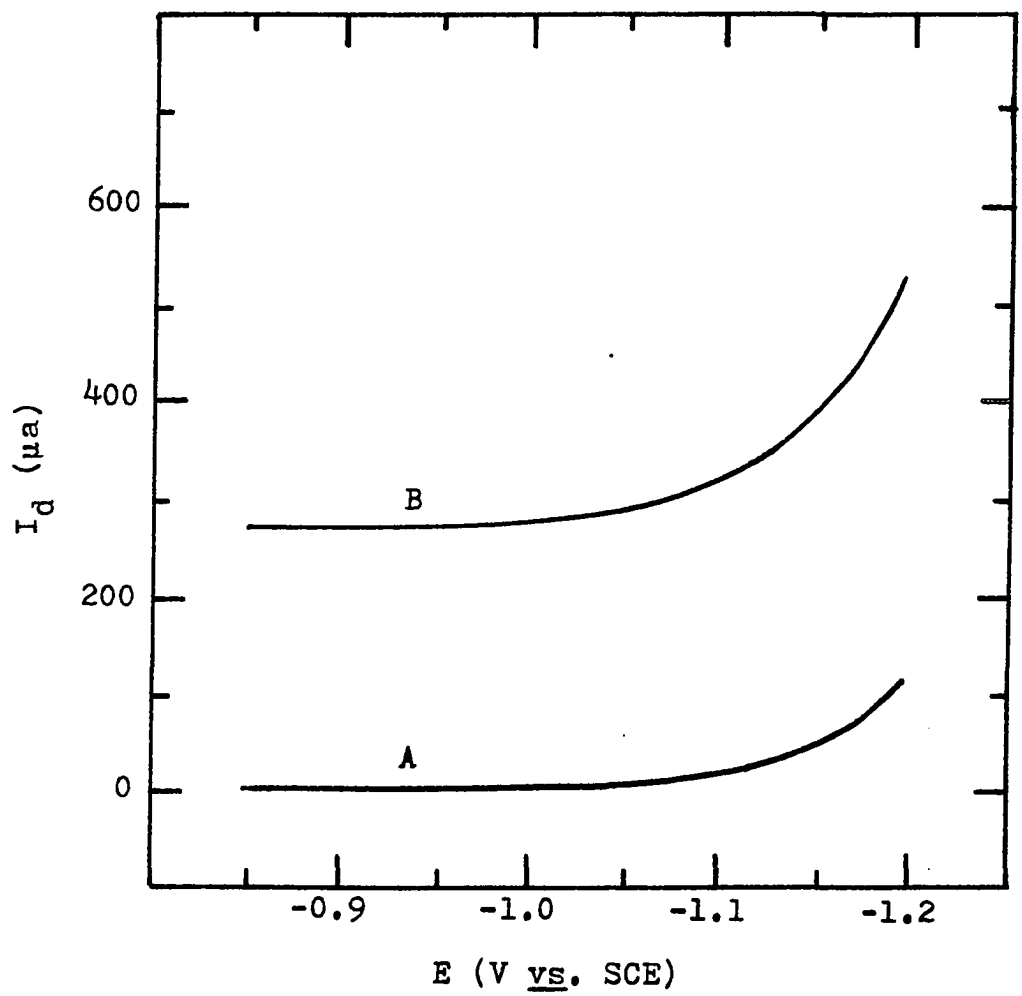

Figure IV. 12. Current-potential curve of O_2 reduction RCDE. Scan rate 1.0 V/min. Rotational velocity 41.9 rad/sec. Electrolyte 0.10 M H_2SO_4 - 5.0 mM $HClO_4$.
A - Deaerated electrolyte
B - Air-equilibrated electrolyte

of 1047 rad/sec (Figure IV. 13).

Oxygen must be excluded from the test solution for two reasons. First, the reduction current due to O_2 cannot be distinquished from that of NO_3^- or NO_2^-, and the presence of dissolved O_2 leads to serious errors. Also, the reduction of O_2 consumes H^+ ions at the electrode surface, as shown below:

$$O_2 + 4H^+ + 4e^- \rightleftarrows 2H_2O \qquad \text{(IV. 14.)}$$

A decrease in the surface H^+ concentration results in a decreased reversibility for the reduction of NO_3^- and NO_2^-, as described above (Figure IV. 6).

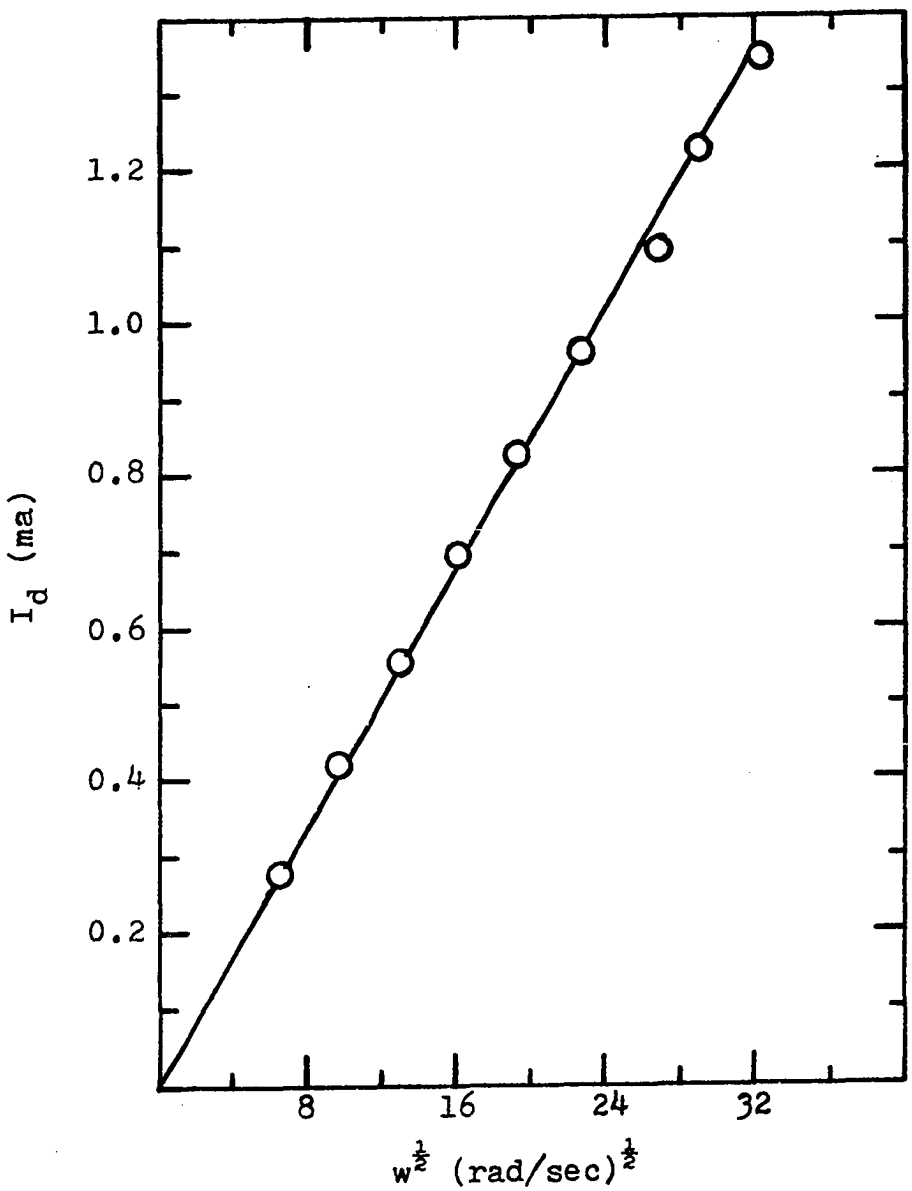

Figure IV. 13. $w^{\frac{1}{2}}$ study of reduction of dissolved O_2 RCDE. Scan rate 1.0 V/min. Air-equilibrated 0.10 M H_2SO_4 - 5.0 mM $HClO_4$ electrolyte. I_d measured at -1.0 V.

V. EVALUATION OF THE CHROMATOGRAPHIC DETERMINATION OF NITRATE AND NITRITE

A. Introduction

Tubular electrodes are conveniently adapted to the amperometric analysis of chromatographic effluents. The relationship between the current measured in a smooth tubular electrode, as an electroactive species continuously flows through it has been reported by Blaedel, et al. (29):

$$I = 5.24 \times 10^5 \, nD^{2/3}L^{2/3}V_f^{1/3}C^b \qquad \text{(V. 1.)}$$

where,

L = length of tubular electrode (cm)

V_f = volumetric flow rate (ml/min)

All other parameters in Equation V. 1 have their usual electrochemical significance.

Electroactive species are eluted from a chromatograph in narrow bands and do not continuously flow through the detector. Chromatographic peaks are the result, and the relationship between the peak areas and the variables in Equation V. 1 was reported by Johnson and Larochelle (113b):

$$Q = k'nFV_f^{-2/3}[\text{moles}] \qquad \text{(V. 2.)}$$

where,

Q = peak area (C)

k' = proportionality constant

[moles] = number of moles of analyte injected into the detector

Equation V. 2 assumes negligible electrolysis of the analyte.

The peak areas are linear functions of the analyte concentration in the sample for reversible reactions if the volume of the injections is constant. From inspection of Equation V. 2, it is seen that good precision in an analysis with a tubular electrode requires the flow rate to be constant.

B. Experimental

1. Chemicals and reagents

All H_2O used was triply distilled and deionized. Solutions used as the chromatographic eluent and electrolyte were prepared by diluting J. T. Baker reagent grade acids with H_2O. These solutions were deaerated by bubbling He through them for 2 hours.

Stock solutions of $NaNO_2$ and $NaNO_3$ were prepared by dissolving the salts (dried 4 hours at 90°C) with known volumes of H_2O. Salts used in the interference study were all reagent grade quality and were not dried before use.

The synthetic unknown was prepared from dried KNO_2 and KNO_3. Solutions of sulfanilamide, N-(1-naphthyl)ethylenediamine, and assorted other solutions required for the spectrophotometric analysis of the synthetic unknown were prepared exactly as prescribed by the Association of Official Analytical Chemists (AOAC) (14).

The Cd reduction column for the AOAC method was held in a 25-ml burette and was 16 cm long. The Cd particles were

prepared from J. T. Baker reagent grade mossy Cd, which was ground in a Waring blender until the particle size was less than 16 mesh. The Cd particles were packed into the burette and the column was back-flushed to remove fines. Thereafter, the reduction column was treated according to the procedure of the AOAC (14).

2. Experimental procedures

The interference study and the analysis of the synthetic unknown utilized 0.010 M $HClO_4$ eluent and 0.20 M H_2SO_4 electrolyte. The flow rate of each was 0.2 ml/min. The tubular detector was potentiostated at -0.90 V, and the sample loop volume was 0.33 ml.

The interference study was carried out over a five-day period. Three consecutive injections of a reference solution, containing 0.500 mM $NaNO_2$ and 0.500 mM $NaNO_3$, were made at the beginning of each day. Then three consecutive injections of a test solution were made. Each test solution contained 0.500 mM $NaNO_2$, 0.500 mM $NaNO_3$, and a possible interference at a concentration of 5.0 mM. The reference solution was injected between injections of different test solutions to ascertain whether the previous interference had permanently affected the chromatograph or detector.

The average NO_3^- peak area and height were calculated from the 15 chromatograms of the reference solution. The average NO_2^- peak area and height were also calculated. Each

average was given the arbitrary value of 100%. The average area and height of both the NO_3^- and NO_2^- peaks were calculated from the chromatograms of each test solution. The averages from each test solution were compared to those of the reference solution, which contained no interference. These results are listed in Table V. 1.

For the long-term precision study, the NO_3^- and NO_2^- peak areas and heights from the 15 chromatograms of the reference solution were statistically evaluated. This data is in Table V. 2. The short-term precision study consisted of a separate statistical evaluation of each of the 5 groups of 3 consecutive chromatograms of the reference solution. This data is presented in Table V. 3.

A synthetic unknown, which contained 5.78 μg KNO_3-N/ml and 5.75 μg KNO_2-N/ml, was analyzed chromatographically and spectrophotometrically. The spectrophotometric procedure was a standard method of the AOAC (14). The total NO_3^- and NO_2^- concentration was found after the NO_3^- present was reduced to NO_2^- in a Cd column. Then all of the NO_2^- in that portion of the sample was diazotized with sulfanilamide and coupled with N-(1-naphthyl)ethylenediamine. The procedure was repeated without the reduction step on another portion of the unknown to calculate the NO_2^- concentration. Then the NO_3^- concentration was found by difference.

The absorbance readings were made at 540 nm using a

Beckman DU-2, and were compared to a calibration curve prepared two days earlier from standard solutions.

The synthetic unknown was analyzed chromatographically by injection immediately after three standard solutions containing 7.278 μg KNO_2-N/ml, 4.852 μg KNO_2-N/ml, and 7.212 μg KNO_3-N/ml, respectively. The injection of the synthetic unknown was followed by an injection of a standard solution containing 4.808 μg KNO_3-N/ml. Linear calibration curves were constructed for NO_3^- and NO_2^- from the peak areas of the chromatograms of the standard solutions. Then the unknown concentrations were calculated from the calibration curves.

All chromatographic peaks were integrated with a Keuffel and Esser planimeter.

C. Results and Discussion

1. The chromatographic separation

All samples can be expected to contain dissolved O_2, and O_2 is electroactive at Cd cathodes as shown in Chapter IV. Furthermore, samples cannot be deaerated because NO_3^- and NO_2^- are volatile and are lost from the sample when a gas is bubbled through it. Therefore, the chromatographic separation must not only separate NO_2^- and NO_3^-, but it must separate dissolved O_2 from them. Most samples will not contain other electroactive anions; however, they may contain electroactive cations (e.g. Fe(II) and Cu(II)). These

cations are removed from the eluent by the cation-exchange column shown in Figure III. 3.

The separation of O_2, NO_2^-, and NO_3^- is easily accomplished with a column of Amberlite IRA-900, a macroreticular, strongly basic anion-exchange resin. Oxygen is not retained on the resin. Nitrite is retained somewhat, but if an acidic eluent is used, most of the NO_2^- in the chromatograph is protonated because HNO_2 is a weak acid ($K_a = 6.0 \times 10^{-6}$). Nitrate is not protonated in a moderately acidic solution, and it is strongly retained on the resin.

Two ion-exchange separations of NO_2^- and NO_3^-, reported previously, used solutions containing NaCl as the eluent (81, 88). The presence of Cl^- in the electrolyte was shown in Chapter IV to decrease the rate of the reductions of NO_2^- and NO_3^- (see Figures IV. 4, IV. 5, and IV. 7). Perchlorate does not decrease the rates of the reductions, and is sorbed strongly on Amberlite IRA-900. Even at low concentrations, $HClO_4$ effectively elutes NO_3^- from the anion-exchange column. The eluent used for most of these studies was 0.010 M $HClO_4$.

The optimum concentration of acid in the electrolyte was shown in Chapter IV to be 0.1 M. However, the separation of dissolved O_2 and NO_2^- will not occur if the eluent is more concentrated than 0.010 M $HClO_4$. Therefore, the eluent was mixed with 0.20 M H_2SO_4 in a 1:1 volumetric ratio after the

separation had been achieved. The solution flowing through the detector was 0.10 M H_2SO_4 - 5.0 mM $HClO_4$. A satisfactory separation was attained when the flow rate of the eluent was 0.2 ml/min.

A chromatogram of 0.500 mM $NaNO_2$ and 0.500 mM $NaNO_3$ is shown in Figure V. 1. The detector potential was -0.90 V, the volume of the injection was 0.33 ml, and the other parameters were those already described. A relatively small O_2 peak in the chromatogram is followed by a sharp peak corresponding to the NO_2^- in the sample. The NO_3^- peak is last and requires 7 - 9 minutes for complete elution.

2. Detector treatment

Cadmium is quickly covered with an oxide layer if it is dried in air. The reductions of NO_2^- and NO_3^- do not readily occur at such an oxide-covered electrode. However, the reduction of NO_3^- or NO_2^- apparently slowly removes the oxide layer and increases the detector sensitivity until the oxide layer has been entirely eliminated. After a few injections of a 1 mM $NaNO_3$ or $NaNO_2$ stock solution, the detector sensitivity increases to the maximum level. Following that pretreatment, the surface of the Cd tube is covered with a mossy, grey coating. The coating can be maintained by storing the detector under a few milliliters of effluent. The detector need not be potentiostated when it is stored, and it requires pretreatment only when it is

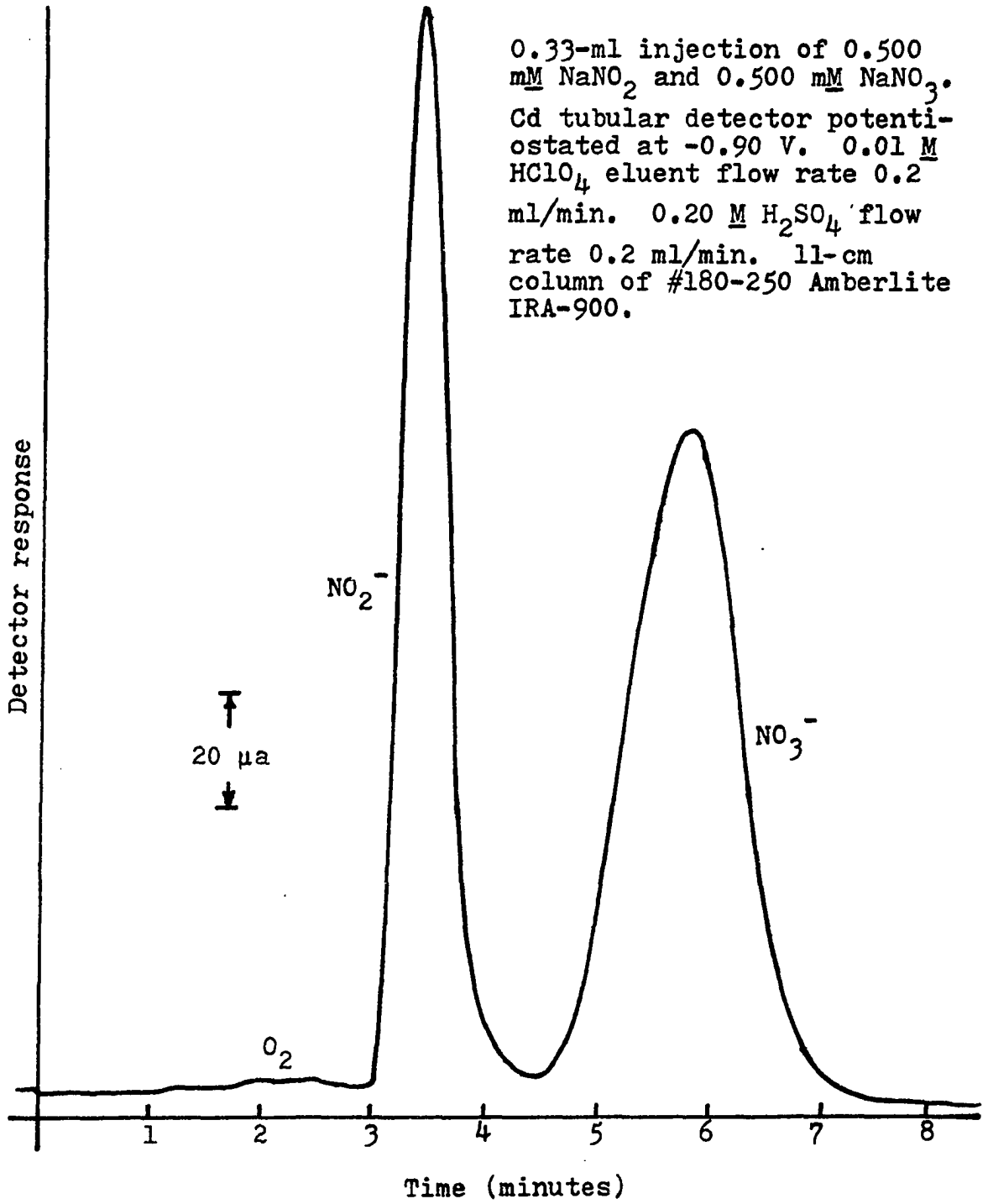

Figure V. 1. Typical chromatogram

allowed to dry.

The nature of the mossy layer on the Cd electrode will be discussed in Chapter VI.

3. Peak areas vs. detector potential

The areas of the NO_3^- and NO_2^- peaks depend on the detector potential in much the same way as the disk current depends on the potential of the RCDE. The peak areas from injections of 0.500 m$\underline{M}$ $NaNO_2$ and 0.507 m$\underline{M}$ $NaNO_3$ solutions are shown as a function of the potential of the detector in Figure V. 2. The base line current is also shown as a function of potential. The Cd detector is oxidized at -0.775 V, and the evolution of H_2 becomes excessive at potentials more negative than -1.0 V.

The peak areas are smaller at the more positive potentials because the rate of the reductions is slower than at more negative potentials (Chapter IV). The peak areas also decrease at the very negative potentials because the large number of H_2 bubbles formed adhere to the walls of the detector and prevent NO_3^- and NO_2^- ions from reaching the electrode surface. The peak areas are a maximum when the detector potential is about -0.90 V. This potential was used for most subsequent studies.

4. Peak areas vs. flow rate

The areas of chromatographic peaks resulting from reversible electrochemical reactions in smooth-walled tubular

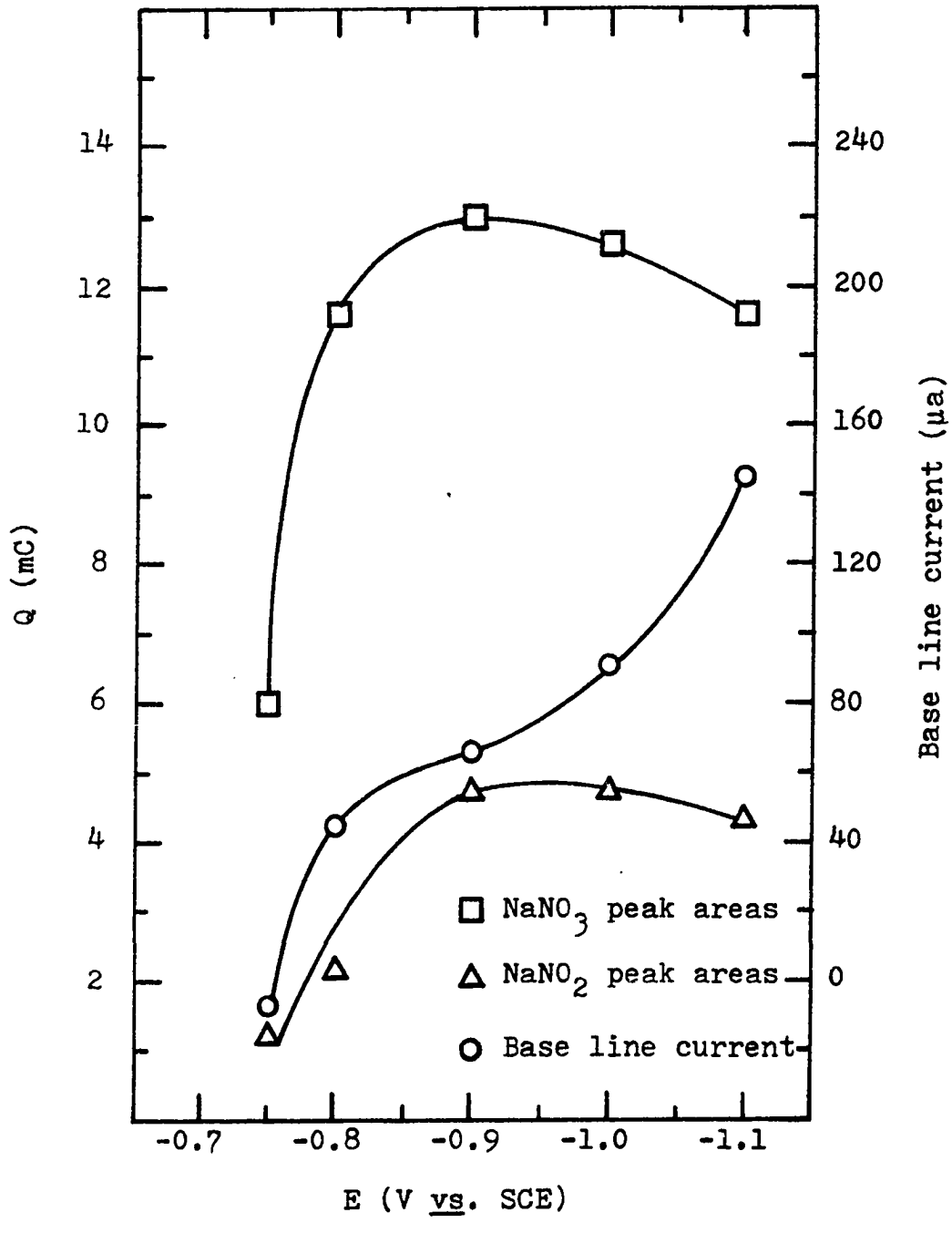

Figure V. 2. Potential dependence of peak areas and base line current
Cd tubular detector. 0.665-ml injections of 0.507 m$\underline{M}$ $NaNO_3$ or 0.500 m$\underline{M}$ $NaNO_2$. Flow rate of 0.010 $\underline{M}$ $HClO_4$ eluent 0.2 ml/min. Flow rate of 0.20 $\underline{M}$ H_2SO_4 0.2 ml/min.

electrodes are proportional to $V_f^{-2/3}$ (Equation V. 2). This proportionality was tested for the Cd tubular electrode with injections of 0.20 m$\underline{M}$ $NaNO_2$ and 0.20 m$\underline{M}$ $NaNO_3$ stock solutions.

The reductions of NO_3^- and NO_2^- at a RCDE are not entirely reversible, and they may not be reversible at a Cd tubular electrode. The reduction of dissolved O_2, however, was shown in Chapter IV to be reversible. Therefore, the areas of the dissolved O_2 peaks in the chromatograms of the 0.20 m$\underline{M}$ $NaNO_3$ stock solution were measured at the three highest flow rates used. The O_2 peak was too broad at the slower flow rates for accurate integration. In all cases, the flow rate of the eluent equaled the flow rate of the 0.20 $\underline{M}$ H_2SO_4.

In Figure V. 3, the peak areas are plotted against the total flow rate. From the slope of each curve, the exponential value of the proportionality can be calculated. In that way, the O_2 peak areas were found to be proportional to $V_f^{-0.91}$. Since the reduction of dissolved O_2 is reversible, the difference between the exponential value of -0.667, predicted from Equation V. 2, and the actual value of -0.91 must be due to the presence of the mossy layer on the interior surface of the Cd tubular electrode. The detector is not smooth-walled, and the convective-diffusional transport in the Cd tube is not that for which Equation V. 2 is applicable.

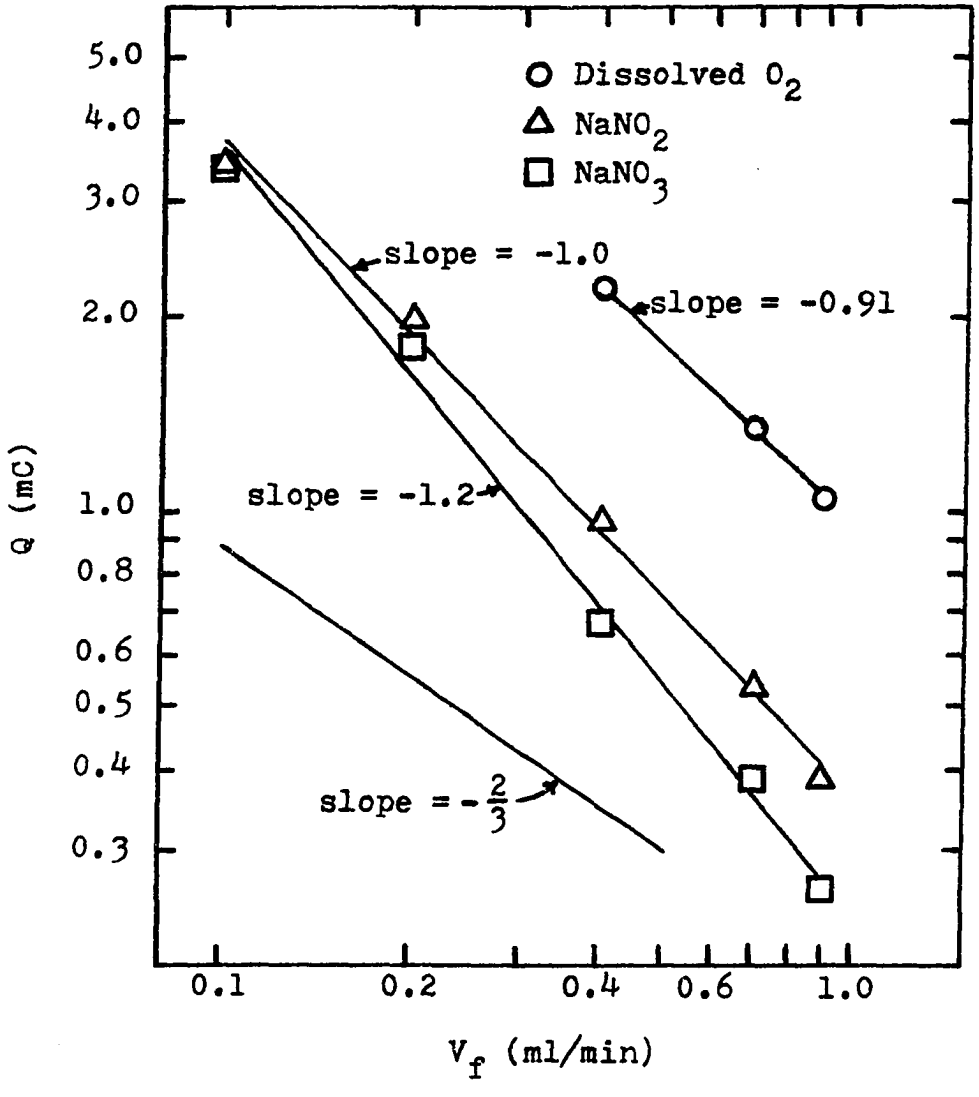

Figure V. 3. Flow rate study
Cd tubular detector potentiostated at -0.90 V. 0.33-ml injections of 0.20 mM $NaNO_3$ or 0.20 mM $NaNO_2$ solutions. Dissolved O_2 peak from NO_3^- chromatograms also measured. 0.010 M $HClO_4$ eluent and 0.2 M H_2SO_4 mixed in 1:1 volumetric ratio.

The areas of the NO_3^- and NO_2^- peaks are proportional to $V_f^{-1.2}$ and $V_f^{-1.0}$, respectively. The larger negative exponents for NO_3^- and NO_2^- reflect that they are reduced more irreversibly than O_2. The difference between the exponential values of NO_2^- and NO_3^- may result from a difference in the rates of the reductions, or the difference in the instantaneous fluxes of NO_2^- and NO_3^- to the Cd surface.

5. Peak areas and heights vs. concentration

The chromatographic peak areas are proportional to the concentration of NO_3^- and NO_2^- in the sample (Figure V. 4). The working range of concentrations is 0.05 - 1.00 mM. The NO_3^- plot intercepts the origin as expected, but the NO_2^- plot does not. In the chromatograms used for this data, the dissolved O_2 peak was not entirely resolved from the NO_2^- peak. A constant error in extrapolating the base line under the NO_2^- peak resulted in the negative intercept observed in Figure V. 4.

The detection limit for both NO_3^- and NO_2^- is about 0.01 mM. The relative uncertainty in the peak area measurement is approximately 100% at this concentration. Figure V. 5 is a chromatogram of NO_2^- and NO_3^- at the detection limit. The NO_2^- peak is a shoulder on the O_2 peak, and the NO_3^- peak is barely distinquishable from the base line.

Manual integration of peak areas is tedious. It is

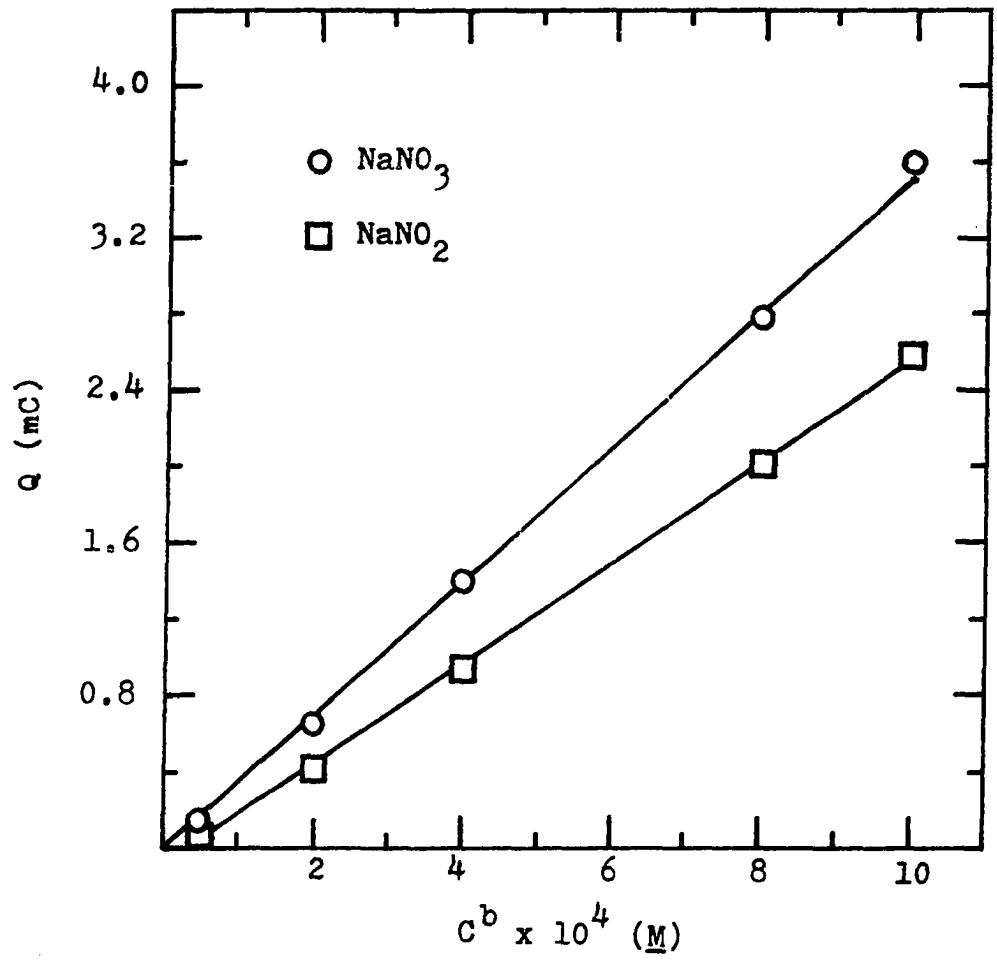

Figure V. 4. Concentration study
Cd tubular detector potentiostated at -0.90 V. 0.33-ml injections. 0.010 M $HClO_4$ eluent flow rate 0.2 ml/min. 0.20 M H_2SO_4 flow rate 0.2 ml/min.

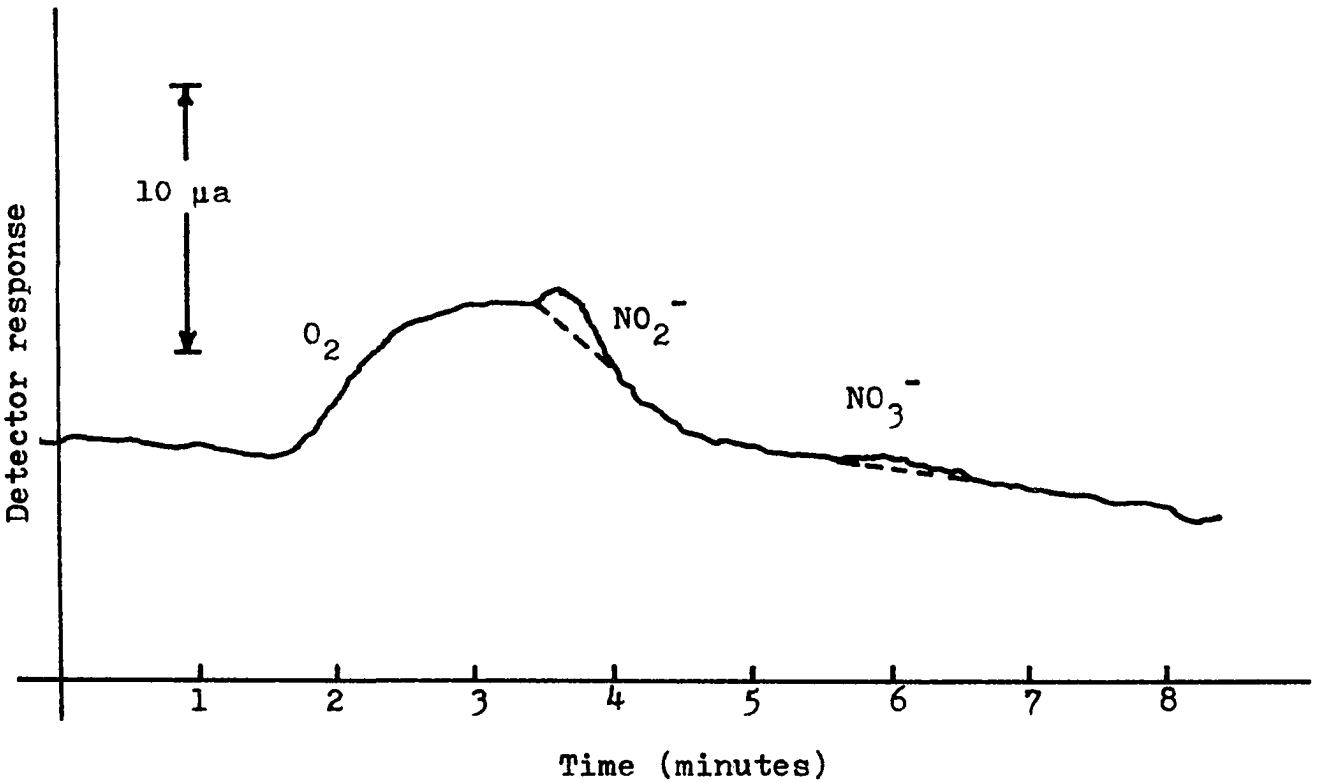

Figure V. 5. Chromatogram of 0.01 m<u>M</u> $NaNO_2$ and 0.01 m<u>M</u> $NaNO_3$ Cd tubular detector potentiostated at -0.90 V. 0.33-ml injection. 0.010 <u>M</u> $HClO_4$ eluent flow rate 0.2 ml/min. 0.20 <u>M</u> H_2SO_4 flow rate 0.2 ml/min.

much more convenient to calculate concentrations from peak heights. Unfortunately, the height of the NO_3^- peaks is not a linear function of concentration (Figure V. 6). Although the NO_2^- peak heights are linear functions of concentration, the next section will show that the height of the NO_2^- peak, but not peak area, is greatly affected by the presence of other salts in the sample. Therefore, the peak areas are much more reliable for the calculation of unknown concentrations.

6. Interference study

The presence of electroinactive salts in the sample affects the height and, to a lesser extent, area of the NO_3^- and NO_2^- peaks. For example, in Figure V. 7 a chromatogram of a solution of 0.500 m$\underline{M}$ $NaNO_2$, 0.500 m$\underline{M}$ $NaNO_3$, and 5.0 m$\underline{M}$ NaCl is compared to a chromatogram of a solution containing 0.500 m$\underline{M}$ $NaNO_2$ and 0.500 m$\underline{M}$ $NaNO_3$. The chromatograms were obtained with identical experimental conditions. The NaCl in the sample results in a shorter, broader NO_2^- peak. The NO_3^- peak is only slightly affected.

The shape of the peaks is affected because when the NO_2^- and NO_3^- ions are in the pure distilled H_2O of the reference solution, they are sorbed onto the anion-exchange resin in a narrow band. They are not eluted until the entire 0.33-ml sample volume has passed the band, and the acidic eluent enters the column. Conversely, if the sample contains

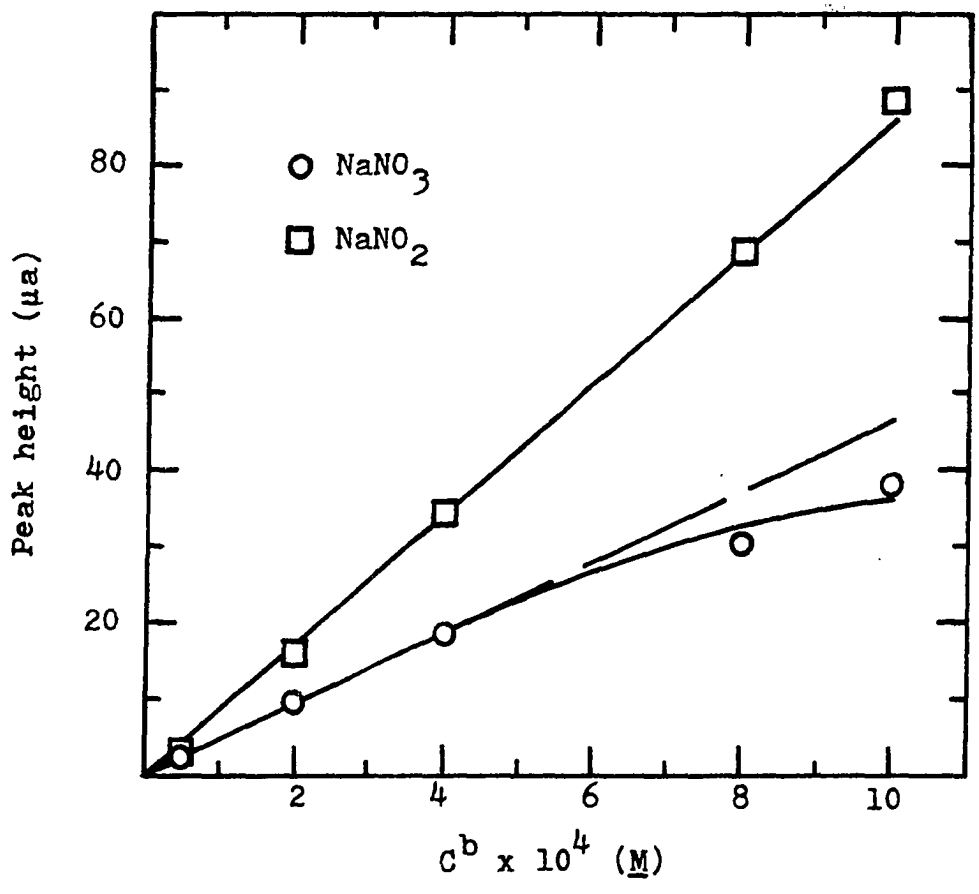

Figure V. 6. Concentration study
Cd tubular detector potentiostated at -0.90 V. 0.33-ml injections. 0.010 M $HClO_4$ eluent flow rate 0.2 ml/min. 0.20 M H_2SO_4 flow rate 0.2 ml/min.

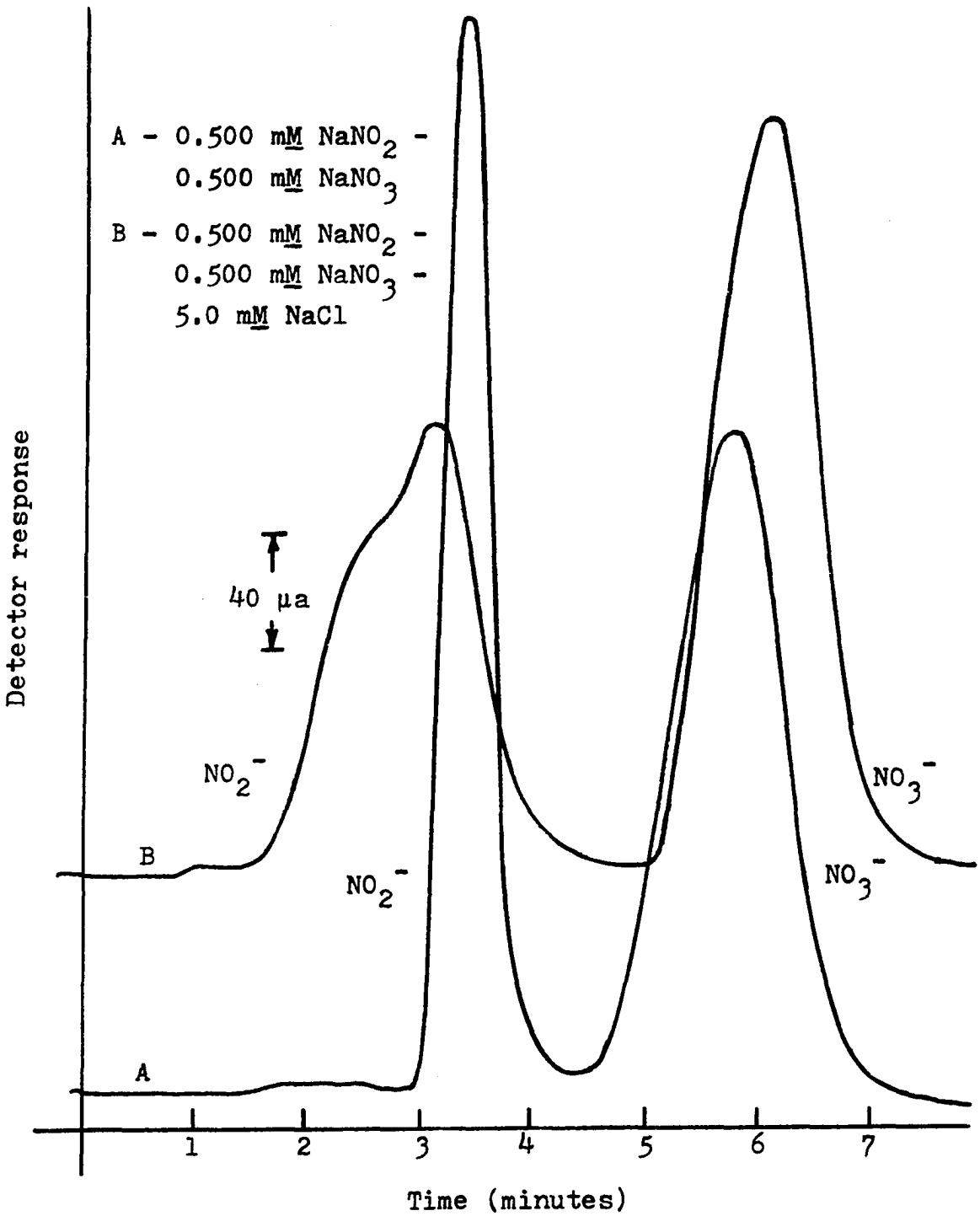

Figure V. 7. Distortion of chromatographic peaks by NaCl Cd tubular detector potentiostated at -0.90 V. 0.33-ml injections. 0.010 M $HClO_4$ eluent flow rate 0.2 ml/min. 0.20 M H_2SO_4 flow rate 0.2 ml/min.

other salts, the NO_2^- and NO_3^- ions may be partially eluted by the anion of that salt while the 0.33-ml sample volume is flowing through the column. Nitrate is less susceptible than NO_2^- to elution by other salts because it is sorbed more strongly on the resin than is NO_2^-. However, some anions (e.g. Br^-, ClO_4^-, and HSO_4^-) broaden the NO_3^- peak if they are in the sample.

The relative effect that various salts have on the chromatographic peaks of 0.500 m$\underline{M}$ $NaNO_2$ and 0.500 m$\underline{M}$ $NaNO_3$ are listed in Table V. 1. The concentration of the salt in each test solution was 5.0 m$\underline{M}$. The peak areas and heights are given relative to the values in the absence of interfering ions.

Nitrite is not stable in acidic solutions and decomposes to NO_3^- and NO (51). Therefore, the NO_2^- peak areas and heights are less than 100% for all solutions containing acidic interferences in Table V. 1, except H_2SO_4. The solution containing H_2SO_4 was analyzed before the decomposition had time to occur. Because NO_3^- is a product of the decomposition, the NO_3^- peak areas are greater than 100% for the acidic test solutions.

Neutral salts affect the NO_2^- and NO_3^- peak areas relatively little. Except where ClO_4^-, Br^-, or HSO_4^- is present, the NO_3^- peak heights are also only slightly affected. However, the NO_2^- peak height is decreased to

Table V. 1. Interference study -- 0.500 mM $NaNO_2$, 0.500 mM $NaNO_3$

Interference (5.0 mM)	Peak Areas		Peak Heights	
	NO_2^-	NO_3^-	NO_2^-	NO_3^-
None	100%	100%	100%	100%
H_2SO_4	114	114	33	60
HCl	58	122	23	125
H_3PO_4	46	126	35	100
$HClO_4$	60	112	24	97
$NaClO_4$	100	112	41	76
NaCl	122	103	42	113
NaBr	120	92	42	57
NaI	81	125	35	97
$NaHSO_4$	62	117	19	57
NaH_2PO_4	110	83	68	86
Na_2HPO_4	112	84	69	86
KCl	108	94	33	106
$CaCl_2$	104	96	27	113
$ZnCl_2$	101	83	29	112
Na_2SO_3	—	86	—	51
$NaBrO_3$	—	116	—	140
$Fe(NH_4)(SO_4)_2$	82	101	22	61
$CuCl_2$	102	91	28	133

Table V. 2. Long-term precision study

Chromatogram Number	Peak Areas (mC)		Peak Heights (μa)	
	NO_2^-	NO_3^-	NO_2^-	NO_3^-
1	4.67	8.54	166	110
2	4.76	8.87	168	110
3	4.73	8.76	170	112
4	5.00	8.35	175	115
5	4.95	8.00	170	113
6	4.84	8.11	166	112
7	5.29	6.66	202	94
8	5.45	6.42	214	91
9	5.35	6.38	211	91
10	5.48	8.11	185	115
11	4.88	8.16	185	114
12	5.36	8.28	183	114
13	6.23	8.04	243	110
14	6.09	8.28	247	114
15	6.47	8.26	249	112
average	5.30	7.95	196	109
average deviation	0.44	0.58	28	6
standard deviation	0.57	0.80	31	9
relative standard deviation	11%	10%	16%	8%

about one-third of its value in the reference solution. Therefore, when samples that contain unknown quantities of salts are to be analyzed, peak areas are much more reliable measures of concentration than are peak heights.

The only salts in Table V. 1 that were severe interferences were $NaBrO_3$, Na_2SO_3, and NaI. Both BrO_3^- and SO_3^{-2}

Table V. 3. Short-term precision study

Chromatograms*	Average Peak Areas (mC)		Average Peak Heights (μa)	
	NO_2^-	NO_3^-	NO_2^-	NO_3^-
#1-3	4.72	8.72	168	111
#4-6	4.93	8.15	170	113
#7-9	5.36	6.49	209	92
#10-12	5.24	8.18	184	114
#13-15	6.26	8.19	246	112
	Relative Standard Deviations			
#1-3	1.1%	2.2%	1.4%	1.1%
#4-6	1.8	2.6	3.1	1.6
#7-9	1.7	2.5	3.4	1.9
#10-12	6.7	1.2	0.6	0.5
#13-15	3.5	1.7	1.4	2.1

*Chromatograms are numbered in Table V. 2.

are electroactive and are eluted simultaneously with NO_2^-. Hence, NO_2^- cannot be determined in their presence.

The NaI interfered because the I^- adsorbed on the Cd electrode surface and decreased the detector sensitivity (Figure IV. 7). Successive injections of the NaI test solution resulted in progressively smaller peaks for NO_2^- and NO_3^-. The data in Table V. 1 for the NaI test solution was taken from the first of the three chromatograms of that

Table V. 4. Comparison of chromatographic and standard methods

Actual Concentration	Chromatographic Result	Standard Method
5.75 μg KNO_2 - N/ml	5.64	5.07
5.78 μg KNO_3 - N/ml	5.86	5.36
	Relative Error	
Determination of NO_2^-	1.9%	11.8%
Determination of NO_3^-	1.4%	7.3%

solution.

Ferric and Cu^{+2} ions did not interfere because they were quantitatively eliminated from the eluent stream by the cation-exchange column.

7. Precision study

The long-term precision study simulates the accuracy obtainable when a calibration curve is constructed and used on subsequent days to determine unknown concentrations. The peak areas and heights from the 15 injections of the 0.500 mM $NaNO_2$ - 0.500 mM $NaNO_3$ reference solution are listed in Table V. 2. Since these chromatograms were made over a 5-day period, the precision of the area and height measurements reflects the day-to-day reproducibility of the flow rate

adjustments and detector sensitivity. The long-term precision represents the accuracy of a single comparison of a peak from an unknown solution to peaks of stock solutions obtained previously.

The relative standard deviations of the measurements of NO_3^- and NO_2^- peak areas in Table V. 2 are 10% and 11%, respectively. The relative standard deviations of the peak heights are 16% for NO_2^- and 8% for NO_3^-. Therefore, about 10% relative error can be expected when a single calibration curve is prepared for routine analyses during a 5-day period.

Greater precision is possible if the unknown injection is made just before or after injections of stock solutions. The accuracy of the determination of an unknown concentration is also greater because the fluctuations in flow rate and detector sensitivity are much less over a period of a few minutes than over several days.

The short-term precision was found by calculating the standard deviation of each of the five groups of three consecutive chromatographic peaks from the reference solution. The standard deviations were calculated according to the method of Dean and Dixon (58), and are listed in Table V. 3. The largest relative standard deviation for the peak area measurements was 6.7% for NO_2^- and 2.6% for NO_3^-, and for peak height measurements it was 3.4% for NO_2^- and 2.1% for

NO_3^-. The average relative standard deviation was 3% or less for either measurement. Therefore, by bracketing the unknown sample injection with injections of standard solutions, the accuracy is improved by a factor of 3 to 4 over the use of a previously prepared calibration curve.

8. Comparison to a standard method

A synthetic unknown was prepared and analyzed chromatographically and spectrophotometrically with a standard method of the AOAC to make certain there were no serious determinate errors inherent in the chromatographic method. The synthetic unknown contained 5.75 μg KNO_2-N/ml (0.411 mM) and 5.78 μg KNO_3-N/ml (0.413 mM). No other salts were added so that both methods would be as accurate as possible. The chromatographic analysis was carried out with injections of stock solutions before and after the unknown injection for maximum accuracy. The spectrophotometric method utilized a calibration curve prepared two days before the analysis of the synthetic unknown. The synthetic unknown was analyzed once by each method.

The results of each analysis are listed in Table V. 4. The chromatographic method reported 5.86 μg KNO_3-N/ml and 5.64 μg KNO_2-N/ml, for a relative error of 1.4% for NO_3^- and 1.9% for NO_2^-. The spectrophotometric method reported 5.36 μg KNO_3-N/ml and 5.07 μg KNO_2-N/ml. The relative errors were 7.3% for NO_3^- and 11.8% for NO_2^-. Had the chromato-

graphic method used a calibration curve prepared a few days earlier, the relative errors of the two methods would have probably been equal.

VI. DETERMINATION OF THE NITRATE AND NITRITE REDUCTION PRODUCTS

A. Introduction

The application of coulometric electrodes as detectors for forced-flow liquid chromatography has been discussed by Johnson and Larochelle (113b). Coulometric detectors are more sensitive than tubular detectors because they electrolyze 100% of the analyte. The peak areas are independent of small variations in the flow rate of the effluent because the analyte is completely electrolyzed; therefore, the coulometric detector offers better precision than does the tubular electrode. The peak area resulting from 100% electrolysis of the electroactive species is given by Equation VI. 1 (113b):

$$Q = nF[\text{moles}] \qquad \text{(VI. 1.)}$$

where each factor has its usual electrochemical significance.

The Cd coulometric electrode used for these studies is shown in Figure III. 2. The electrode was not durable, but the value of n in Equation VI. 1 was determined using the coulometric detector.

Additional voltammetric studies were made to determine the product of the reduction of NO_3^- and NO_2^-. A rotating glassy-carbon disk/Pt-ring electrode was used. The products of reactions at the disk electrode are transported by diffusion and radial convection to the ring where they can be identified. The RRDE has been used to detect Cu(I), an

intermediate in the reduction of Cu(II) in Cl^- media (7b); H_2O_2, an intermediate in the reduction of O_2 (7b); and H_2O_2 in the reduction of O_3 to H_2O (113a).

The product of the reductions of NO_3^- and NO_2^- was sought because of the variety of possible products that exist. Depending on the experimental conditions, the reduction of NO_3^- has been shown to produce NO_2^- at Hg cathodes (141); NH_3 at Pb (117), Cu (5, 62, 140), Ti (5), Pt (62), and Hg (62, 119) cathodes; and NH_2OH at Cu (62), Pt (62), Sn (7a), Pb (7a), Pb(Hg) (5), Cu(Hg) (5, 221), and Hg (5, 6, 7a, 62, 119, 141) cathodes. The reduction of NO_3^- to NH_2OH is 90% complete at Hg cathodes in solutions of H_2SO_4 at pH 0.56 to 1.22 (141). The reduction is quantitative if the electrolyte is 46% H_2SO_4 (6).

B. Experimental

1. Chemicals and reagents

All H_2O used was triply distilled and deionized. All chemicals were reagent grade quality. Stock solutions of $NaNO_2$ and $NaNO_3$ were prepared by dissolving the salts, dried 4 hours at 90°C, in H_2O. Other solutions were prepared by dissolving undried salts or diluting reagent grade acids with H_2O.

2. Experimental procedures

The coulometric electrode, shown in Figure III. 2, was used in the detector cell shown in Figure III. 1. The Cd

coulometric detector was pretreated like the tubular electrode and was stored under a few milliliters of effluent (Chapter V).

The cation-exchange column was not used with the chromatograph shown in Figure III. 3 for these studies. The anion-exchange column was 7 cm long. The eluent was 1.0 m$\underline{M}$ $HClO_4$ - 2.0 m$\underline{M}$ H_2SO_4, and was mixed in a 1:1 volumetric ratio with 0.2 $\underline{M}$ H_2SO_4 before entering the detector. The volume of the sample loop was 0.665 ml. All other procedures and parameters used in these chromatographic studies are described in Chapter V.

The RCDE and the rotating glassy-carbon disk/Pt-ring electrode were used for voltammetric studies. These electrodes are described in Chapter III.

The glassy-carbon disk electrode of the RRDE was plated with Cd in a solution of 0.1 $\underline{M}$ K_2SO_4 and 1 m$\underline{M}$ $CdCl_2$. The RRDE was rotated at 41.9 rad/sec, and the potential of the disk electrode was scanned from -0.85 to -1.2 V for 3 minutes. The scan rate was 1.0 V/min. The Pt-ring electrode was potentiostated at 0.0 V. The RRDE was then removed from the plating solution, rinsed, and transferred to the voltammetric cell that contained 400 ml of the 0.10 $\underline{M}$ H_2SO_4 - 5.0 m$\underline{M}$ $HClO_4$ electrolyte. The Cd-plated disk was potentiostated at -0.90 V, and the Pt ring was scanned from -0.2 to +1.4 V at a rate of 1.0 V/min. The rotational velocity of the RRDE was 41.9

rad/sec. Current-potential (I-E) curves were obtained of the reduction products of NO_3^- and NO_2^- at the Pt-ring electrode after aliquots of the stock solutions were added to the deaerated electrolyte.

Current-potential curves of NO_2^- and NH_2OH were obtained at the Pt-ring electrode for comparison. The glassy-carbon disk was not plated with Cd in this instance, and was potentiostated at 0.0 V, at which no electrochemical reaction occurred.

Current-potential curves of the NO_3^- and NO_2^- reductions at the RCDE were obtained at very low rotational velocities with a servo-controlled, variable-speed motor, Model ASR from Pine Instrument Co. The RCDE had been oxidized at 0.0 V for 90 seconds (Chapter IV).

All other voltammetric procedures were those discussed in Chapter IV.

C. Results and Discussion

1. Coulometric detector

Several injections of 1.0 mM $NaNO_2$ or $NaNO_3$ stock solutions were made before the Cd coulometric detector electrolyzed 100% of the NO_3^- and NO_2^- injected into it. After this pretreatment, the spaces between the wires in the detector were partially filled with the grey, mossy material that had previously been observed on the walls of the pretreated Cd tubular electrode. The mossy material

completely plugged the end of the coulometric detector nearest the SCE after a few hours of work and stopped the flow of eluent. The deposited material could only be removed from the detector by unpacking the electrode, wiping the Cd wires, and repacking the detector. The Cd coulometric detector was deemed unsuitable for routine applications for this reason.

The mossy coating in the detector was Cd resulting from dissolution of Cd in the upstream end of the detector, and the deposition of that Cd^{+2} in the end of the detector nearest the SCE. In normal use, the detector was potentiostated at -0.90 V. The internal resistance in the electrode produced a potential gradient through the length of the detector whenever an electrical current flowed. The end of the detector nearest the SCE was maintained by the potentiostat at -0.90 V, but the upstream end was at a more positive potential; the potential difference between the ends being equal to the product of the current and the internal resistance by Ohm's Law. Cadmium is rapidly oxidized in this medium at potentials more positive than -0.76 V. Peak currents of 1 ma were common when 1.0 m$\underline{M}$ stock solutions of $NaNO_2$ or $NaNO_3$ were injected, and an internal resistance of only a few hundred ohms would make the potential of the upstream end of the coulometric detector more positive than -0.76 V. The Cd^{+2} ions from the

dissolution were eluted down the detector until they were reduced to Cd^{o} in a portion of the detector at which the potential was more negative than -0.76 V. A potential gradient of this sort in a porous Cd anode was reported by Bro and Kang (34).

The deposition of the mossy layer of Cd in the tubular electrode is not a problem since there are no capillary spaces to be clogged.

2. Nitrate and nitrite reduction products

A criterion of coulometric efficiency for a detector is the invariance of peak areas with changes in the flow rate of the effluent. The peak areas from injections of a 0.500 mM $NaNO_2$ solution are shown in Figure VI. 1 to be constant with effluent flow rates of 0.2 - 0.4 ml/min. At lower flow rates, the efficiency of the detector decreases because H_2 bubbles formed in it are not expelled as they are at higher flow rates.

Injections of stock solutions of 0.500 mM $NaNO_2$ and 0.507 mM $NaNO_3$ were made with a flow rate of 0.3 ml/min to determine the electrode potential at which the efficiency of the detector is a maximum. The peak areas at various detector potentials are shown in Figure VI. 2. The maximum efficiency for both NO_2^- and NO_3^- is at -0.865 V, and the maxima in Figure VI. 2 exist for the same reasons as the maxima in Figure V. 2.

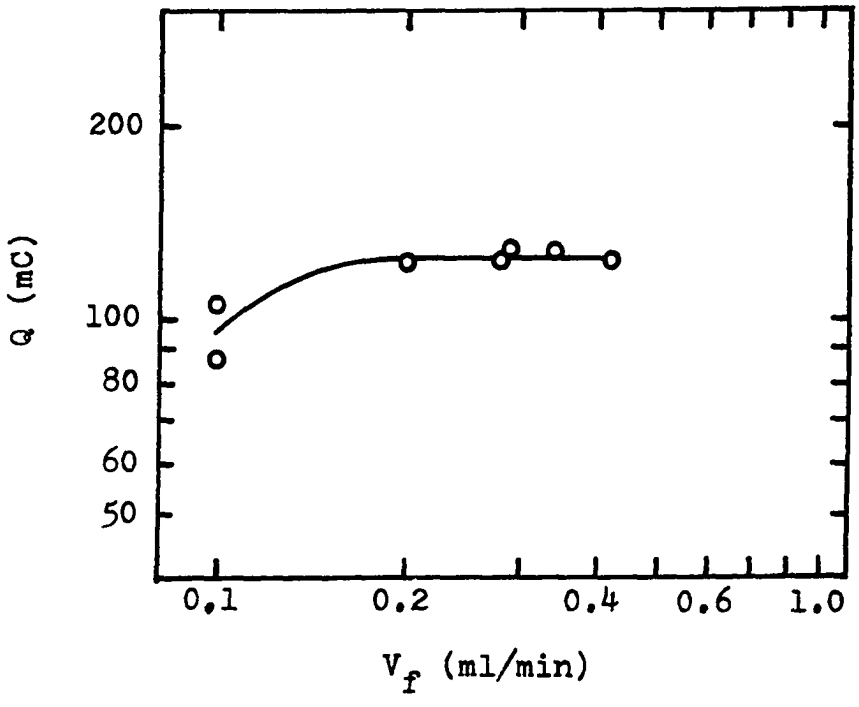

Figure VI. 1. Flow rate study
Cd coulometric detector potentiostated at -0.90 V. 0.665-ml injections of 0.500 m<u>M</u> $NaNO_2$. 1.0 m<u>M</u> $HClO_4$ - 2.0 m<u>M</u> H_2SO_4 eluent mixed with 0.20 <u>M</u> H_2SO_4 in a 1:1 volumetric ratio.

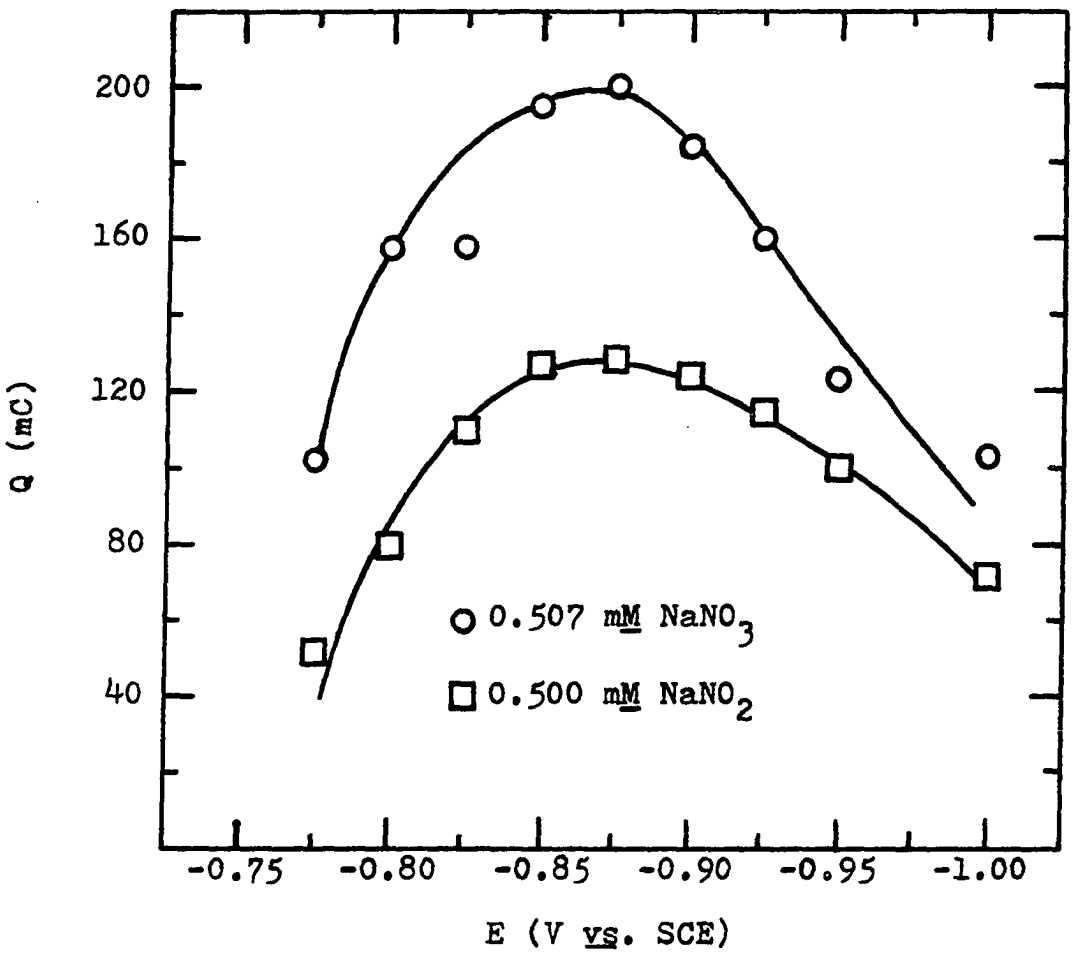

Figure VI. 2. Potential dependence of peak areas Cd coulometric detector. 0.665-ml injections. 1.0 mM $HClO_4$ - 2.0 mM H_2SO_4 eluent flow rate 0.15 ml/min. 0.20 M H_2SO_4 flow rate 0.15 ml/min.

The peak areas at -0.865 V in Figure VI. 2 are concluded to correspond to the total electrolysis of the NO_2^- and NO_3^-. Equation VI. 1 was solved for the value of n with the data in Figure VI. 2. For NO_2^- and NO_3^-, n equals 4.0 and 6.1, respectively. These values correspond to the formation of NH_2OH as the sole product of both reductions within the uncertainty of the integration of the peaks. Hence, the reductions occur according to the following equations in this medium:

$$NO_3^- + 7H^+ + 6e^- \rightarrow NH_2OH + 2H_2O \qquad \text{(VI. 2.)}$$

$$HNO_2 + 4H^+ + 4e^- \rightarrow NH_2OH + H_2O \qquad \text{(VI. 3.)}$$

These reactions are consistent with the fact that NH_2OH is not reduced at a Cd cathode in 0.10 M H_2SO_4 - 5.0 mM $HClO_4$.

3. Reduction products at the RCDE

A characteristic of an electrochemical reaction controlled by the rate of convective-diffusional mass transport is that the concentrations at the electrode surface of the reactant and all intermediate states are virtually zero. The limiting current is related to the concentration of the reactant in the bulk electrolyte by Equation IV. 1. The voltammetric data obtained for the reduction of NO_2^- and NO_3^- in 0.10 M H_2SO_4 were characteristic of faradaic reactions partially controlled by slow reaction kinetics at the electrode surface. Semi-stable intermediates produced electrochemically in a kinetically controlled reaction may

be transported away from the electrode surface by convection and diffusion. These kinetically controlled reactions and reaction intermediates are amenable to study with the RRDE. Products and semi-stable intermediates of electrochemical reactions at the surface of the disk electrode are transported by diffusion and radial convection to the ring electrode where they can be electrolyzed and possibly identified.

The RRDE used for these studies had a glassy-carbon disk and Pt ring. Nitrate, NO_2^-, and NH_2OH are not electroactive at glassy-carbon electrodes. Nitrate and NO_2^- are reduced at the disk at -0.90 V when it is plated with Cd. Current-potential curves of the reduction products and intermediates can then be obtained at the Pt-ring electrode.

An I-E curve of the reduction products of NO_3^- is shown in Figure VI. 3. Nitrate is not electroactive at the Pt ring and does not interfere. The I-E curve of the NO_3^- reduction products is compared to that of the Pt ring in supporting electrolyte. The I-E curve of the reduction products exhibits a small cathodic wave at potentials more negative than 0.0 V, and a large anodic wave at potentials more positive than +0.8 V.

The same anodic wave is observed in an I-E curve of NH_2OH (Figure VI. 4). However, the I-E curve of NH_2OH does not exhibit a cathodic wave at 0.0 V. This cathodic wave

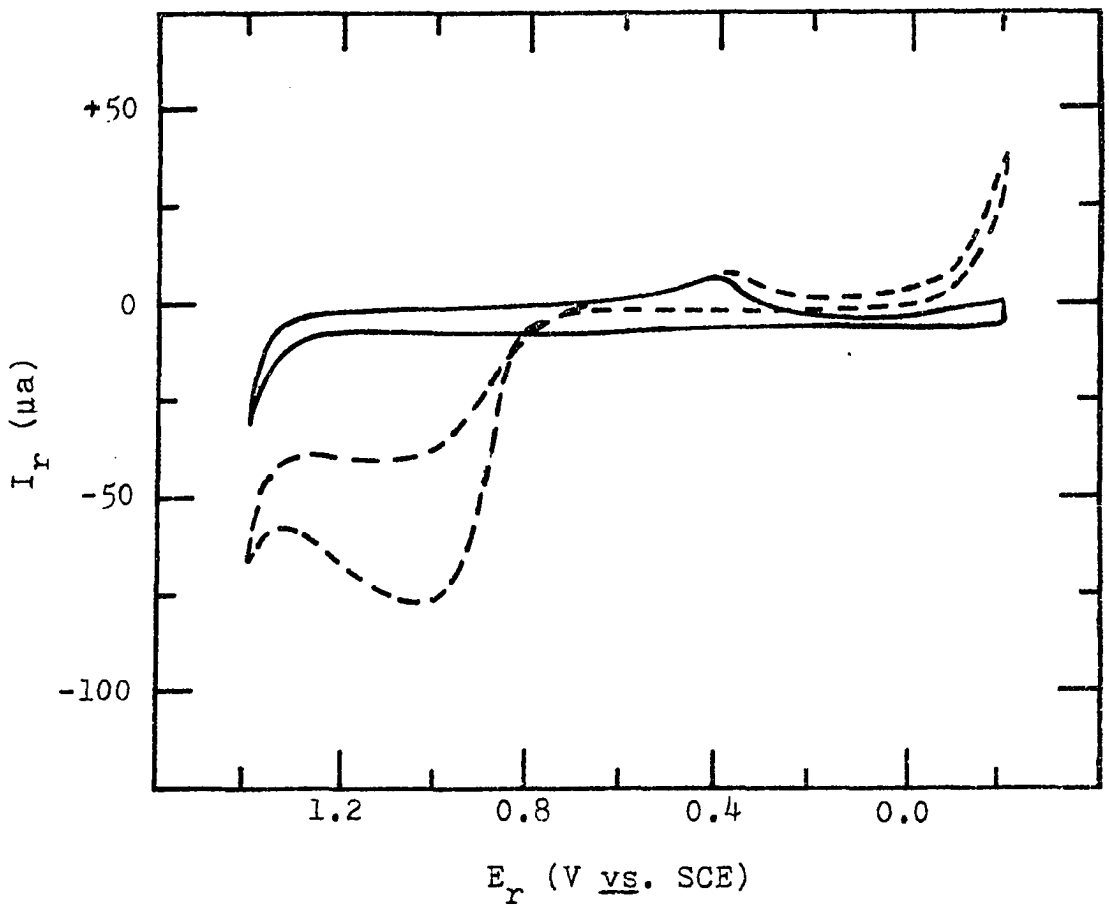

Figure VI. 3. Current-potential curve of the reduction products of $NaNO_3$

Cd-plated disk potentiostated at -0.90 V. Scan rate at Pt-ring electrode 1.0 V/min. Rotational velocity 41.9 rad/sec. 0.10 M H_2SO_4 - 5.0 mM $HClO_4$ electrolyte.

——— no $NaNO_3$

– – – 0.987 mM $NaNO_3$

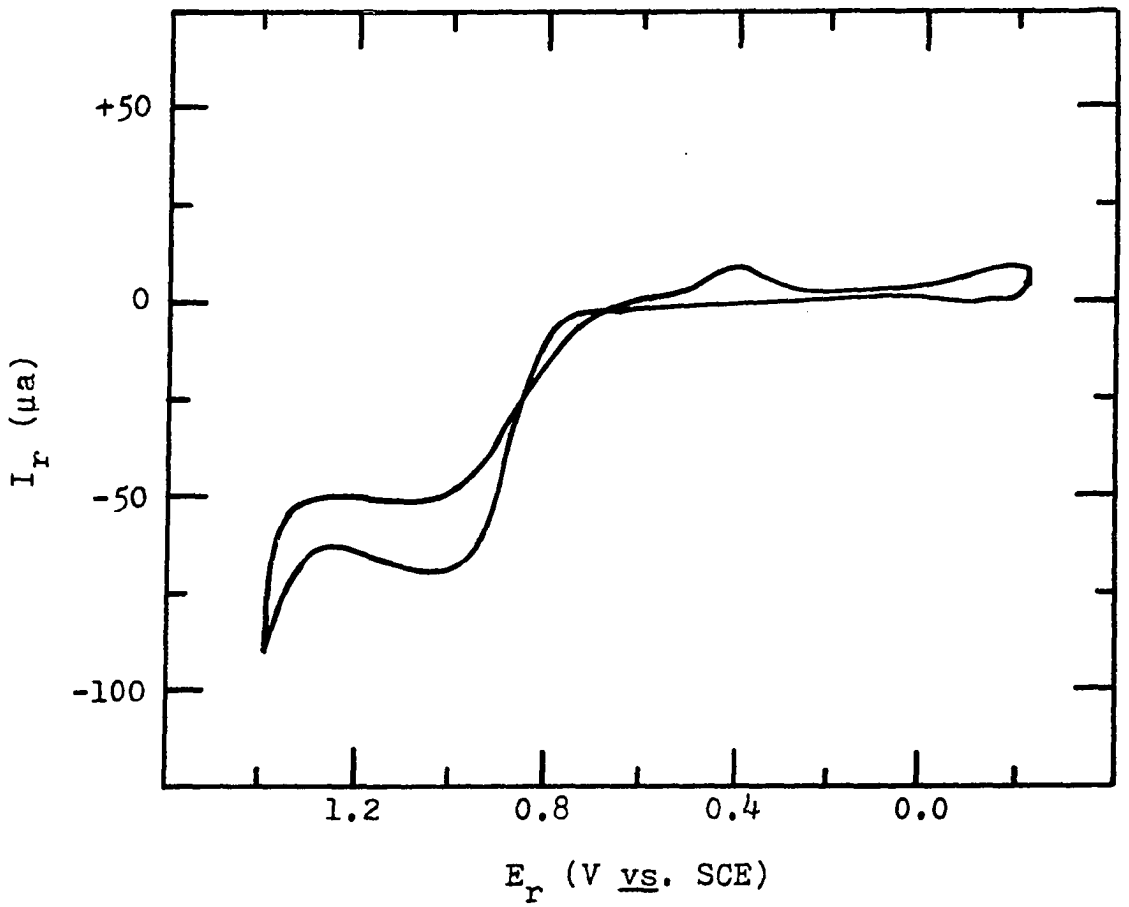

Figure VI. 4. Current-potential curve of NH_2OH at Pt-ring electrode
Glassy-carbon disk potentiostated at 0.0 V. Rotational velocity 41.9 rad/sec. Scan rate 1.0 V/min. 0.2 m$\underline{M}$ $NH_2OH \cdot HCl$ in 0.10 $\underline{M}$ H_2SO_4 - 5.0 m$\underline{M}$ $HClO_4$.

is a characteristic of the I-E curve of NO_2^- at a Pt electrode.

An I-E curve of 0.993 m$\underline{M}$ $NaNO_2$ at the Pt-ring electrode is shown in Figure VI. 5. Nitrite is oxidized at Pt electrodes ($E > 0.8$ V) as well as reduced ($E < 0.0$ V), and the anodic waves of NO_2^- and NH_2OH are indistinquishable. The addition of NH_2OH to a solution containing NO_2^- only increases the height of the single anodic wave (Figure VI. 5). It is concluded that the reduction of NO_3^- to NH_2OH at a RCDE produces some NO_2^-.

Investigations of the reduction products of NO_2^- is complicated because NO_2^- is electroactive at the Pt-ring electrode. Current-potential curves at the ring electrode are shown in Figure VI. 6 when NO_2^- is simultaneously reduced at the disk, and when there is no reaction at the disk electrode. The I-E curve, obtained while NO_2^- was reduced at the disk, exhibits a smaller cathodic wave and larger anodic wave than the other I-E curve. This indicates the expected consumption of NO_2^- at the disk during its reduction there, and the presence of the larger anodic wave implies the formation of NH_2OH.

Equation IV. 1 can be used to calculate n, the average number of equivalents per mole of reactant transported to the RDE surface, from the slopes of plots of I_d $\underline{vs}$. $w^{\frac{1}{2}}$. This was done with the RCDE for 0.499 m$\underline{M}$ $NaNO_2$ and 0.496 m$\underline{M}$ $NaNO_3$

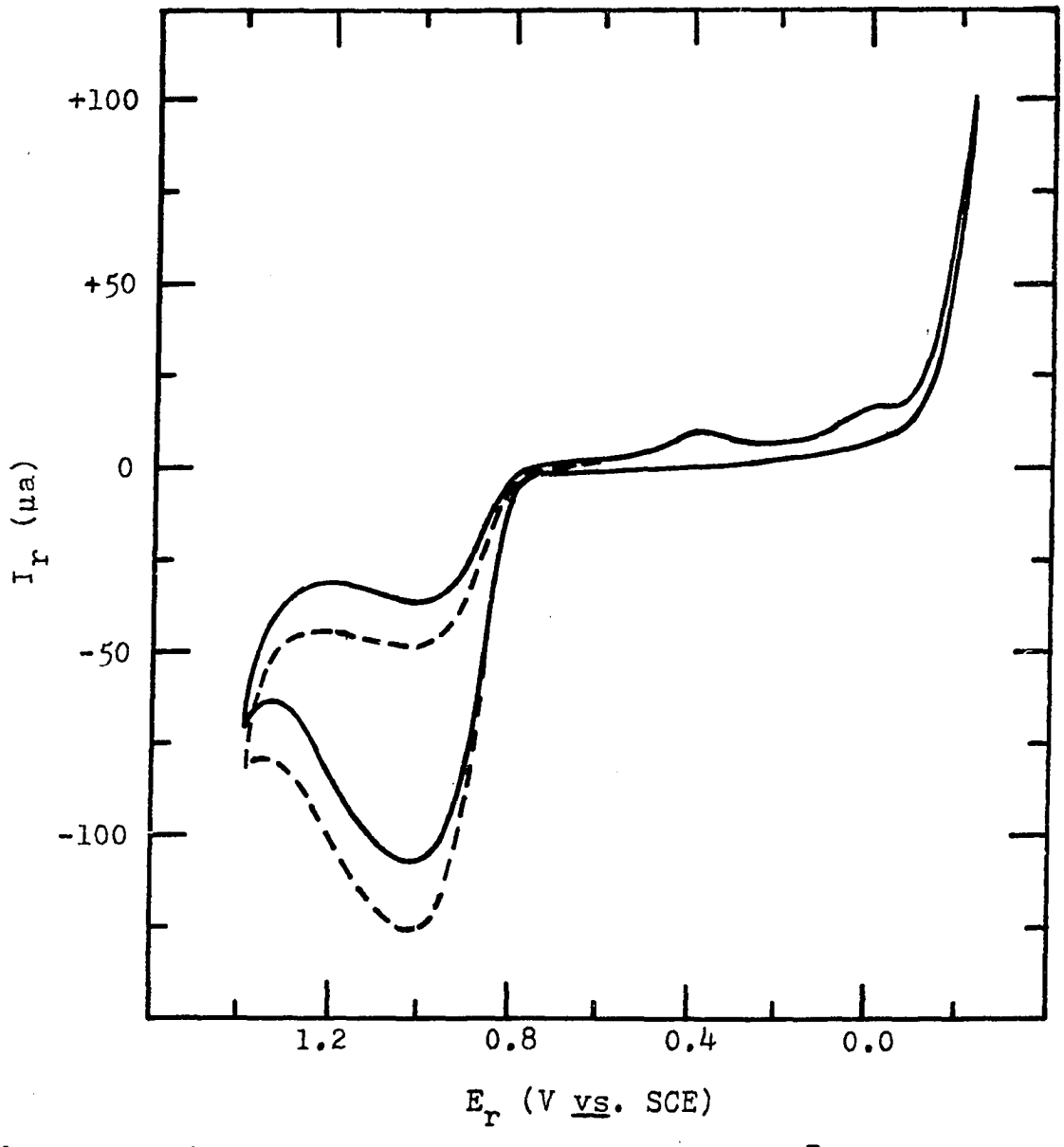

Figure VI. 5. **Current potential curves of NO_2^- and NH_2OH at Pt-ring electrode**

Rotational velocity 41.9 rad/sec. Scan rate 1.0 V/min. 0.10 M H_2SO_4 - 5.0 mM $HClO_4$ electrolyte. Glassy-carbon disk potentiostated at 0.0 V.

——— 0.993 mM $NaNO_2$

– – – 0.993 mM $NaNO_2$ - 0.1 mM $NH_2OH \cdot HCl$

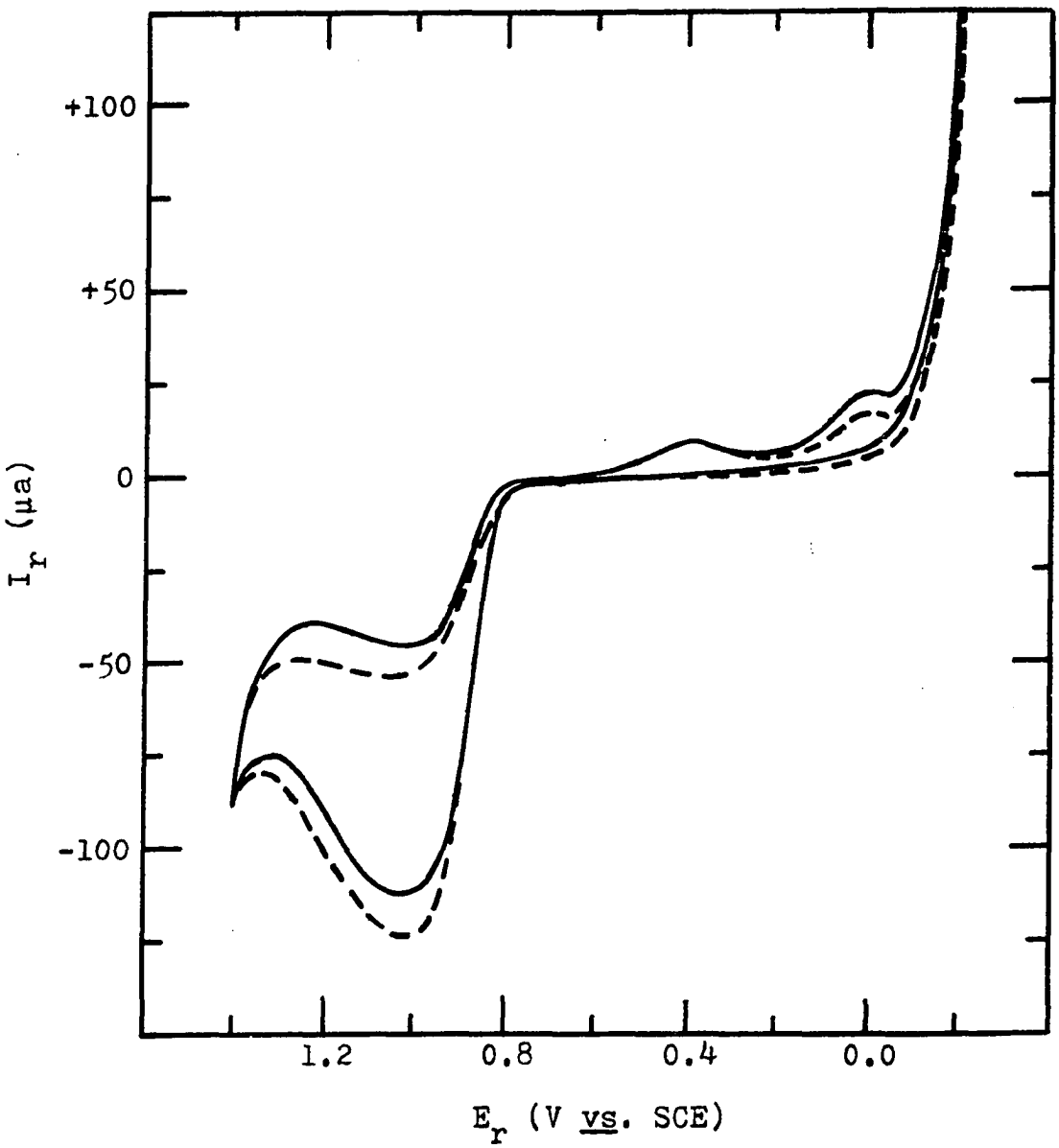

Figure VI. 6. Current-potential curves of NO_2^- and the reduction products of NO_2^- at Pt-ring electrode

Rotational velocity 41.9 rad/sec. Scan rate 1.0 V/min. 0.10 M H_2SO_4 - 5.0 mM $HClO_4$ electrolyte. Concentration of $NaNO_2$ is 0.993 mM.

——— Glassy-carbon disk potentiostated at 0.0 V

– – – Cd-plated disk electrode potentiostated at -0.90 V

in 0.10 M H_2SO_4 - 5.0 mM $HClO_4$. The RCDE was oxidized at 0.0 V for 90 seconds to expose the polycrystalline structure of the disk. This maximized the reversibility of the reductions of NO_2^- and NO_3^- (Chapter IV). The disk current was measured at -1.05 V at rotational velocities as low as 5.25 rad/sec, and the results are shown in Figure VI. 7. The extrapolated intercepts of the plots of I_d vs. $w^{\frac{1}{2}}$ approximate the non-faradaic residual current as expected from Equation IV. 1.

The slope of the plot for NO_2^- in Figure VI. 7, calculated for the lowest two values of $w^{\frac{1}{2}}$, is 0.0516 ma(sec/rad)$^{\frac{1}{2}}$. The value of n calculated for NO_2^- is 2.4, using 0.01 cm^2/sec for ν (4) and assuming the literature value of D for NO_3^-, equal to 1.9 x 10^{-5} cm^2/sec (228), applies to NO_2^-. The value of n equal to 2.4 is just 60% of the value of 4.0 expected for the total conversion of NO_2^- to NH_2OH. The value of n calculated for larger values of $w^{\frac{1}{2}}$ was less than 2.4, which is consistent with the diagnosis of slow reaction kinetics.

The slope of the plot for NO_3^- in Figure VI. 7, calculated for the lowest two values of $w^{\frac{1}{2}}$, is 0.0905 ma(sec/rad)$^{\frac{1}{2}}$, and the value of n calculated from Equation IV. 1 is 4.3. This is 72% of the value of 6.0 expected for the total conversion of NO_3^- to NH_2OH.

Studies with the RRDE at $w^{\frac{1}{2}}$ equal to 6.47 (rad/sec)$^{\frac{1}{2}}$

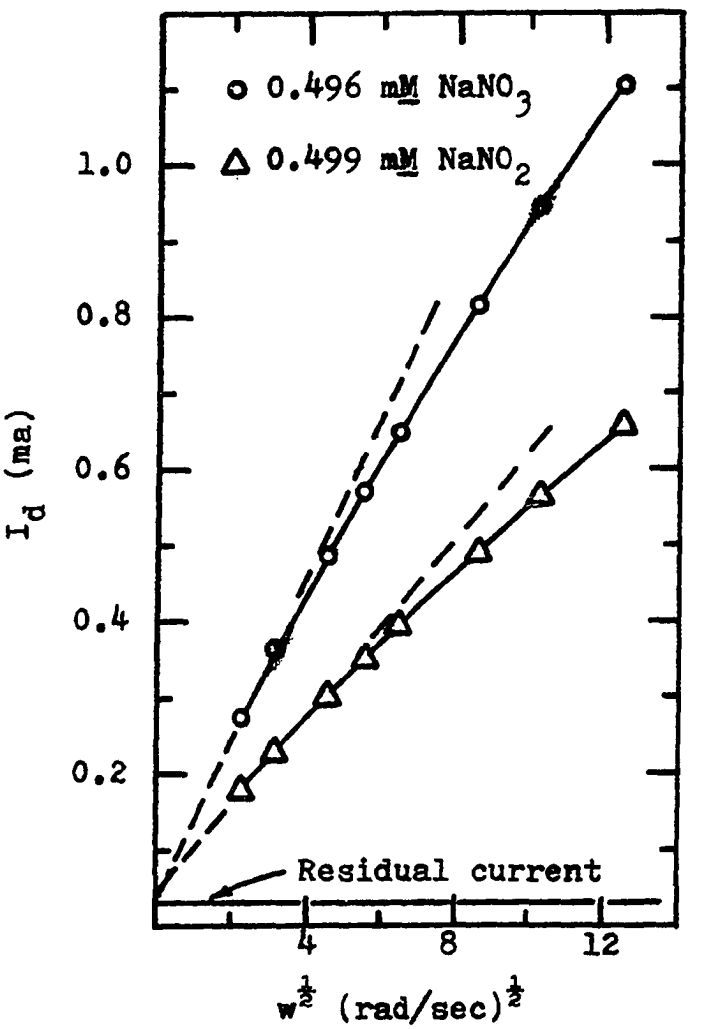

Figure VI. 7. $w^{\frac{1}{2}}$ study of $NaNO_3$ and $NaNO_2$

RCDE, oxidized at 0.0 V for 90 sec. Scan rate 1.0 V/min. I_d measured at -1.05 V. 0.10 M H_2SO_4 - 5.0 mM $HClO_4$ electrolyte.

revealed that NO_2^- is one product of the reduction of NO_3^- at the RCDE. From the data in Figure VI. 7, it was shown that only 60% of the NO_2^- is reduced to NH_2OH for $2.3 \leq w^{\frac{1}{2}} \leq 3.2$ $(rad/sec)^{\frac{1}{2}}$. It is assumed that the only stable products produced from the reduction of NO_3^- are NO_2^- and NH_2OH. The efficiency of the conversion of NO_3^- to NO_2^- can be calculated if the reduction of NO_3^- to NH_2OH proceeds through NO_2^-, which is 60% reduced to NH_2OH as shown in Equations VI. 4 and VI. 5.

$$NO_3^- + 2H^+ + 2e^- \rightarrow NO_2^- + H_2O \qquad \text{(VI. 4.)}$$

$$NO_2^- + 5H^+ + 4e^- \xrightarrow{60\%} NH_2OH + H_2O \qquad \text{(VI. 5.)}$$

The efficiency of the reduction of NO_3^- to NO_2^-, X, can be calculated from the average value of n found for the reduction of NO_3^- to NH_2OH (4.3) and the equivalents per mole in Equations VI. 4 and VI. 5.

$$2X + (0.60)\ (4)\ X = 4.3 \qquad \text{(VI. 6.)}$$

$$X = 98\%$$

Similar calculations show that at higher rotational velocities the reductions shown in Equations VI. 4 and VI. 5 are decreased in efficiency. When $w^{\frac{1}{2}}$ equals 5.6 $(rad/sec)^{\frac{1}{2}}$, VI. 4 is 93% complete and VI. 5 is 58% complete. At the highest rotational velocities in Figure VI. 7, VI. 4 is 85% complete, and VI. 5 is only 50% complete. Neither reduction is extremely fast, but the rate of reduction of NO_2^- to

NH_2OH is slower than that for the reduction of NO_3^- to NO_2^-.

The reduction of NO_3^- and NO_2^- is incomplete at the RCDE at the lowest rotational velocities available; yet, the reduction is complete in the Cd coulometric detector. The incomplete reduction at the RCDE is due to the much greater rate of mass transport at a RDE than at the coulometric electrode. The flux of an electroactive species to an electrode is related to the Reynolds number, N_{Re} (4). The Reynolds number for a RDE is given by Equation VI. 7 (4).

$$N_{Re} = \frac{(r')^2 w}{\nu} \qquad \text{(VI. 7.)}$$

In Equation VI. 7, r' equals the overall radius of the RDE. The Reynolds number of the RCDE at 5.25 rad/sec equals 425, if ν equals 0.01 cm^2/sec.

The Reynolds number for the Cd coulometric detector can be calculated from Equation VI. 8 (4).

$$N_{Re} = \frac{UL}{\nu} \qquad \text{(VI. 8.)}$$

In Equation VI. 8,

U = solution velocity (cm/sec)

L = length of electrode (cm)

The Reynolds number of the coulometric detector, neglecting the volume of the mossy layer of deposited Cd, is only 11 at a flow rate of 0.3 ml/min. Since the flux of NO_2^- and NO_3^- to the surface of the coulometric electrode is much less than to the RCDE, the ions have more time to react and the

efficiency of the reductions is greater. The rates of the reductions are sufficiently slow that NO_3^- and NO_2^- cannot be reversibly reduced at the RCDE even at the lowest rotational velocities.

VII. CHROMATOGRAPHIC ANALYSIS OF SAMPLES

A. Introduction

The reductions of NO_3^- and NO_2^- have been studied with both the RCDE and the Cd tubular detector, and the optimum chromatographic and electrochemical parameters have been determined. In this chapter, procedures are discussed for the application of the chromatographic method to the routine analysis of samples. The results of some of the analyses are compared to those obtained with a standard spectrophotometric method.

B. Experimental

1. Reagents and stock solutions

All H_2O used was triply distilled and deionized, and all other chemicals were reagent grade quality. Stock solutions of $NaNO_2$ and $NaNO_3$ were prepared from dried salts (4 hours at 90°C). The chromatographic eluent and the 0.20 M H_2SO_4 were prepared by diluting J. T. Baker reagent grade acids with H_2O.

2. Chromatographic procedure

The Cd tubular detector, shown in Figure III. 1, and the forced-flow liquid chromatograph, shown in Figure III. 3, were used. Detailed instructions are given below for the routine use of the chromatograph.

Deaerate the solution in each reagent tank by bubbling He through it for 2 hours. This need not be done each time

the chromatograph is used if the tanks are sealed and pressurized when they are not in use.

Seal the tanks and pressurize them to 25 psi with He. After pressurization, adjust the flow rate of both the 0.01 M $HClO_4$ eluent and the 0.20 M H_2SO_4 electrolyte to approximately 0.2 ml/min. Insert a tube connected to an aspirator into the detector cell to remove excess effluent. Eliminate any bubbles of He from the eluent stream through the 3-way valve #1. Allow the flow rates of the eluent and electrolyte to stabilize.

Attach the leads from the potentiostat to the SCE, counter electrode, and Cd tubular detector. If the Electroscan is used, balance the potentiometer and adjust the working electrode potential to -0.90 V. Turn the potentiostat on. Adjust the recorder chart speed and current sensitivity to the desired values.

When the base line no longer drifts, inject the sample and stock solutions. Calculate the unknown concentration from peak area measurements.

To shut down the chromatograph, stop the flow of eluent and electrolyte by tightening the flow-controlling screw clamps. Attach screw clamps to the Teflon tubes running from the manifold to each reagent tank. This prevents mixing of the solutions. Turn off the He at the regulator, and open each reagent tank to release the

pressure. If the chromatograph will be used again soon, leave the tanks pressurized, the He regulator turned on, and only stop the flow of eluent and electrolyte.

Turn the potentiostat off (if the Electroscan is used, leave the main power switch on), and remove the SCE, counter electrode, and aspirator tube from the detector cell. Cover the cell with a watch glass to prevent evaporation of the effluent in it.

3. Preparation of samples

a. Cornstalks Aqueous extracts of cornstalks were provided by the Iowa State University Veterinary Diagnostic Laboratory. The top, middle, and bottom of the cornstalks were separated, air-dried, and chopped. Ten grams of each sample were mixed with 100 ml of H_2O in a 250-ml erlenmeyer flask 1 hour in a wrist-action shaker. The mixtures were filtered, and the aqueous extracts were refrigerated prior to the chromatographic analysis.

The extract of the top of the cornstalks was chromatographically analyzed without dilution. A 0.400-ml aliquot of the middle extract and a 1.00-ml aliquot of the bottom extract were each diluted to 50.0 ml with H_2O.

Stock solutions of $NaNO_2$ and $NaNO_3$ were injected before and after the cornstalk extracts to prepare a calibration curve.

b. Oat hay A sample of oat hay was analyzed after

10.1 g of the finely chopped, air-dried hay was mixed with 100 ml of H_2O in a Waring blender at the highest speed for 5 minutes in this laboratory. A portion of the mixture was centrifuged and filtered through Whatman 41 paper. This extract was chromatographically analyzed immediately after its preparation.

A 2.00-ml aliquot of the extract was diluted to 100 ml with H_2O prior to the chromatographic analysis. The NO_3^- peak area was compared to the peak areas from 0.200 mM and 0.400 mM $NaNO_3$ stock solutions.

c. Water A sample of H_2O, from Squaw Creek in Ames, Iowa, was collected, and particulate material was allowed to settle to the bottom of the collection vessel. The H_2O was chromatographically analyzed without dilution soon after it was collected. The NO_3^- peak area from the H_2O sample was compared to peak areas from 0.400, 0.600, and 0.800 mM $NaNO_3$ stock solutions.

The cornstalk extracts and the oat hay were analyzed by the I.S.U. Veterinary Diagnostic Laboratory. The Diagnostic Laboratory analyzed the same cornstalk extracts that were analyzed chromatographically, but prepared their own extract of the oat hay using the procedure for the cornstalks. The Diagnostic Laboratory determined NO_3^- spectrophotometrically by reducing it to NO_2^- with N_2H_4. The NO_2^- was diazotized with sulfanilamide and coupled with N-(1-naphthyl)ethylene-

diamine. The total NO_2^- and NO_3^- concentration was reported as NO_3^-. The oat hay extract prepared by the Diagnostic Laboratory was decolorized with activated charcoal.

C. Results and Discussion

The cornstalks taken for analysis were suspected of containing a toxic concentration of NO_3^-. Five cattle had eaten some of the cornstalks and died, exhibiting symptoms of methemoglobinemia. The top, the middle, and the bottom of the cornstalks were sampled and analyzed for NO_3^- by the I.S.U. Veterinary Diagnostic Laboratory.

The extract of the tops was slightly yellow. The other extracts were colorless, and none were turbid. The spectrophotometric results from the Diagnostic Laboratory compared well with the chromatographic results, as shown in Table VII. 1. The results from the two methods agree to within 10% for the middle and bottom of the cornstalks. The chromatographic method showed that the top of the cornstalks contained 140 ppm NO_2^- in addition to 580 ppm NO_3^-. The spectrophotometric method did not report the NO_2^- because NO_2^- was not expected to be present and was not sought. Nitrite is considerably more toxic than NO_3^- (54, 78a); therefore, it is advantageous to detect NO_2^- even when it is not expected to be in a sample. Nitrite was not detected in the extract of the middle or the bottom of the cornstalks.

The extract of the oat hay was turbid and brown, but it

Table VII. 1. Analytical results

Sample	Chromatographic Results	Spectrophotometric Results
Top of cornstalks	5.8×10^2 ppm NO_3^- 1.4×10^2 ppm NO_2^-	7.22×10^2 ppm NO_3^-
Middle of cornstalks	3.4×10^3 ppm NO_3^- NO_2^- not detected	3.1×10^3 ppm NO_3^-
Bottom of cornstalks	3.8×10^3 ppm NO_3^- NO_2^- not detected	3.7×10^3 ppm NO_3^-
Oat hay	6.27×10^3 ppm NO_3^-	4.8×10^3 ppm NO_3^-
Squaw Creek water	34.1 ppm NO_3^-	———

was analyzed chromatographically without difficulty. A chromatogram of the diluted extract is shown in Figure VII. 1 with a chromatogram of a 0.200 m$\underline{M}$ $NaNO_3$ stock solution for comparison.

Figure VII. 2 is a calibration curve prepared for the analysis of the oat hay. A straight line was drawn through two points, corresponding to peak areas from standard solutions of $NaNO_3$, and the origin. The diluted oat hay

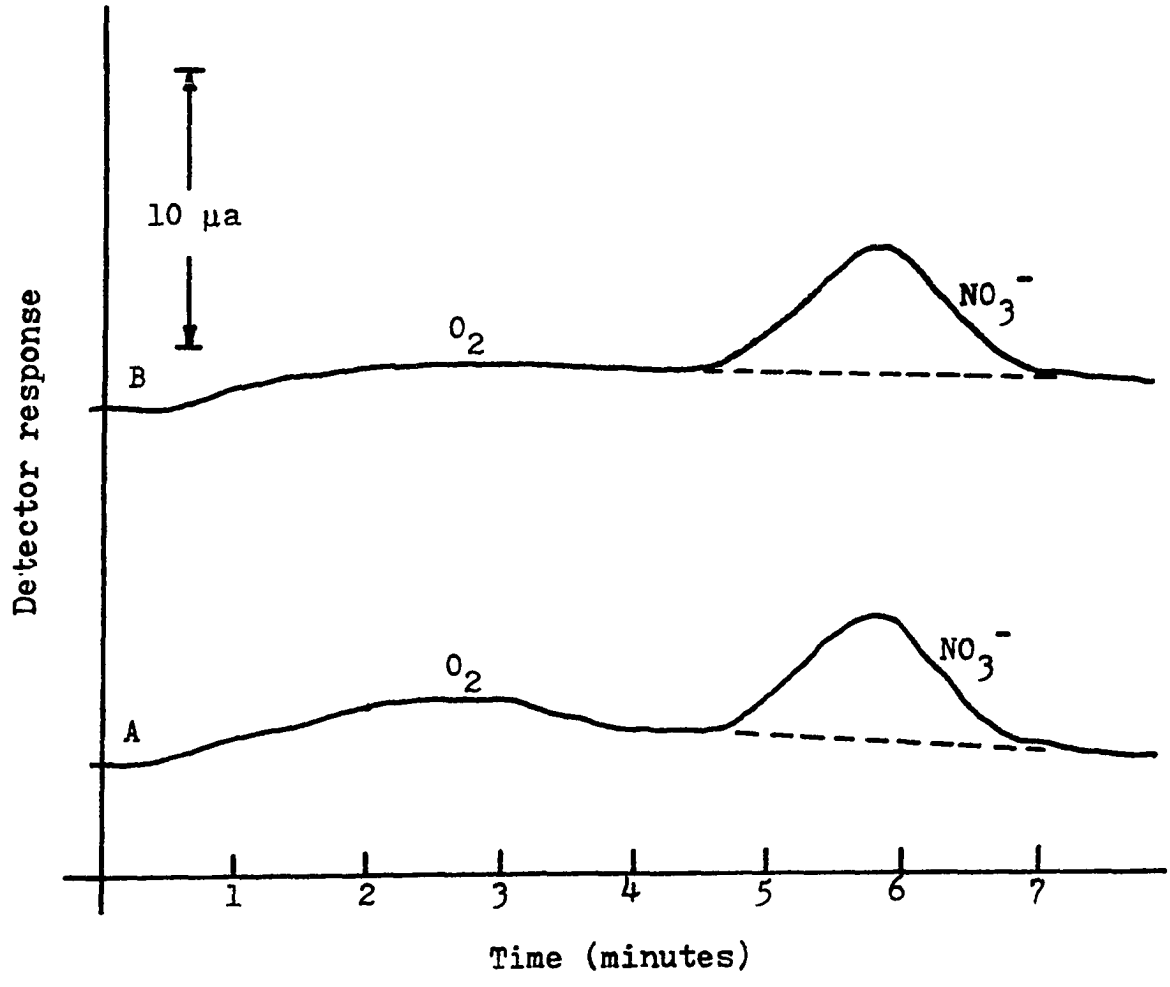

Figure VII. 1. Analysis of oat hay
Cd tubular detector potentiostated at -0.90 V. 0.010 M $HClO_4$ eluent flow rate 0.2 ml/min. 0.20 M H_2SO_4 flow rate 0.2 ml/min. 0.33-ml injections.
A - 0.200 mM $NaNO_3$ stock solution
B - Oat hay extract, diluted 1:50

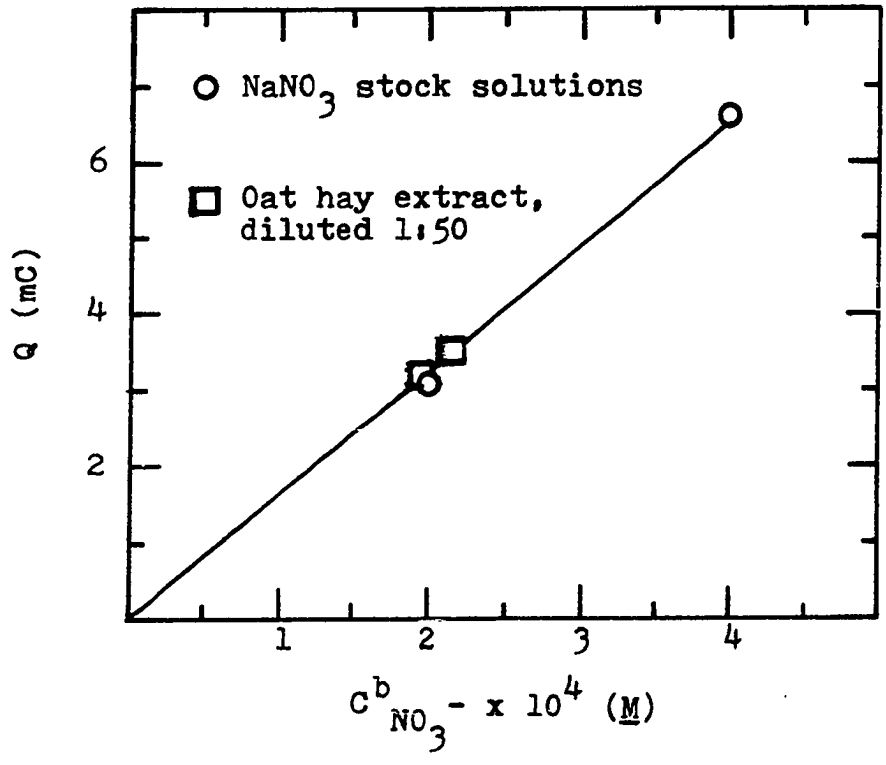

Figure VII. 2. Calibration curve for analysis of oat hay
Cd tubular detector potentiostated at -0.90 V. 0.010 M $HClO_4$ eluent flow rate 0.2 ml/min. 0.20 M H_2SO_4 flow rate 0.2 ml/min. 0.33-ml injections

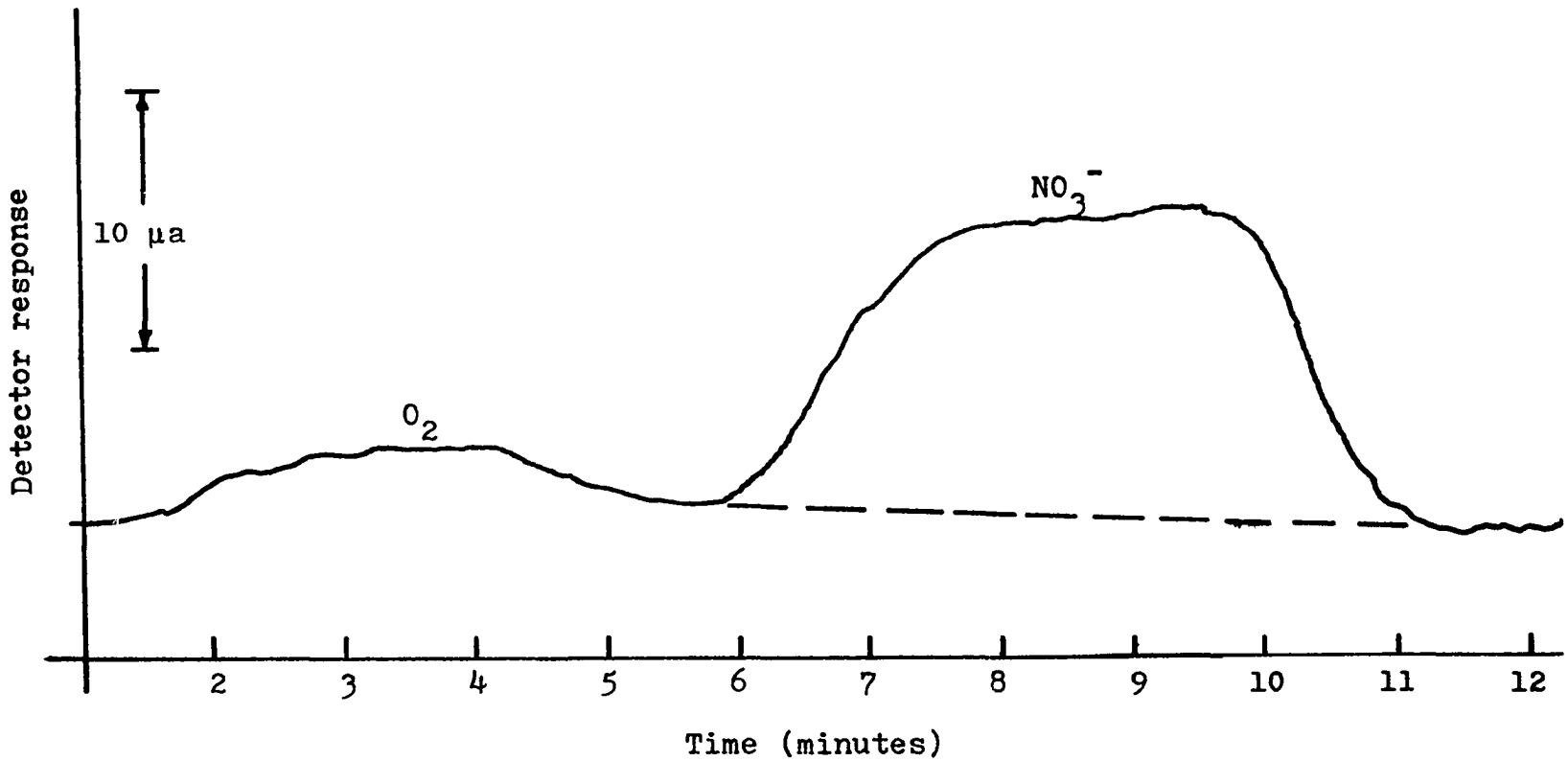

Figure VII. 3. Chromatogram of H_2O from Squaw Creek Cd tubular detector potentiostated at -0.90 V. 0.010 M $HClO_4$ eluent flow rate 0.15 ml/min. 0.20 M H_2SO_4 flow rate 0.15 ml/min. 0.33-ml injection.

extract was injected twice, and the two NO_3^- peak areas correspond to concentrations of 0.215 and 0.195 mM NO_3^- from the calibration curve. The average of the concentrations of NO_3^- calculated for the oat hay is 6.27×10^3 ppm (Table VII. 1).

The spectrophotometric result from the analysis of the oat hay was 4.8×10^3 ppm NO_3^-. Assuming the extraction procedure used by the Diagnostic Laboratory was quantitative, the large discrepancy between the results of the chromatographic and spectrophotometric methods may be a result of the decolorization of the extract with activated charcoal prior to the spectrophotometric analysis. Some NO_3^- may have been adsorbed on the charcoal and lost from the solution. This discrepency in the results emphasizes the possible errors inherent in some clarification procedures.

A chromatogram of H_2O from Squaw Creek is shown in Figure VII. 3. The flow rate of the eluent was decreased from 0.2 to 0.15 ml/min to resolve the NO_3^- peak from the very large dissolved O_2 peak. The NO_3^- concentration was calculated from a calibration curve like that in Figure VII. 2 to be 0.552 mM (34.1 ppm NO_3^-). Nitrite was not detected.

The broad shape of the NO_3^- peak implies the presence of large quantities of electroinactive salts (Chapter V). These salts cause little error in the chromatographic method (see Table V. 1), but do cause significant errors in the

standard spectrophotometric methods (156). Therefore, the chromatographic method is expected to provide more accurate results than the spectrophotometric method for many clear samples.

VIII. SUMMARY

Nitrate and NO_2^- are reduced to NH_2OH at Cd cathodes in 0.10 M H_2SO_4 - 5.0 mM $HClO_4$. Nitrite is an intermediate in the reduction of NO_3^-. The reduction of NO_3^- to NO_2^- is nearly complete at a RCDE at low rates of mass transport, but the reduction of NO_2^- is kinetically slower.

The rates of the reductions of NO_3^- and NO_2^- are decreased as the acidity of the electrolyte is decreased. Nitrate is quantitatively reduced to NO_2^- in a Cd reduction column in a standard spectrophotometric procedure of the AOAC because the pH equals 9.6 and the rate of the reduction of NO_2^- at Cd is slow (14).

The rates of the reductions of NO_2^- and NO_3^- at a RCDE are increased when the electrode is oxidized to expose more active sites on the electrode surface. The reductions approach convective-diffusion control at low rates of mass transport at the oxidized RCDE.

A Cd coulometric detector cannot be used for routine analyses because it is quickly plugged with deposited Cd. However, a Cd tubular electrode is durable and can be used as the detector for a forced-flow liquid chromatograph. Dissolved O_2, NO_2^-, and NO_3^- are separated in 8 - 9 minutes using Amberlite IRA-900 resin and 0.010 M $HClO_4$ as the eluent.

The peak areas for NO_2^- and NO_3^- are linear functions

of concentration when the eluent is mixed with 0.20 M H_2SO_4 to increase its acidity. The working range of concentrations is 0.05 - 1.0 mM, and the detection limit is 0.01 mM for NO_2^- and NO_3^-.

Only BrO_3^-, SO_3^{-2}, and I^- were found to interfere with the analysis. Cationic interferences were removed from the eluent by a cation-exchange column in the chromatograph.

Analysis of samples can be accomplished with relative errors less than 2% and relative standard deviations of 3%. Cornstalks, oat hay, and surface H_2O samples were analyzed, and the chromatographic results compared well with spectrophotometric results.

The chromatographic method is well-suited for the analysis of colored and turbid samples and samples that contain large concentrations of Cl^- and other salts that interfere with standard methods. The chromatographic method is rapid, convenient, and requires little laboratory skill.

IX. SUGGESTIONS FOR FUTURE WORK

Oxidation of a polished RCDE exposes the polycrystalline inner-structure of the electrode to the solution, and the rates of the reductions of NO_2^- and NO_3^- at the RCDE are increased. Some of the crystal planes of Cd may be particularly reactive, and these planes may be exposed when the RCDE is oxidized. Voltammetric studies with an electrode constructed from a single crystal of Cd might prove that hypothesis. The reductions of NO_2^- and NO_3^- at the different faces of the crystal would be compared.

A major advantage of any chromatographic method is the rapidity of each analysis. The chromatographic determination of NO_3^- and NO_2^- requires 7 to 9 minutes per sample. This time could be shortened to 3 to 4 minutes with higher eluent flow rates and a longer, high-resolution anion-exchange column. The cation-exchange column is unnecessary for most samples, and its removal would shorten the time per analysis. A shorter tubular detector could be used to achieve higher resolution.

Coulometric detectors are more sensitive and precise than tubular detectors, but the Cd coulometric detector was quickly plugged with deposited Cd. A coulometric detector might be made from a carbon tube packed with carbon particles. The packed carbon detector would be plated with Cd for coulometric efficiency in the determination of NO_3^- and NO_2^-.

When it became plugged, the Cd would be anodically stripped from the electrode, and a fresh layer of Cd would be deposited. Thus, the electrode could be rejuvenated without disassembly.

More samples should be analyzed after the above improvements have been made to evaluate the method. Fertilizers and meat products should be analyzed, and the results compared to a standard method.

The chromatographic determination of NO_3^- might be applied to the determination of the total nitrogen content of samples. Oxidation of nitrogen species during the Kjeldahl digestion leads to errors in that method. Total oxidation of organic samples with $HClO_4$ or some other strong oxidizing agent, possibly in a sealed container to avoid the loss of gaseous intermediates, may quantitatively convert those nitrogen species to NO_3^-. Then the NO_3^- concentration would be determined chromatographically.

The large hydrogen overpotential of Cd electrodes might be useful in the analysis of some reducible organic compounds. Nitrobenzenes are electroactive at Cd cathodes, and other organic compounds may be determined chromatographically with a Cd tubular detector.

X. BIBLIOGRAPHY

1. W. Abbott, J. Miss. Acad. Sci. 14, 11 (1968).

2. F. N. Abercrombie and A. L. Caskey, Trans. Ill. State Acad. Sci. 62, 161 (1969).

3. M. K. Achtzehn and H. Hawat, Lebensm.-Ind. 19, 482 (1972).

4. R. N. Adams, Electrochemistry at Solid Electrodes (Marcel Dekker, New York, 1969), pp. 43-104.

5. R. I. Agladze, D. E. Karchava, and R. K. Kvaratskheliya, Soobshch. Akad. Nauk Gruz. SSR 52, 75 (1968).

6. R. I. Agladze, D. E. Karchava, and R. K. Kvaratskheliya, Soobshch. Akad. Nauk Gruz. SSR 53, 345 (1969).

7a. R. I. Agladze, D. E. Karchava, and R. K. Kvaratskheliya, Soobshch. Akad. Nauk Gruz. SSR 56, 89 (1972).

7b. W. J. Albery and M. L. Hitchman, Ring-Disc Electrodes (Oxford University Press, London, 1971), pp. 17-28.

8a. R. E. Allen, Department of Chemistry, Iowa State University, personal communication.

8b. American Public Health Association, Standard Methods for Examination of Water and Wastewater, 12th ed. (American Public Health Assoc., New York, 1965), pp. 195-200.

9. S. Aoyagi, J. Chem. Soc. Japan 78, 369 (1957).

10. S. Aoyagi, Tokyo Kogyo Daigaku Gakuho, Ser. A, 1 (1959).

11. J. Armand and P. Souchay, Chim. Anal. (Paris) 44, 239 (1962).

12. F. A. J. Armstrong, C. R. Stearns, and J. D. H. Strickland, Deep-Sea Res. Oceanogr. Abstr. 14, 381 (1967).

13. E. A. Ashikhmin, Uch. Zap., Permsk. Gos. Univ. 25, 34 (1963).

14. Association of Official Analytical Chemists, Official Methods of Analysis of the Association of Official Analytical Chemists, edited by W. Horwitz (AOAC, Washington, D.C., 1970), p. 126.

15. E. L. Atlas, S. W. Hager, L. I. Gordon, and P. K. Park, U.S. Nat. Tech. Infor. Serv., AD Rep. No. 730482, 1971.

16. M. Aulesheva, M. T. Saibova, and Kh. R. Rustamov, Uzb. Khim. Zh. 17, 18 (1973).

17. W. I. Awad and S. S. M. Hassan, Talanta 16, 1383 (1969).

18. W. I. Awad, S. S. M. Hassan, and M. T. M. Zaki, Talanta 18, 219 (1971).

19. A. S. Baker and R. Smith, J. Agr. Food Chem. 17, 1284 (1969).

20. M. Bartik and J. Kupka, Slov. Akad. Vied. Folia Veterin. Fac. Med. Veterin. Cas. 1, 229 (1956).

21. R. Bastian, R. Weberling, and F. Palilla, Anal. Chem. 29, 1795 (1957).

22. F. Baumann, J. Electroanal. Chem. 6, 245 (1963).

23. P. H. T. Beckett, Nature 186, 879 (1960).

24. F. A. Belinskaya, E. A. Materova, L. A. Karmanova, and V. I. Kozyreva, Elektrokhimiya 7, 214 (1971).

25. M. L. Bernard, A. Barbey, J. Breqeon, and M. Lezay, Compt. Rend. 260, 6101 (1965).

26. V. M. Bhuchar and V. K. Amar, Indian J. Technol. 10, 433 (1972).

27. W. J. Blaedel and S. L. Boyer, Anal. Chem. 43, 1538 (1971).

28. W. J. Blaedel and L. N. Klatt, Anal. Chem. 38, 879 (1966).

29. W. J. Blaedel, C. L. Olson, and R. L. Sharma, Anal. Chem. 35, 2100 (1963).

30. R. M. Bly, Ph.D. thesis, University of Illinois (1961) (unpublished).

31. V. A. Bork, L. A. Shvyrkova, and M. I. Aparsheva, Tr. Konf. Anal. Khim. Nevodn. Rastvorov Ikh Fiz.-Khim. Svoistvam 1, 186 (1968).

32. N. Bousset-Fatianoff, Ph. Gouet, C. Bes, and N. Mouhous, Ann. Biol. Anim., Biochim., Biophys. 11, 705 (1971).

33. J. A. Brabson and W. G. Burch, Jr., J. Ass. Off. Agr. Chem. 47, 1035 (1964).

34. P. Bro and H. Y. Kang, J. Electrochem. Soc. 118, 519 (1971).

35. S. Bruckenstein and B. Miller, J. Electrochem. Soc. 117, 1040 (1970).

36. N. G. Bunton and N. T. Crosby, Water Treat. Exam. 18, 338 (1969).

37. M. Busch, Ber. 38, 861 (1905).

38. K. Cammann, Beckman Rep. 1, 21 (1970).

39. D. J. Cantliffe, G. E. MacDonald, and N. H. Peck, N. Y. Food Life Sci. Bull., No. 3 (1970).

40. D. Ceausescu and F. Pirvu, Rev. Chim. (Bucharest) 9, 305 (1958).

41. D. Ceausescu and A. Sirbu, Chim. Anal. (Bucharest) 2, 187 (1972).

42. B. Chapman, G. H. Cooke, and R. Whitehead, Water Pollut. Contr. 66, 185 (1967).

43. S. S. Chaterjee and B. K. Banerjee, Technology 8, 285 (1971).

44. R. Chavdarova, Dokl. Bolg. Akad. Nauk 26, 227 (1973).

45. R. Chavdarova, Dokl. Bolg. Akad. Nauk 26, 403 (1973).

46. D. Chow and R. Robinson, Anal. Chem. 25, 1493 (1953).

47. G. Cinquina, Chimica 3, 363 (1948).

48. R. G. Clem, Anal. Chem. 43, 1853 (1971).

49. C. J. Coetzee and H. Freiser, Anal. Chem. 40, 2071 (1968).

50. C. J. Coetzee and H. Freiser, Anal. Chem. 41, 1128 (1969).

51. F. A. Cotton and G. Wilkinson, Advanced Inorganic Chemistry (Interscience, New York, 1967), p. 349.

52. D. J. Curran, Ph.D. thesis, University of Illinois (1961) (unpublished).

53. R. J. Davenport and D. C. Johnson, Anal. Chem. 45, 1979, (1973).

54. I. Davidsohn and J. B. Henry, Clinical Diagnosis by Laboratory Methods, 14th ed. (W. B. Saunders Co., Philadelphia, 1969), pp. 135, 592.

55. A. W. Davies and K. Taylor, 2nd Technicon Symp., New York, London, 1965.

56. J. E. W. Davies, G. J. Moody, and J. D. R. Thomas, Analyst (London) 97, 87 (1972).

57. G. S. Davtyan, Soobshch. Inst. Agrokhim. Probl. Gidroponiki, Akad. Nauk Arm, SSR No. 12, 116 (1972).

58. R. B. Dean and W. J. Dixon, Anal. Chem. 23, 636 (1951).

59. J. H. de Lange, Chem. Tech. Rev. 21, 636 (1966).

60. W. L. Delvin and L. R. Duncan, USAEC Report No. HW-SA-2635, 1962 (unpublished).

61. G. S. Deshmukh and S. V. S. S. Murty, Indian J. Chem. 1, 316 (1963).

62. B. M. Dikova, Khim. Ind. (Sofia) 43, 35 (1971).

63. T. N. Dobbelstein and H. Diehl, Talanta 16, 1341 (1969).

64. L. J. Dombrowski and E. J. Pratt, Anal. Chem. 44, 2268 (1972).

65. L. R. Duncan, USAEC Report No. HW-SA-2118, 1961 (unpublished).

66. R. A. Durst, Ion-Selective Electrodes, Natl. Bur. Std. Special Publication No. 314, pp. 375-414.

67. H. Fadrus and J. Maly, Fresenius' Z. Anal. Chem. 246, 239 (1969).

68. R. F. Falcao, Rev. Port. Farm. 17, 460 (1967).

69. G. Faraone and M. Trozzi, Atti Soc. Peloritana Sci. Fis. Mat. Nat. 7, 233 (1961).

70. W. Fiddler, E. G. Piotrowski, J. W. Pensabene, R. C. Doerr, and A. E. Wasserman, J. Food Sci. 37, 668, (1972).

71. J. G. A. Fiskell and H. L. Breland, Soil Crop Sci. Soc. Fla., Proc. 29, 63 (1970).

72. R. E. Frazier, J. Am. Waterworks Ass. 55, 624 (1968).

73. J. R. Freney, Commun. Soil Sci. Plant Anal. 2, 479 (1971).

74. J. R. Freney and R. Wetselaar, Aust. Commonwealth Sci. Ind. Res. Organ. Div. Plant Ind., Tech. Paper No. 23, 1967.

75. A. N. Frumkin and G. M. Florianovich, Doklady Akad. Nauk SSSR 80, 907 (1951).

76. A. N. Frumkin and S. I. Zhdanov, Doklady Akad. Nauk SSSR 97, 867 (1954).

77. R. Fudge and R. W. Truman, J. Ass. Pub. Anal. 11, 19 (1973).

78a. R. J. Garner, Veterinary Toxicology, 2nd ed. (The Williams and Wilkins Co., Baltimore, 1963), p. 111.

78b. D. G. Gehring, W. A. Dippel, and R. S. Boucher, Anal. Chem. 42, 1686 (1970).

79. A. Ya. Getmanets and G. G. Farenik, Khim. Sel. Khoz. 9, 867 (1971).

80. C. Ghimicescu and V. Dorneanu, Talanta 19, 1474 (1972).

81. T. W. Gilbert and R. A. Dobbs, Anal. Chem. 45, 1390 (1973).

82. L. Giuffre, E. Losio, and R. F. Lamma, Ann. Chim. (Rome) 57, 1450 (1967).

83. G. I. Gleason, J. Chem. Ed. 50, 718 (1973).

84. I. T. Glover and F. T. Johnson, J. Chem. Ed. 50, 426 (1973).

85. Z. R. Grabowski, Roczniki Chem. 27, 285 (1953).

86. D. N. Gritsan, G. V. Pentsova, V. D. Kalugin, and L. D. Gritsan, Dopov. Akad. Nauk Ukr. SSR, Ser. B 33, 543 (1971).

87. O. Guertler and H. Holzapfel, Angew. Makromol. Chem. 7, 194 (1969).

88. A. Gutbier, Z. Angew. Chem. 18, 494 (1905).

89. S. W. Hager, E. L. Atlas, L. I. Gordon, A. W. Mantyla, and P. K. Park, Limnol. Oceanogr. 17, 931 (1972).

90. G. P. Haight, Jr., Acta Chem. Scand. 15, 2012 (1961).

91. G. P. Haight, Jr. and A. Reynard, presented at the ACS Conf. Anal. Chem., Pittsburgh, 1952; Anal. Chem. 24, 499 (1952).

92. H. Hamaguchi, J. Hashimoto, and N. Fukushi, Nippon Kagaku Zasshi 79, 1482 (1958).

93. H. Hamaguchi, R. Kuroda, and S. Endo, Bunseki Kagaku 7, 409 (1958).

94. R. E. Hamm and C. D. Withrow, Anal. Chem. 27, 1913 (1955).

95. W. E. Harris and I. M. Kolthoff, J. Am. Chem. Soc. 67, 1484 (1945).

96. A. M. Hartley and R. M. Bly, Anal. Chem. 35, 2094 (1963).

97. A. M. Hartley and D. J. Curran, Anal. Chem. 35, 686 (1963).

98. H. Hawat and M. K. Achtzehn, Nahrung 16, 359 (1972).

99. E. Hein, Arch. Tierernaehr. 23, 165 (1973).

100. C. R. Hipkin and P. J. Syrett, New Phytol. 72, 47 (1973).

101. L. Holleck, Z. Electrochem. 49, 400 (1943).

102. J. G. Holty and H. S. Potworowski, Environ. Sci. Technol. 6, 835 (1972).

103. H. Holzapfel and O. Guertler, J. Prakt. Chem. 35, 70 (1967).

104. M. E. Houser and M. I. Fauth, Microchem. J. 15, 399 (1970).

105. Y. Inoue, Hisoshima Daigaku Igaku Zasshi 20, 347 (1972).

106. Y. Inoue, Hisoshima Daigaku Igaku Zasshi 20, 357 (1972).

107. M. Ishidate, A. Tanimura, Y. Ito, A. Sakai, H. Sakuta, T. Kawamura, K. Sakai, F. Miyazawa, and H. Wada, Nippon Yakuzaishikai Zasshi 23, 47 (1971).

108. S. Ivanko and A. Branik, Pol'nohospodarstvo 18, 627 (1972).

109. I. Izumi, Denki Kagaku 40, 358 (1972).

110. D. Jenkins and L. L. Medsker, Anal. Chem. 36, 610 (1964).

111. G. S. Johar and G. D. Tiwari, Fresenius' Z. Anal. Chem. 265, 32 (1973).

112. D. B. Johnson, Ir. J. Agr. Res. 9, 271 (1970).

113a. D. C. Johnson, D. T. Napp, and S. Bruckenstein, Anal. Chem. 40, 482 (1968).

113b. D. C. Johnson and J. Larochelle, Talanta 20, 959 (1973).

114. J. W. Johnson, E. Deng, S. C. Lai, and W. J. James, J. Electrochem. Soc. 114, 424 (1967).

115. M. G. Johnson and R. J. Robinson, Anal. Chem. 24, 366 (1952).

116. E. Julien and M. Comtat, Rev. Chim. Miner. 6, 885 (1969).

117. B. N. Kabanov, N. N. Tomashova, and I. G. Kiseleva, Elektrokhimiya 6, 612 (1970).

118. L. J. Kamphake, S. A. Hannah, and J. M. Cohen, Water Res. 1, 205 (1967).

119. D. E. Karchava and R. K. Kvaratskheliya, Soobshch. Akad. Nauk Gruz. SSR 65, 361 (1972).

120. Y. Katsube, K. Uesugi, and J. H. Yoe, Bull. Chem. Soc. Japan 34, 743 (1961).

121. E. A. Khomskaya and A. S. Kolosov, Elektrokhimiya 8, 918 (1972).

122. N. E. Khomutov and U. S. Stamkulov, Elektrokhimiya 7, 332 (1971).

123. S. Kihara, Electroanal. Chem. Interfac. Electrochem. 45, 31 (1973).

124. S. Kihara, Electroanal. Chem. Interfac. Electrochem. 45, 45 (1973).

125. Y. S. Kim, K. Y. Yim, and K. S. Lee, Kungnip Kongop Yonguso Pogo 15, 146 (1965).

126. O. Klee, Mikrokosmos 58, 42 (1969).

127. B. M. Kneebone and H. Freiser, Anal. Chem. 45, 449 (1973).

128. J. Knoeck, Anal. Chem. 41, 2069 (1969).

129. I. M. Kolthoff, W. E. Harris, and G. Matsuyama, J. Am. Chem. Soc. 66, 1782 (1944).

130. I. M. Kolthoff and I. Hodara, J. Electroanal. Chem. 5, 2 (1963).

131. I. M. Kolthoff and J. J. Lingane, Polarography, 2nd ed. (Interscience, New York, 1952), p. 537.

132. I. M. Kolthoff, E. B. Sandell, E. J. Meehan, and S. Bruckenstein, Quantitative Chemical Analysis, 4th ed. (Macmillan, New York, 1969), pp. 821-822, 834.

133. J. Koryta, Chem. Listy 49, 17 (1955).

134. J. Koryta, Coll. Czech. Chem. Comm. 20, 667 (1955).

135. E. L. Kothny, W. A. Cook, B. Dimitriades, E. F. Ferrand, G. D. Nifong, P. W. McDaniel, B. E. Saltzman, and F. T. Weiss, Health Lab. Sci. 9, 324 (1972).

136. A. P. Kreshkov, V. A. Bork, K. S. Sal'nikova, Zh. Anal. Khim. 22, 224 (1967).

137. V. N. Kudeyarov, Agrokhimiya No. 1, 102 (1969).

138. D. Kuroda, Kagaku To Kogyo (Osaka) 45, 304 (1971).

139. T. R. N. Kutty, Curr. Sci. 42, 18 (1973).

140. R. K. Kvaratskheliya, Soobshch. Akad. Nauk Gruz. SSR 50, 631 (1968).

141. R. K. Kvaratskheliya, Soobshch. Akad. Nauk Gruz. SSR 59, 341 (1970).

142. D. H. K. Lee, Environ. Res. 3, 484 (1970).

143. K. Lemieszek-Chodorowska, I. Michalak, W. Pukorska, W. Lisowska, J. Kotlarek, M. Cywinska, H. Kula, K. Mazurkiewicz, M. Jarysz, et al., Rocz. Panstw. Zakl. Hig. 23, 549 (1972).

144. V. G. Levich, Physicochemical Hydrodynamics (Prentice-Hall, Englewood Cliffs, New Jersey, 1962) pp. 60-72.

145. L.-T. Li, Nung Yeh Yen Chiu 17, 49 (1968).

146. S.-J. Liu and S. I. Zhdanov, Zh. Fiz. Khim. 37, 1750 (1963).

147. A. R. Mack and R. B. Sanderson, Can. J. Soil Sci. 51, 95 (1971).

148. S. E. Manahan, Proceeding 3rd Univ. Mo. Annu. Conf., 1969, pp. 353-357.

149. S. E. Manahan, M. Smith, D. Alexander, and R. Hamilton, U.S. Clearinghouse Fed. Sci. Tech. Inform, P. B. Report No. 192809 (1970).

150. J. F. Marten, Ind. Chim. Belge 32, 1319 (1967).

151. F. B. Martinez and M. Z. Perez, Inform. Quim. Anal. 26, 163 (1972).

152. J. Masek, Advan. Polarog. Proceedings 2nd Intern. Congr., Cambridge, England, 1959, p. 340.

153. R. Mazoyer and I. Agius, Ann. Agron. 23, 673 (1972).

154. B. D. McCaslin, W. T. Franklin, M. A. Dillon, J. Am. Soc. Sugar Beet Technol. 16, 64 (1970).

155. N. I. McClelland and K. H. Nancy, J. Amer. Waterworks Ass. 64, 795 (1972).

156. E. F. McFarren and R. J. Lishka, Advances in Chemistry Series, No. 73 (American Chemical Society, Washington, D.C., 1968), p. 253.

157. Ph. Mechelynck and C. Mechelynck-David, Anal. Chim. Acta 21, 432 (1959).

158. L. Meites, J. Am. Chem. Soc. 73, 4115 (1951).

159. J. Mertens and D. L. Massart, Bull. Soc. Chim. Belg. 82, 179 (1973).

160. P. J. Milham, A. S. Awad, R. E. Paull, and J. H. Bull, Analyst (London) 95, 751 (1970).

161. A. S. Millar, Effluent Water Treat. J. 7, 468 (1967).

162. A. Mirna and G. Schuetz, Fleischwirtschaft 52, 1337 (1972).

163. J. I. Monselise, Isr. J. Technol. 11, 163 (1973).

164. M. I. Montenegro, M. J. Cruz, and M. L. Matias, Rev. Port. Quim. 13, 217 (1971).

165. K. Mori, Y. Yamamoto, Y. Akahane, and S. Oyabu, Nippon Suisan Gakkaishi 38, 1373 (1972).

166. G. P. Morie, C. J. Ledford, and C. A. Glover, Anal. Chim. Acta 60, 397 (1972).

167. M. Morimoto, A. Hirakoba, and R. Ishibashi, Bunseki Kagaku 16, 1335 (1967).

168. H. J. Mortko and R. E. Cover, Anal. Chem. 45, 1983 (1973).

169. R. J. K. Myers and E. A. Paul, Can. J. Soil Sci. 48, 369 (1968).

170. I. Nagai and H. Reizen, Eisei Kagaku 18, 329 (1972).

171. D. T. Napp, D. C. Johnson, and S. Bruckenstein, Anal. Chem. 39, 481 (1967).

172. R. Navone, J. Amer. Waterworks Ass. 59, 1193 (1967).

173. R. A. Nicholas and J. B. Fox, Jr., J. Ass. Off. Anal. Chem. 56, 922 (1973).

174. M. S. Nichols, J. Am. Waterworks Ass. 57, 1319 (1965).

175. M. Nishimura, K. Matsunaga, and K. Matsuda, Bunseki Kagaku 19, 1096 (1970).

176. A. Oeien and A. R. Selmer-Olsen, Analyst (London) 94, 888 (1969).

177. S. Okada, Hokkaidoritsu Eisei Kenkyushoho No. 22, 96 (1972).

178. M. Olaru and M. Basceanu, Chim. Anal. (Bucharest) 2, 233 (1972).

179. A. B. Onken and H. D. Sunderman, Commun. Soil Sci. Plant Anal. 1, 155 (1970).

180. N. S. Ormerod, Inst. Sewage Purif. J. Proc., 471 (1966).

181. T. Panalaks, J. R. Iyengar, and N. P. Sen, J. Ass. Off. Anal. Chem. 56, 621 (1973).

182. V. A. Panin and K. V. Rybalka, Elektrokhimiya 8, 1202 (1972).

183. N. K. Podberezskaya, E. A. Shilenko, and V. A. Sushkova, Issled. Obl. Khim. Fiz. Metod. Anal. Miner. Syr'ya, 90 (1971).

184. S. S. Potterton and W. D. Shults, Anal. Lett. 1, 11 (1967).

185. H. Przewlocka, Zesz. Nauk Politech. Czestochow. Nauki Tech.-Hutn. 3, Pt. 2, 549 (1969).

186. T. P. Ramachandran, Ph.D. thesis, Louisiana State University (1966) (unpublished).

187. M. C. Rand and H. Heuklekian, Anal. Chem. 25, 878 (1953).

188. G. A. Rechnitz, Chem. Eng. News 45, 146 (1967).

189. A. M. Relimpio, M. G. Guerro, A. Paneque, and M. Losada, Z. Pflanzenphysiol. 66, 290 (1971).

190. Resources Agency of California, Water Quality Criteria, State Water Quality Control Board Publication No. 3-A, edited by J. E. McKee and H. W. Wolf (Sacramento, California, 1963), p. 224.

191. N. G. Rokova, Agrokhimiya No. 1, 126 (1973).

192. A. Roy and S. K. Ghosh, Technology 7, 169 (1970).

193. E. N. Rozenblyum, R. V. Vauchskaya, and M. N. Sorokina, Sb. Rabot Khim. Istoch. Toka, 273 (1966).

194. S. Sadowski, Rocz. Panstw. Zakl. Hig. 20, 527 (1969).

195. D. Sam, U.S. Nat. Tech. Inform. Serv., AD Rep. No. 755697, 1972.

196. J. Sander and F. Schweinsberg, Zentralbl. Bakteriol., Parasitenk., Infektionskr. Hyg. 156B, 299 (1972).

197. J. Sander and F. Schweinsberg, Zentralbl. Bakteriol., Parasitenk., Infektionskr. Hyg. 156B, 321 (1972).

198. I. Sarudisen, Elelmiszervizsgalati Kozlem. 14, 47 (1968).

199. K. Sasaki, J. Electrochem. Soc. 11, 758 (1970).

200. D. Saunders and R. L. Pecsok, Anal. Chem. 40, 44 (1968).

201. G. Schmid and M. A. Lobeck, Ber. Bunsenges. Phys. Chem. 73, 189 (1969).

202. G. Schmid, M. A. Lobeck, and H. Keiser, Ber. Bunsenges. Phys. Chem. 74, 1035 (1970).

203. J. A. Schmit and R. A. Henry, Chromatographia 3, 497 (1970).

204. E. Schulek, K. Burger, and M. Feher, Z. Anal. Chem. 167, 423 (1959).

205. E. Scott and K. Bamback, Ind. Eng. Chem., Anal. Ed. 14, 136 (1942).

206. M. D. Seymour, J. P. Sickafoose, and J. S. Fritz, Anal. Chem. 43, 1734 (1963).

207. L. R. Sharma and J. Dutt, Ind. J. Chem. 6, 593, 597 (1968).

208. L. R. Sharma and J. Dutt, Ind. J. Chem. 7, 485 (1969).

209. L. R. Sharma and J. Dutt, Ind. J. Chem. 8, 170 (1970).

210. D. V. Singh and P. P. Mukherjee, Indian J. Technol. 10, 469 (1972).

211. S. I. Sinyakova and G. G. Karanovich, Tr. Komisii Anal. Khim., Otdel. Khim. Nauk, Akad. Nauk SSSR 2, 65 (1949).

212. R. E. Sioda and T. Kambara, J. Electroanal. Chem. Interfac. Electrochem. 38, 51 (1972).

213. E. M. Skobets, V. A. Chernyi, and P. I. Drutstsa, Tr. Nikoloev Korablestroit Inst. 36, 171 (1970).

214. M. I. V. Soares, P. G. S. Pereira, and A. M. Antunes, Rev. Port. Quim. 13, 151 (1971).

215. J. T. Stock and R. G. Bjork, Microchem. J. 6, 219 (1962).

216. J. T. Stock and R. G. Bjork, Talanta 11, 315 (1964).

217. J. Subert and L. Knazko, Zentralbl. Pharm., Pharmakother. Laboratoriumsdiagn. 112, 241 (1973).

218. Y. Takata and G. Muto, Anal. Chem. 45, 1864 (1973).

219. K. Tanaka, Bull. Chem. Soc. Japan 43, 2030 (1970).

220. N. Tanaka and T. Ito, Bull. Chem. Soc. Japan 39, 1043 (1966).

221. R. Thangappan, S. P. Nachiappan, S. Sampath, and H. V. K. Udupa, Metals Miner. Rev., 9 (1970).

222. M. Tokuoka, Coll. Czech. Chem. Comm. 4, 444 (1932).

223. M. Tokuoka and J. Ruzicka, Coll. Czech. Chem. Comm. 6, 339 (1934).

224. N. M. Trepak, Tr. Molodykh Uch., Saratov. Univ., Vyp. Khim. No. 2, 113 (1971).

225. N. M. Trepak, L. K. Il'ina, A. L. L'vov, and V. N. Rodnikova, Elektrokhimiya 8, 939 (1972).

226. V. A. Trukhacheva, N. F. Zakharchuk, and I. G. Yudelevich, Izv. Sib. Otd. Akad. Nauk SSSR, Ser. Khim. Nauk No. 1, 157 (1970).

227. D. D. Van Slyke and A. F. LoMonte, Microchem. J. 14, 608 (1969).

228. V. M. Vdovenko, Yu. V. Gurikov, and E. K. Legin, Radiokhimiya 8, 323 (1966).

229. B. Vennesland and C. Jetschmann, Biochim. Biophys. Acta 227, 554 (1971).

230. A. I. Vogel, A Text-Book of Quantitative Inorganic Analysis Including Elementary Instrumental Analysis, 3rd ed. (John Wiley and Sons, New York, 1961), pp. 322, 583, 956, 1088-1089.

231. E. Wada and A. Hattori, Anal. Chim. Acta 56, 233 (1971).

232. C. M. Weiss, Water Poll. Control Fed. 43, 933 (1971).

233. P. West and T. P. Ramachandran, Anal. Chim. Acta 35, 317 (1966).

234. J. H. Wetters and K. L. Uglum, Anal. Chem. 42, 335 (1970).

235. H. W. Wharton, J. Electroanal. Chem. 9, 134 (1965).

236. A. Wilhelms and H. Bernhardt, Vom Wasser 36, 353 (1969).

237. D. N. Willett, H. P. Peterson, and R. J. Moubry, J. Ass. Off. Agr. Chem. 51, 658 (1968).

238. R. J. B. Williams, Chem. Ind. (London) 48, 1735 (1969).

239. T. Williamson and A. Millar, Water Treat. Exam. 18, 150 (1969).

240. H. S. Wroblowa, J. Electroanal. Chem. Interfac. Electrochem. 42, 321 (1973).

241. H. S. Wroblowa and A. Saunders, J. Electroanal. Chem. Interfac. Electrochem. 42, 329 (1973).

242. R. T. Yang and M. J. D. Low, U.S. Nat. Tech. Inform. Serv., AD Report No. 755750, 1973.

243. Y. Yoshida, Nippon Suisan Gakkaishi 33, 348 (1967).

XI. ACKNOWLEDGEMENTS

This thesis and the research described in it would not have been possible without the inspiration and guidance of Dr. Dennis C. Johnson, whose belief that Nature is trying to tell us something seems justified. The pursuit of this research would not have been as enjoyable without him.

The author wishes to thank the University Research Grants Committee and the Graduate College of Iowa State University for the Dissertation Research Assistantship. The author also wishes to thank the Department of Chemistry of Iowa State University, the National Science Foundation, and Pine Instrument Co. for research funds and equipment used in this research.

The author thanks Bruce Parkinson, Cathy Wottreng, Bobby Snider, and Janan Hagen for contributions made to this research, and Walter Hyde of the Iowa State University Veterinary Diagnostic Laboratory for consultation and samples supplied for analysis.

The author thanks his wife, Rita, for help in preparing this thesis, and especially for tolerating a grumpy chemist.